Forecasting Hurricane Intensity: Lessons from Application of the Coupled Hurricane Intensity Prediction System (CHIPS)

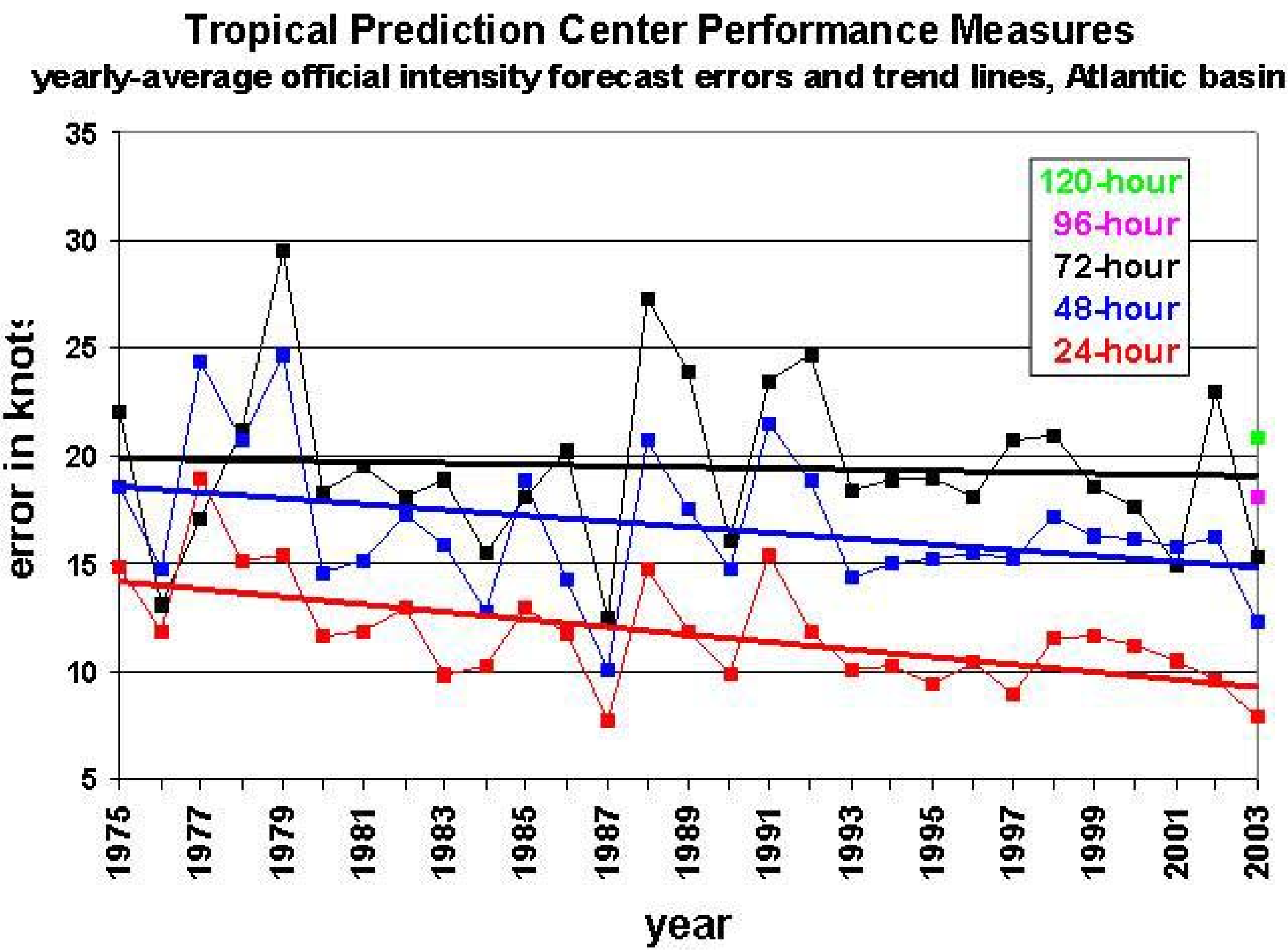

Tropical Prediction Center Performance Measures
yearly-average official intensity forecast errors and trend lines, Atlantic basin
120-hour
96-hour
72-hour
48-hour
24-hour
error in knots
35
30
25
20
15
10
5
1975
1977
1979
1981
1983
1985
1987
1989
1991
1993
1995
1997
1999
2001
2003
year

Coupled Model Design

- **Atmospheric Component:** (from Emanuel, 1995)
  - Gradient and hydrostatic balance
  - Potential radius coordinates give very fine (~ 1 km) resolution in eyewall
  - Interior structure constrained by assumption of moist adiabatic lapse rates on angular momentum surfaces
  - Axisymmetric
  - Entropy defined in PBL and at single level in middle troposphere
  - Convection based on boundary layer quasi-equilibrium postulate
  - Surface fluxes by conventional aerodynamic formulae
  - Thermodynamic inputs: Environmental potential intensity and storm-induced SST anomalies

- **Ocean Component**

  (Schade, L.R., 1997: A physical interpreatation of SST-feedback. Preprints of the 22nd Conf. on Hurr. Trop. Meteor., Amer. Meteor. Soc., Boston, pgs. 439-440.)

- **Mixing by bulk-Richardson number closure**
- **Mixed-layer current driven by hurricane model surface wind**

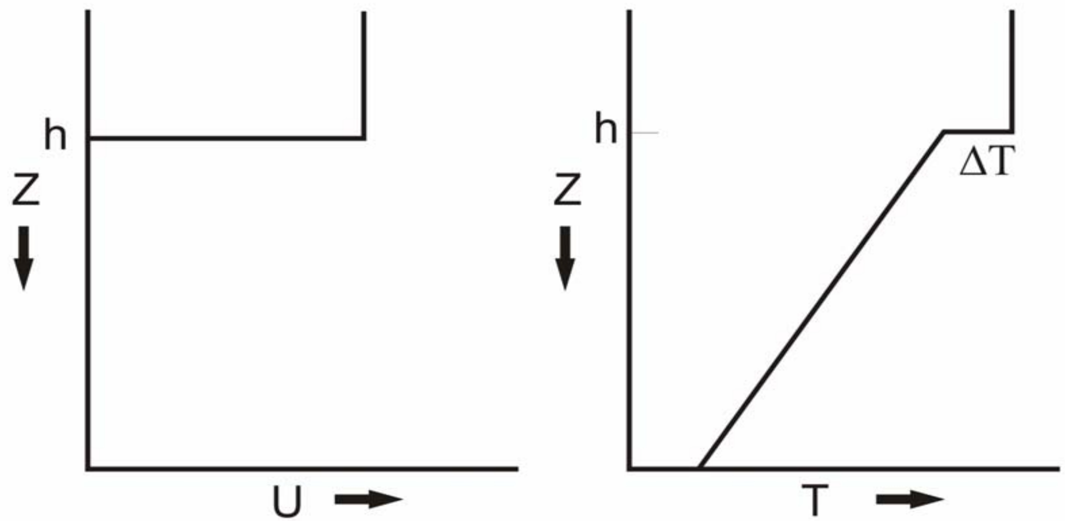

Ocean columns integrated only Along predicted storm track. Predicted storm center SST anomaly used for input to ALL atmospheric points.

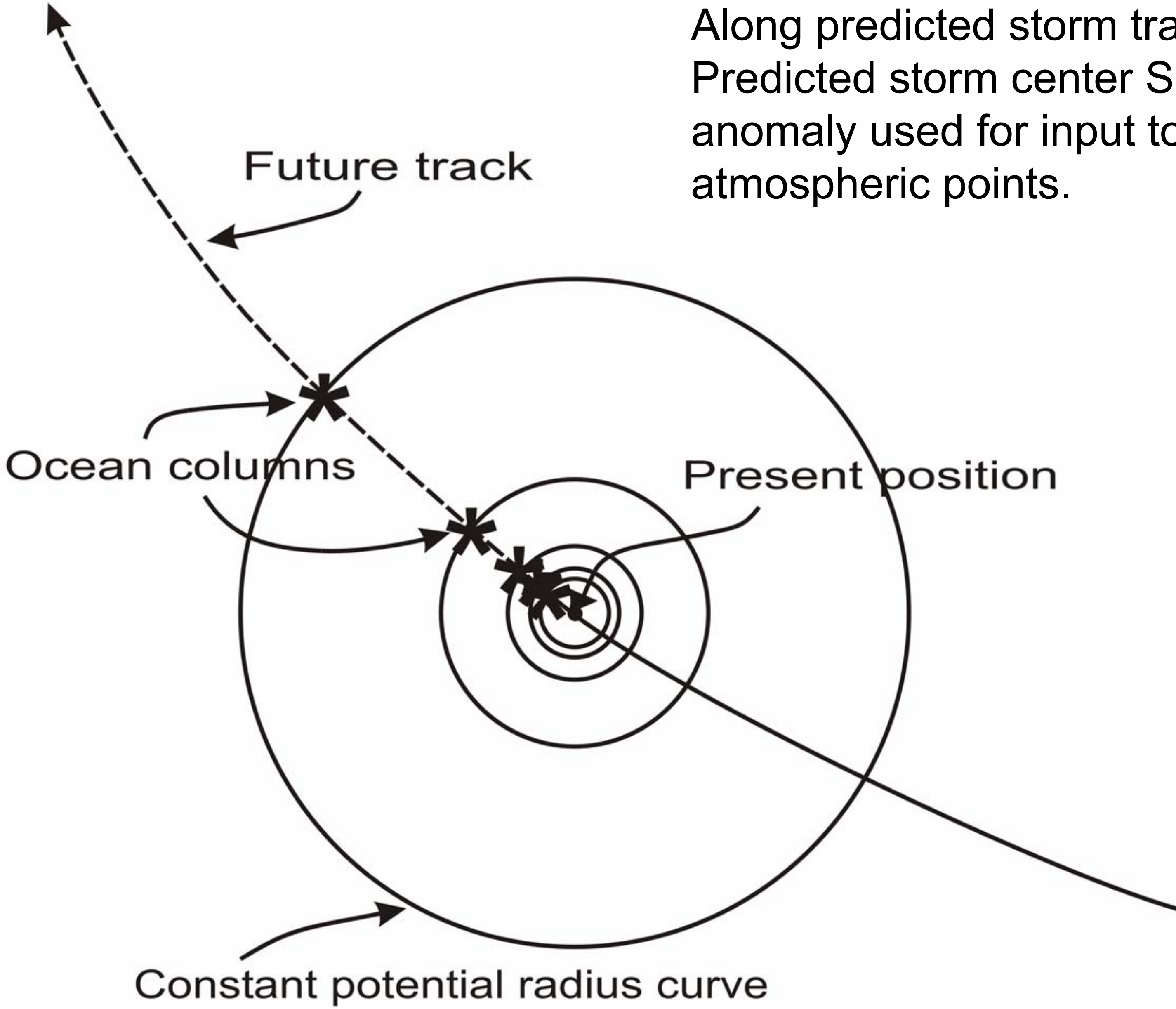

- **Data Inputs:**
  - **Weekly updated potential intensity (1 X 1 degree)**
  - **Official track forecast and storm history (NHC & JTWC)**
  - **Monthly climatological ocean mixed layer depths (1 X 1 degree)**
  - **Monthly climatological sub-mixed layer thermal stratification (1 X 1 degree)**
  - **Bathymetry (1/4 X 1/4 degree)**

Initialization:

- **Synthetic, warm core vortex specified at beginning of track**
- **Radial eddy flux of entropy at middle levels adjusted so as to match storm intensity to date**
- **This matching procedure effectively initializes middle tropospheric humidity as well as balanced flow**

Comparison with same atmospheric model coupled to 3-D ocean model; idealized runs:
Full model (black), string model (red)

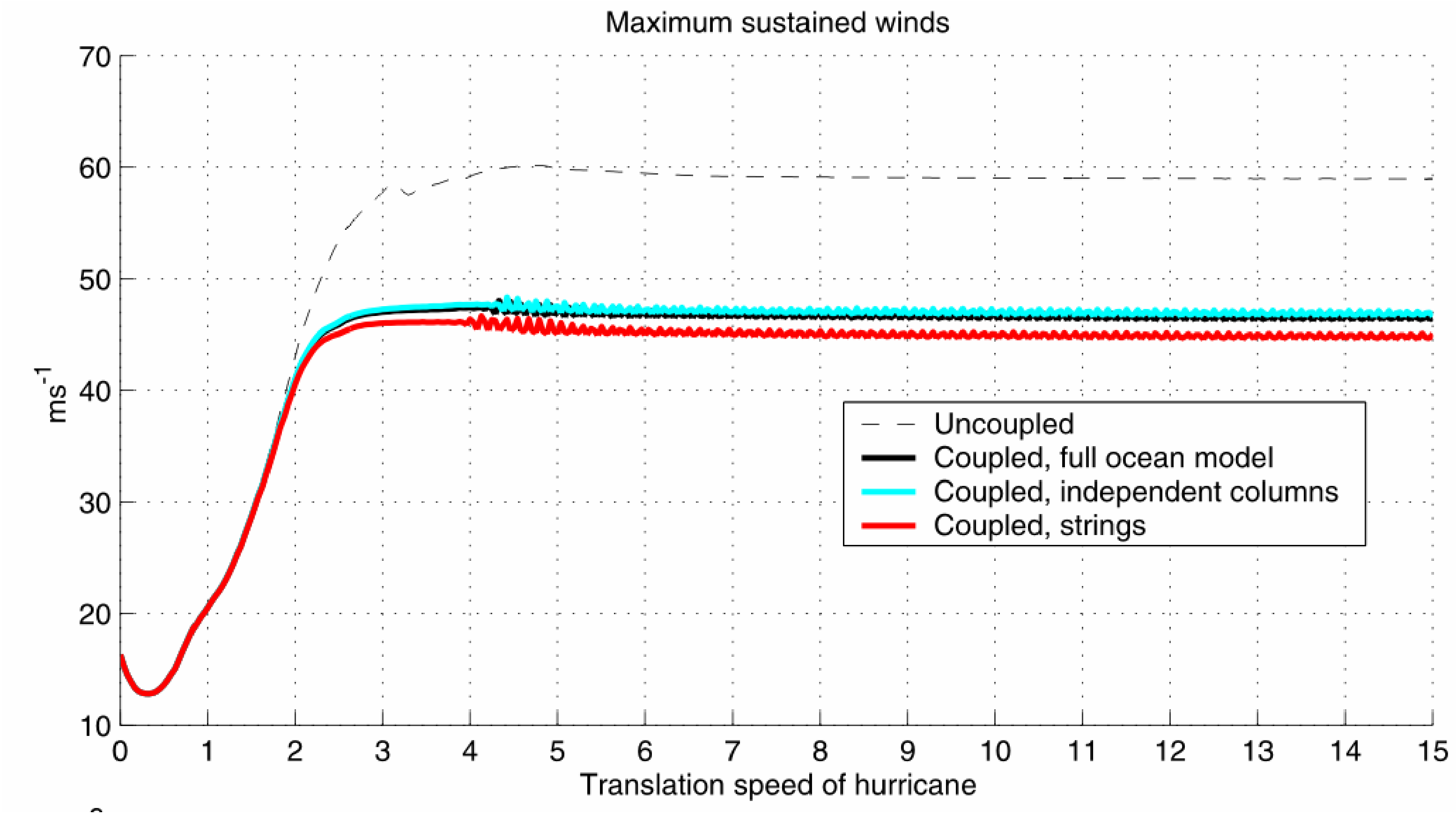

Mixed layer depth and currents

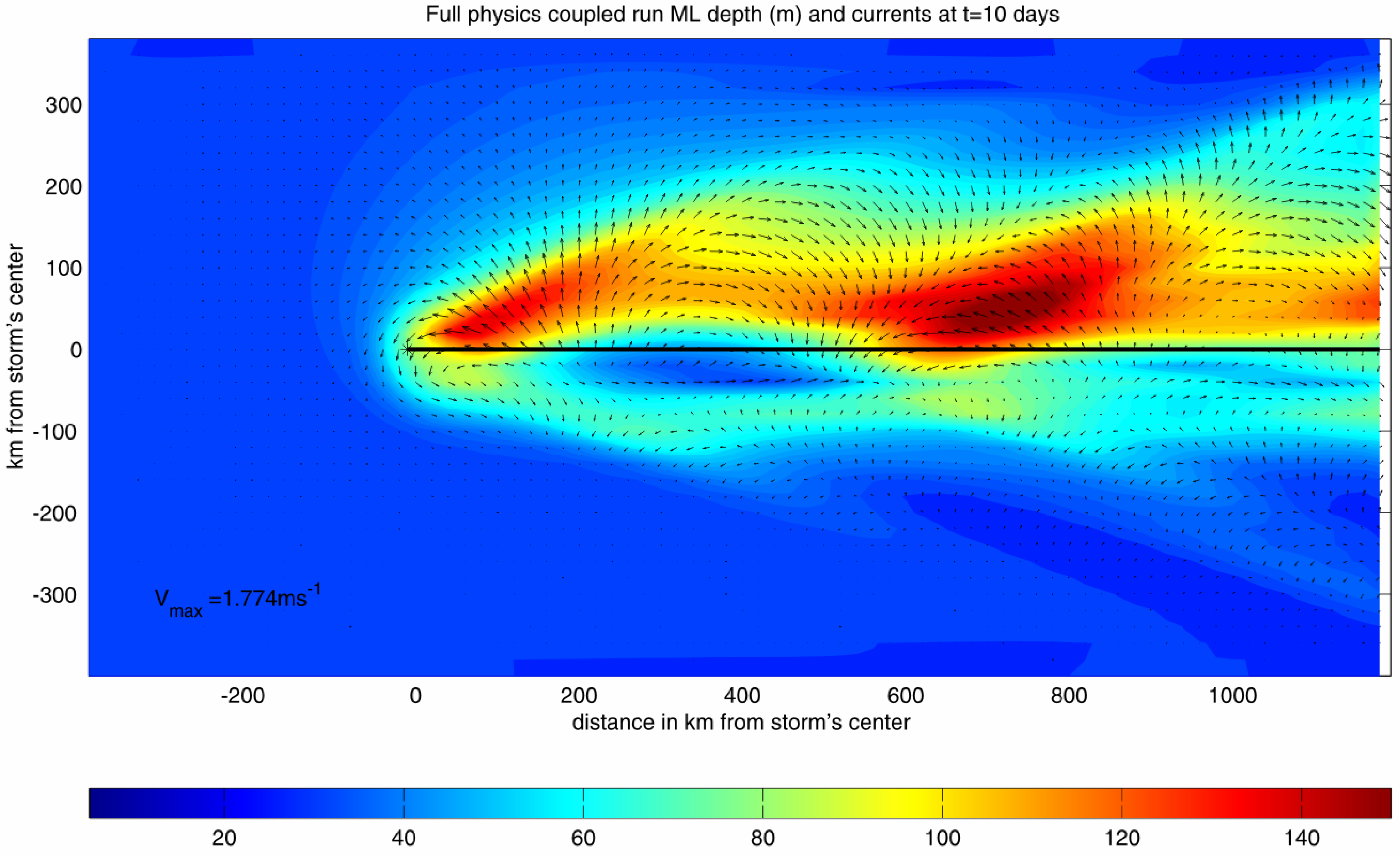

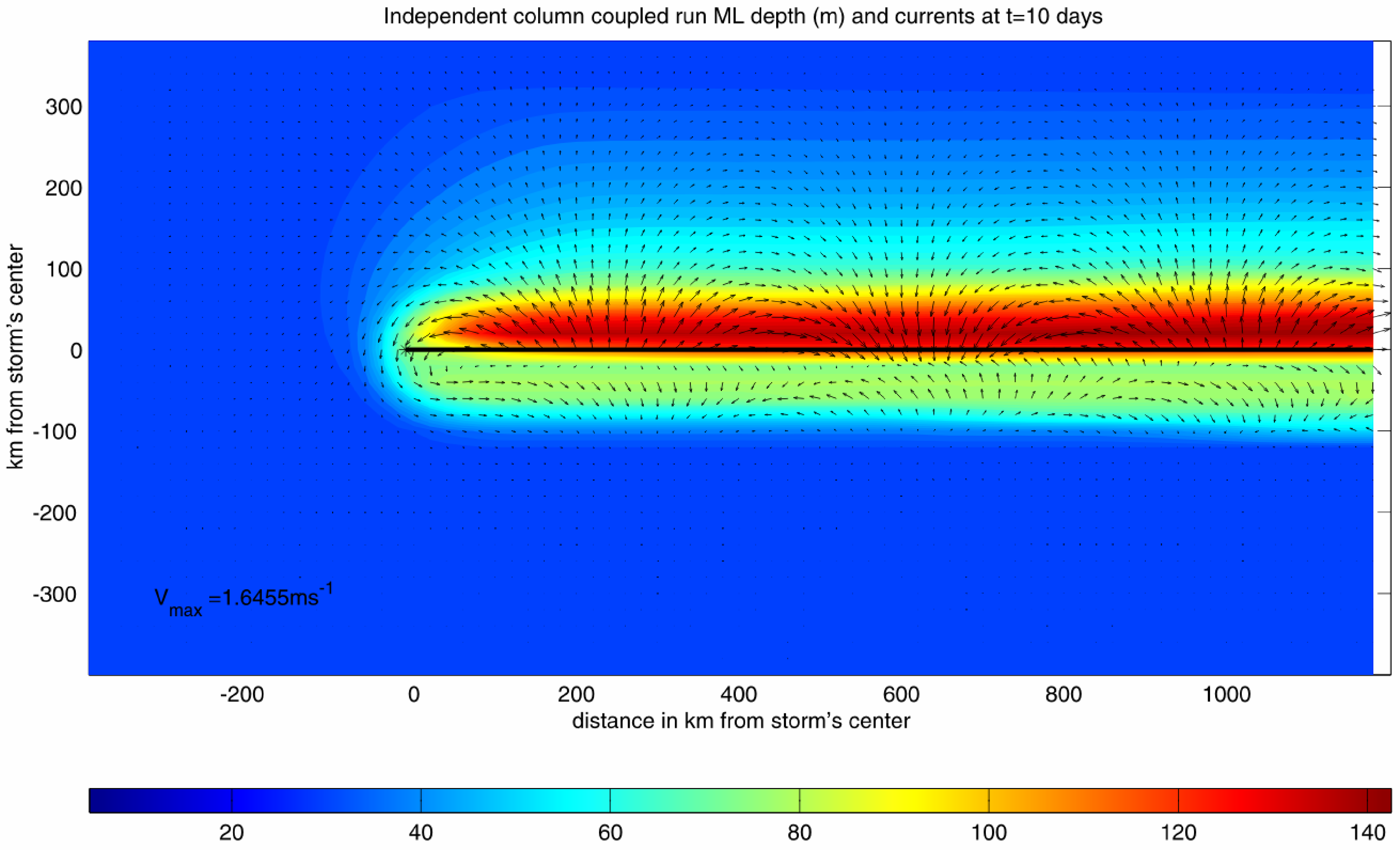

Independent column coupled run ML depth (m) and currents at t=10 days
km from storm's center
300
200
100
0
-100
-200
-300
V_{max} =1.6455ms^{-1}
-200
0
200
400
600
800
1000
distance in km from storm's center
20
40
60
80
100
120
140

SST Change

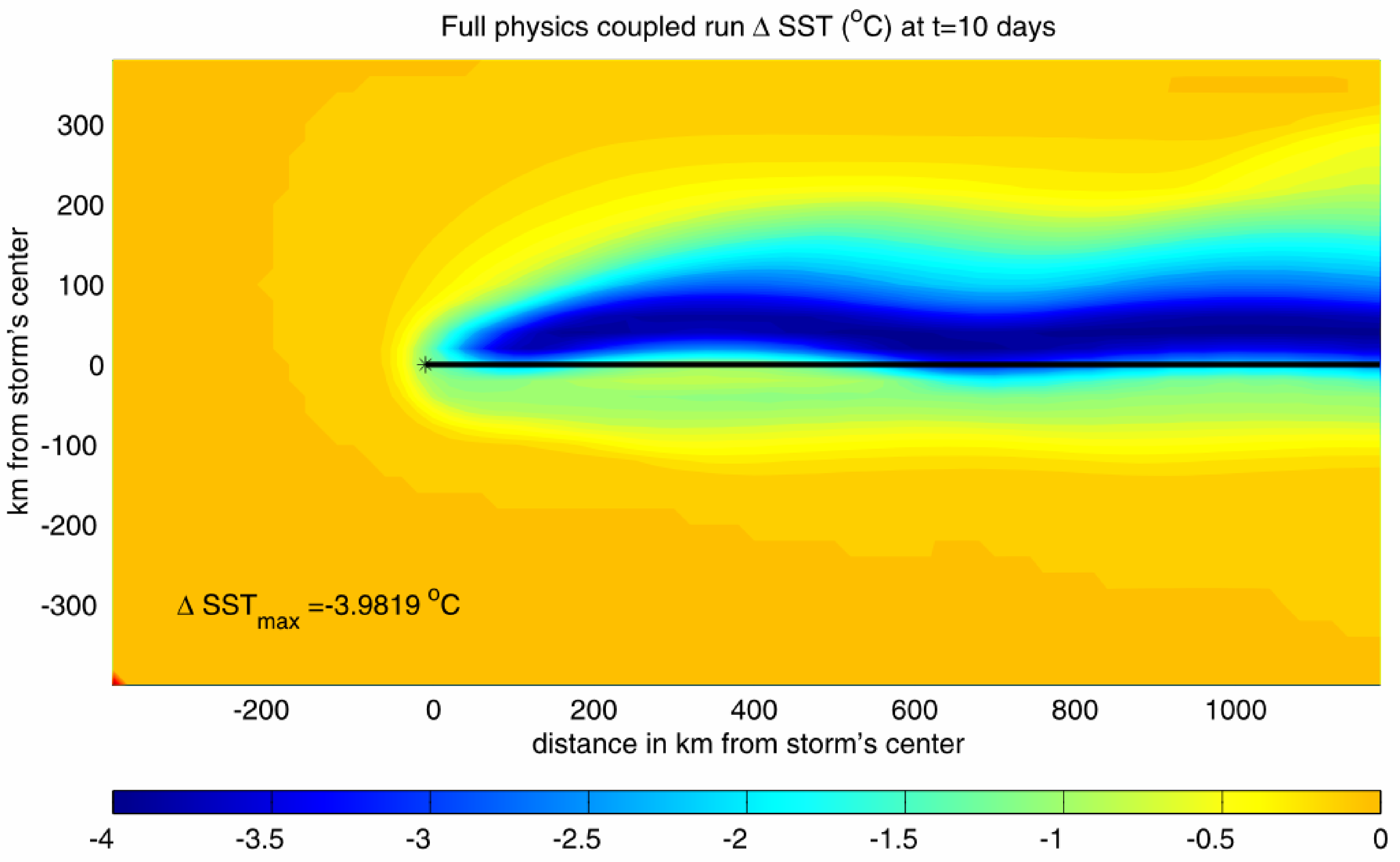
Full physics coupled run Δ SST (°C) at t=10 days
300
200
100
0
-100
-200
-300
km from storm's center
Δ SSTmax =-3.9819 °C
-200
0
200
400
600
800
1000
distance in km from storm's center
-4
-3.5
-3
-2.5
-2
-1.5
-1
-0.5
0

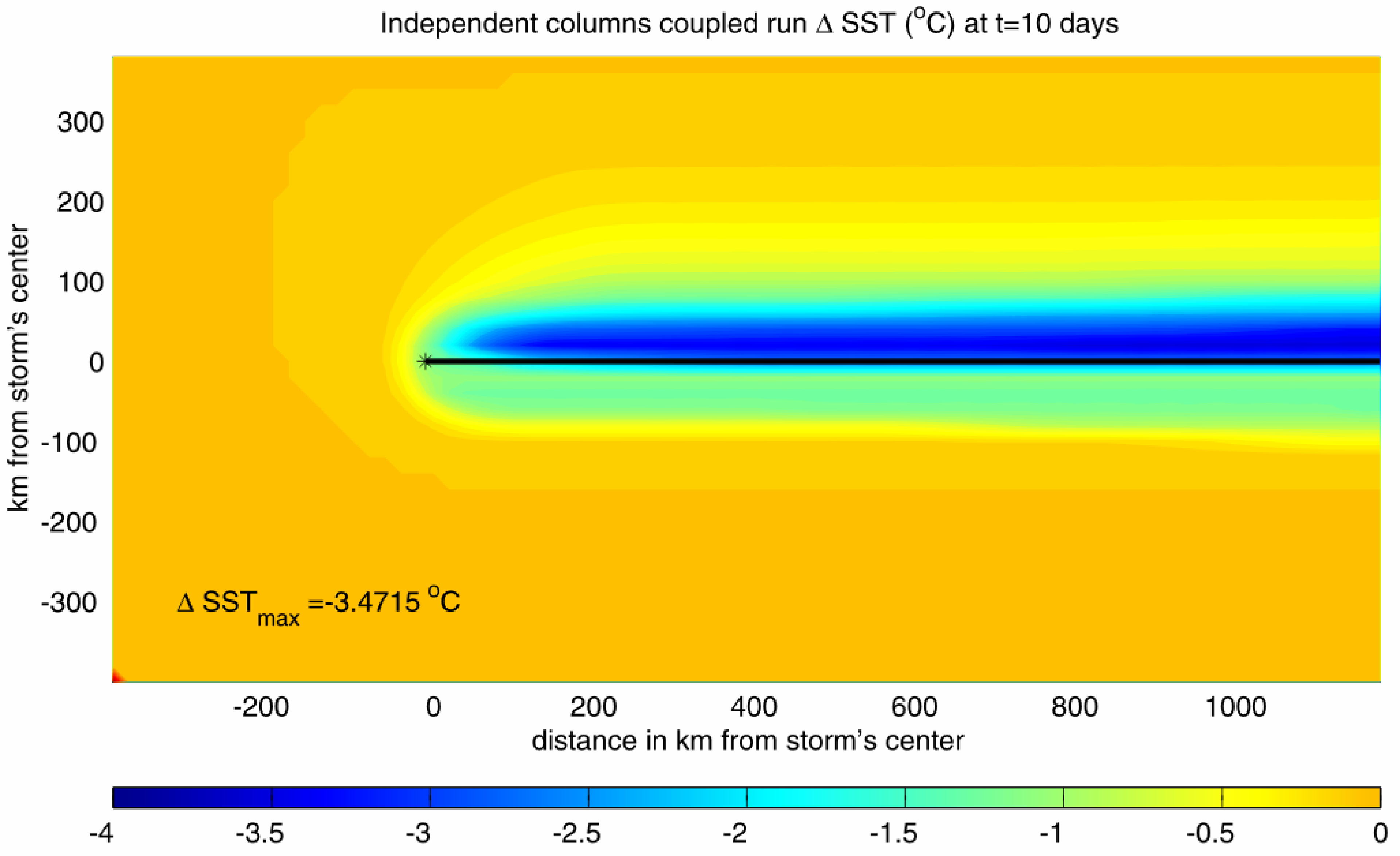

Independent columns coupled run Δ SST (°C) at t=10 days
300
200
100
0
-100
-200
-300
km from storm's center
Δ SST$_{max}$ =-3.4715 °C
-200
0
200
400
600
800
1000
distance in km from storm's center
-4
-3.5
-3
-2.5
-2
-1.5
-1
-0.5
0

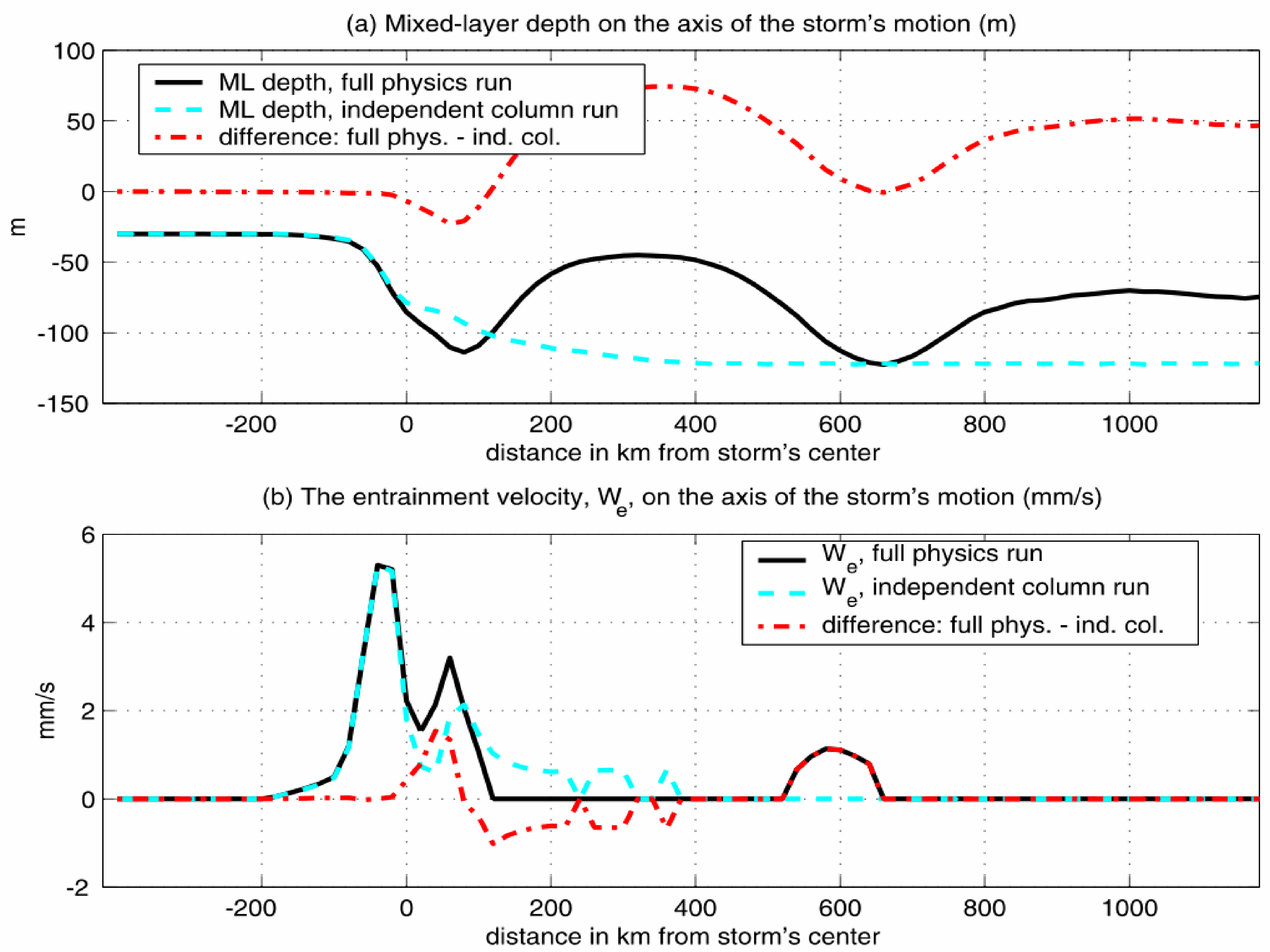

(a) Mixed-layer depth on the axis of the storm's motion (m)
ML depth, full physics run
ML depth, independent column run
difference: full phys. - ind. col.
m
100
50
0
-50
-100
-150
-200
0
200
400
600
800
1000
distance in km from storm's center
(b) The entrainment velocity, W_e, on the axis of the storm's motion (mm/s)
W_e, full physics run
W_e, independent column run
difference: full phys. - ind. col.
mm/s
6
4
2
0
-2
-200
0
200
400
600
800
1000
distance in km from storm's center

Landfall Algorithm:

- Enthalpy exchange coefficient decreases linearly with land elevation, reaching zero when h = 40 *m*
- This accounts in a crude way for heat fluxes from low-lying, swampy or marshy terrain

Real-Time Forecasts Posted at http://wind.mit.edu/~emanuel/storm.html

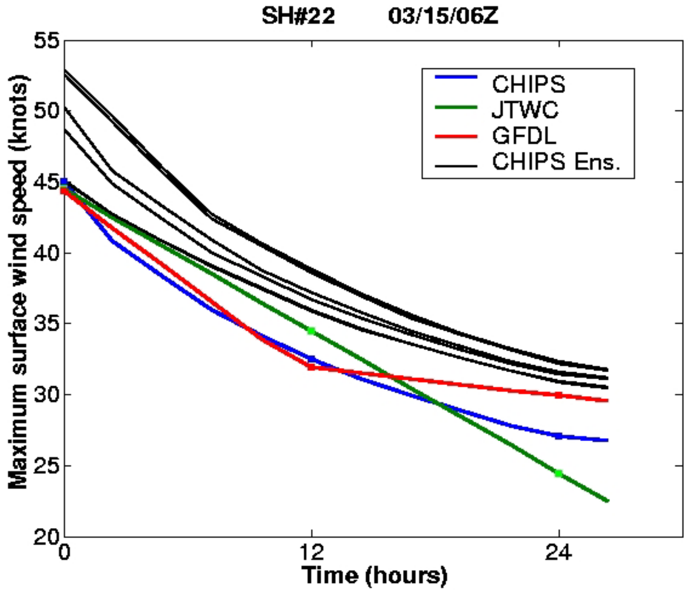

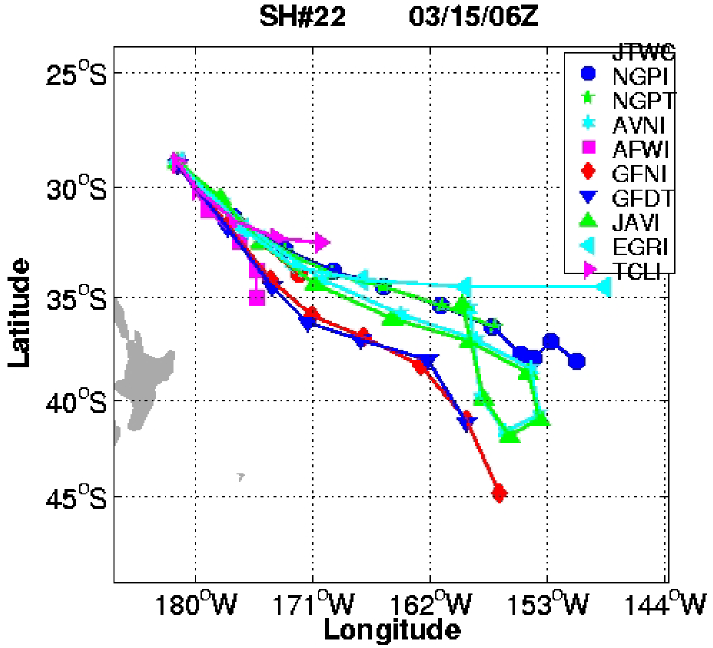

Overall Forecast Performance:
2002 Atlantic Intensity Errors

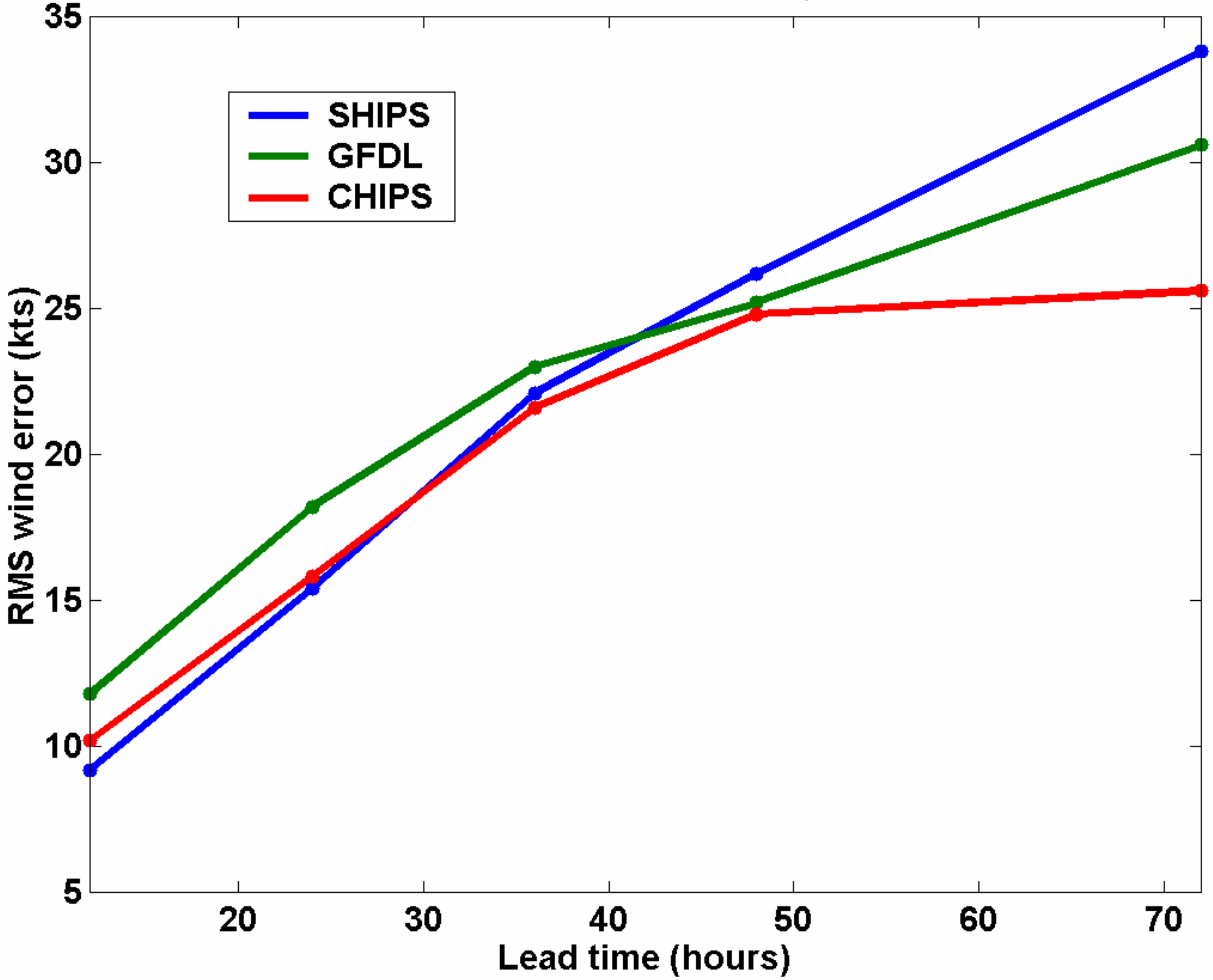

Hurricane Gert occurred in a low-shear environment and moved over an ocean close to its climatological mean state.

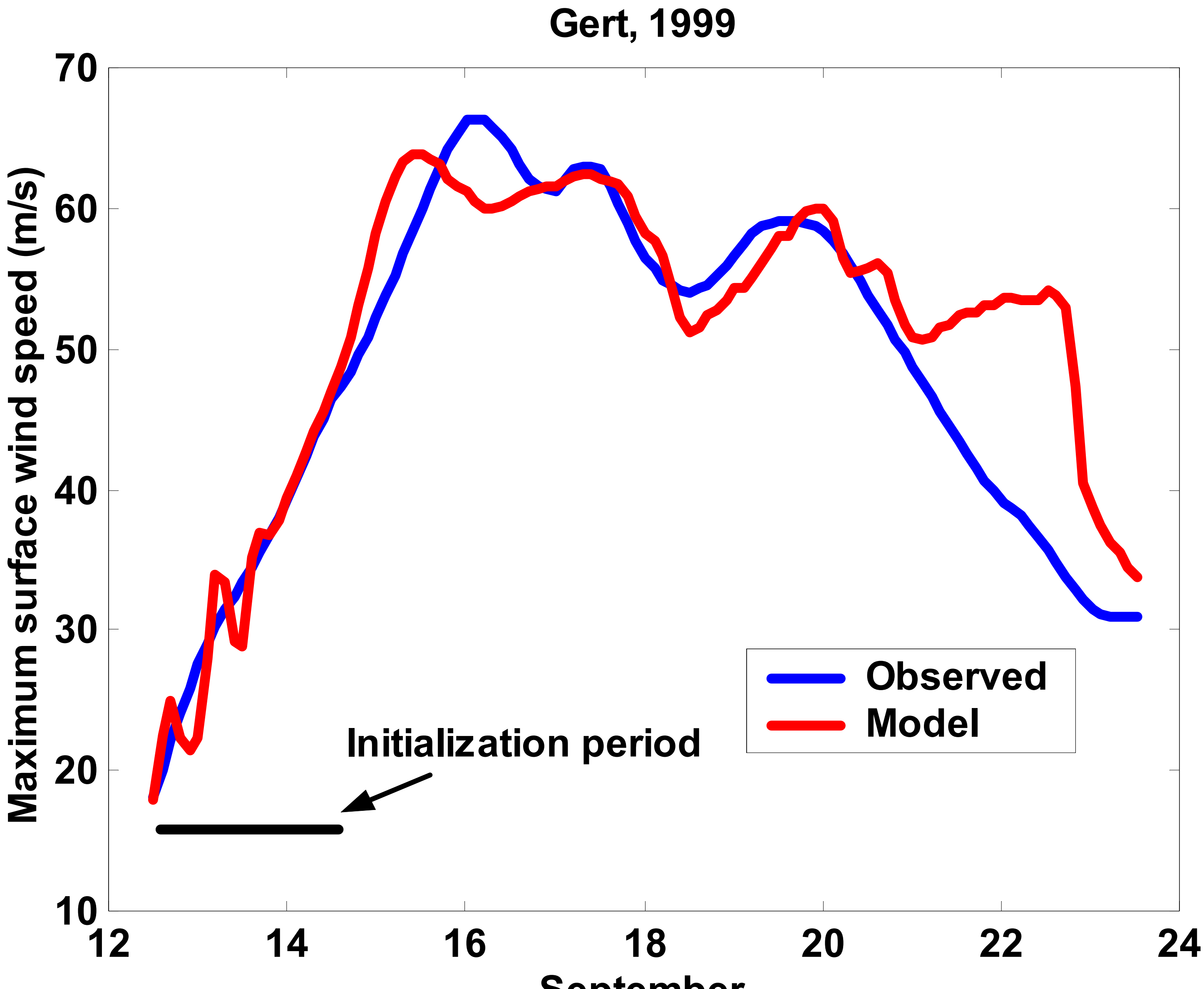

Same simulation, but with fixed SST:

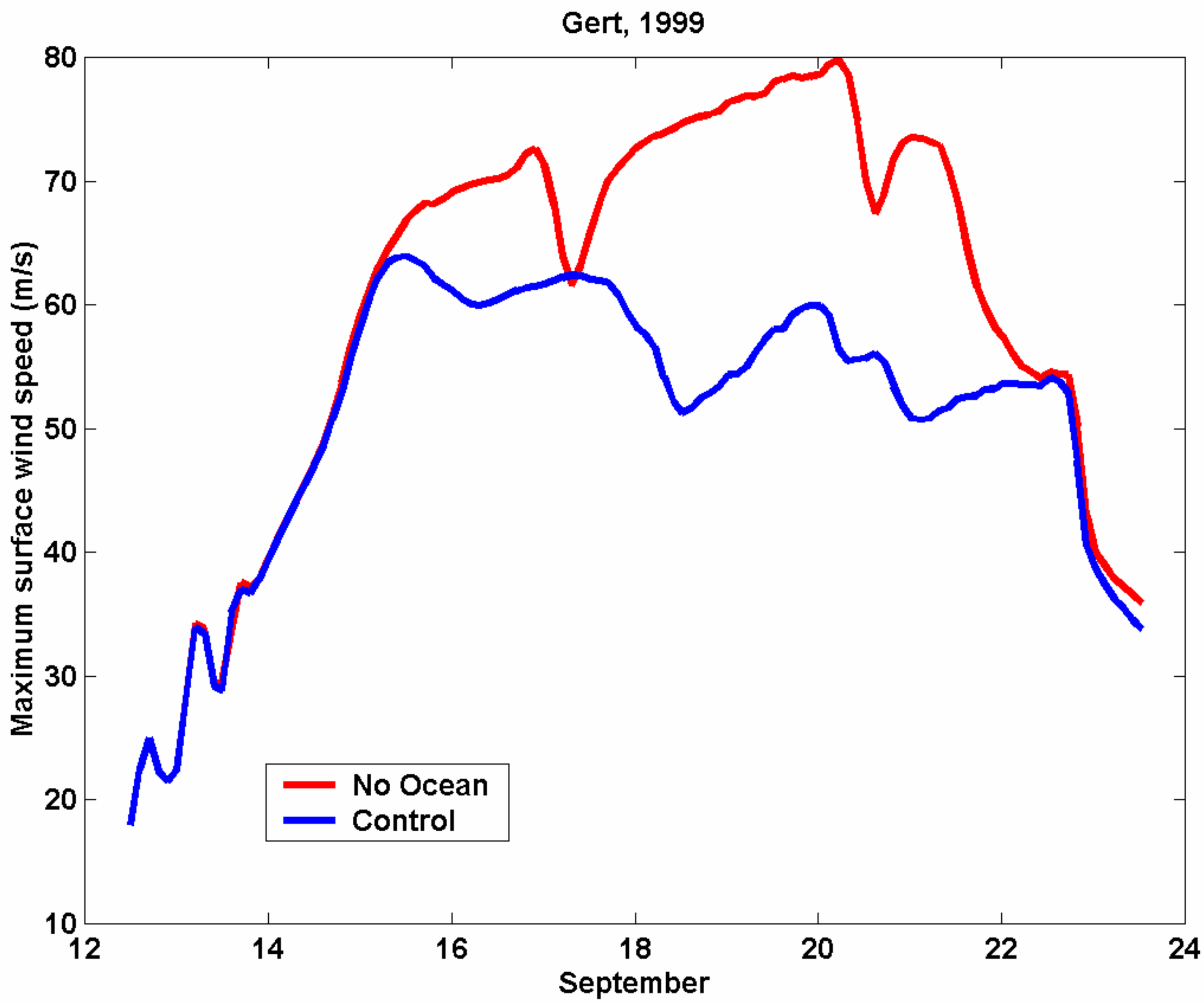

Sensitivity to initial intensity error and length of matching period:

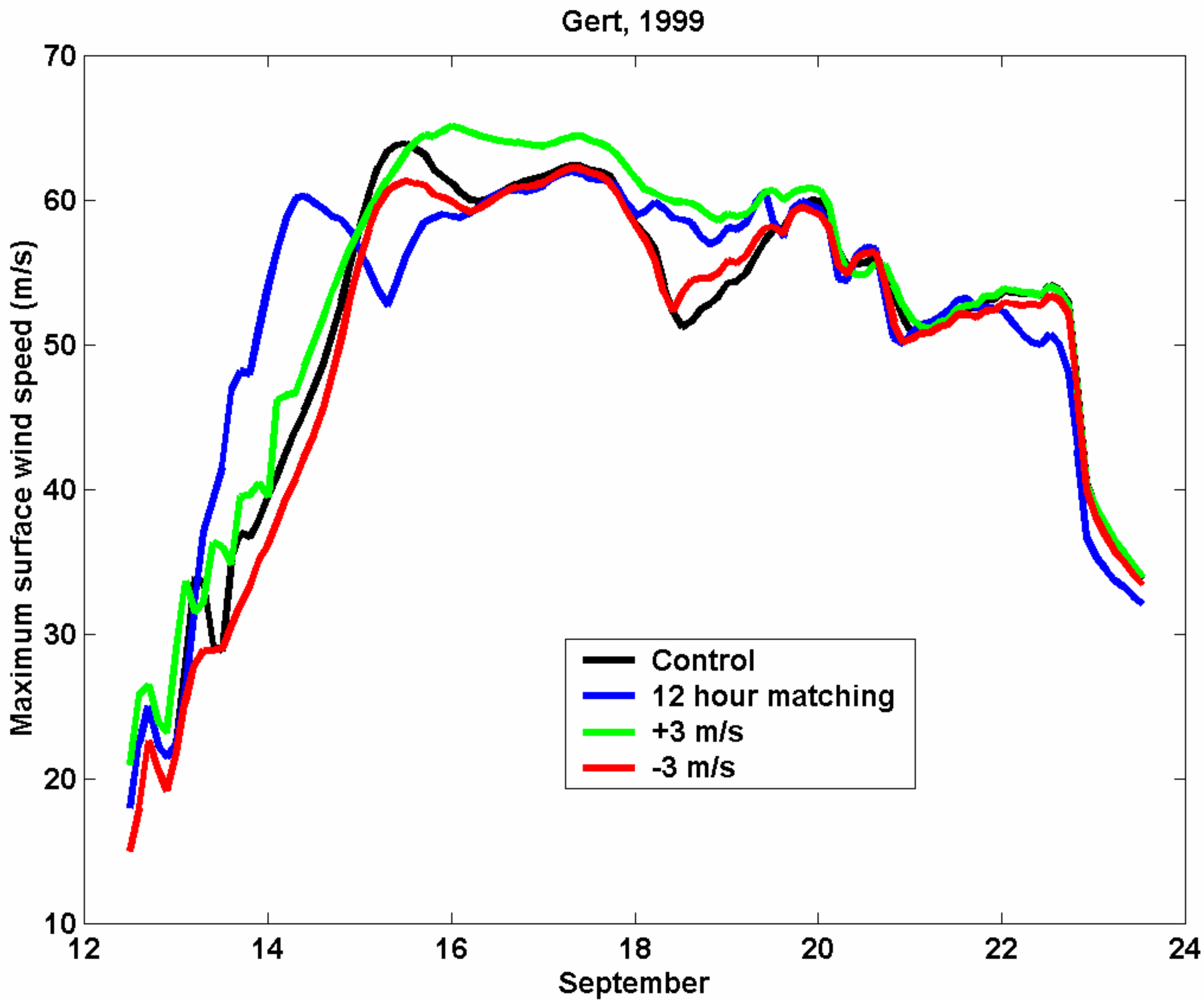

Sensitivity to size of starting vortex

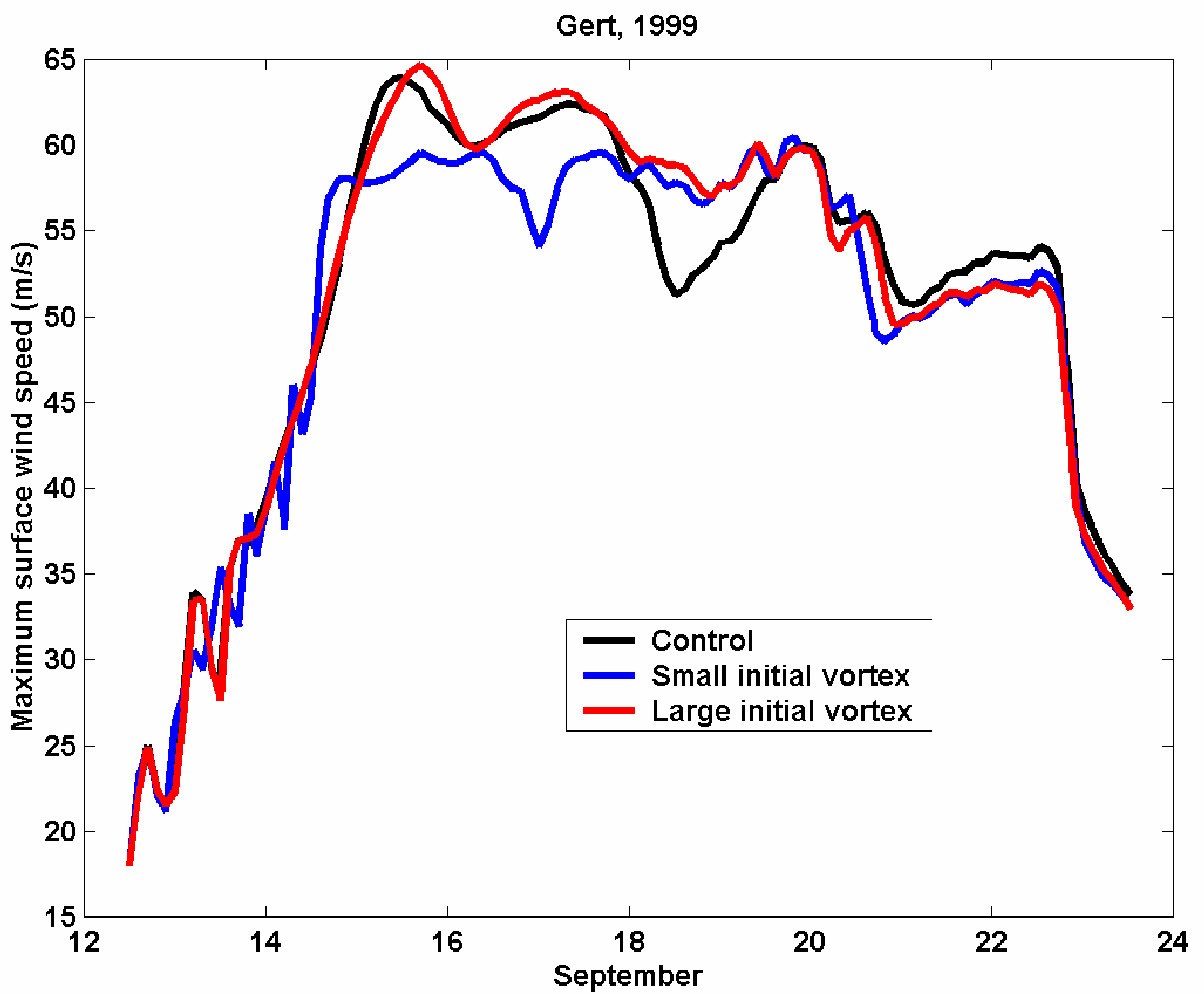

Model performs poorly when substantial shear is present, as in Chantal, 2001:

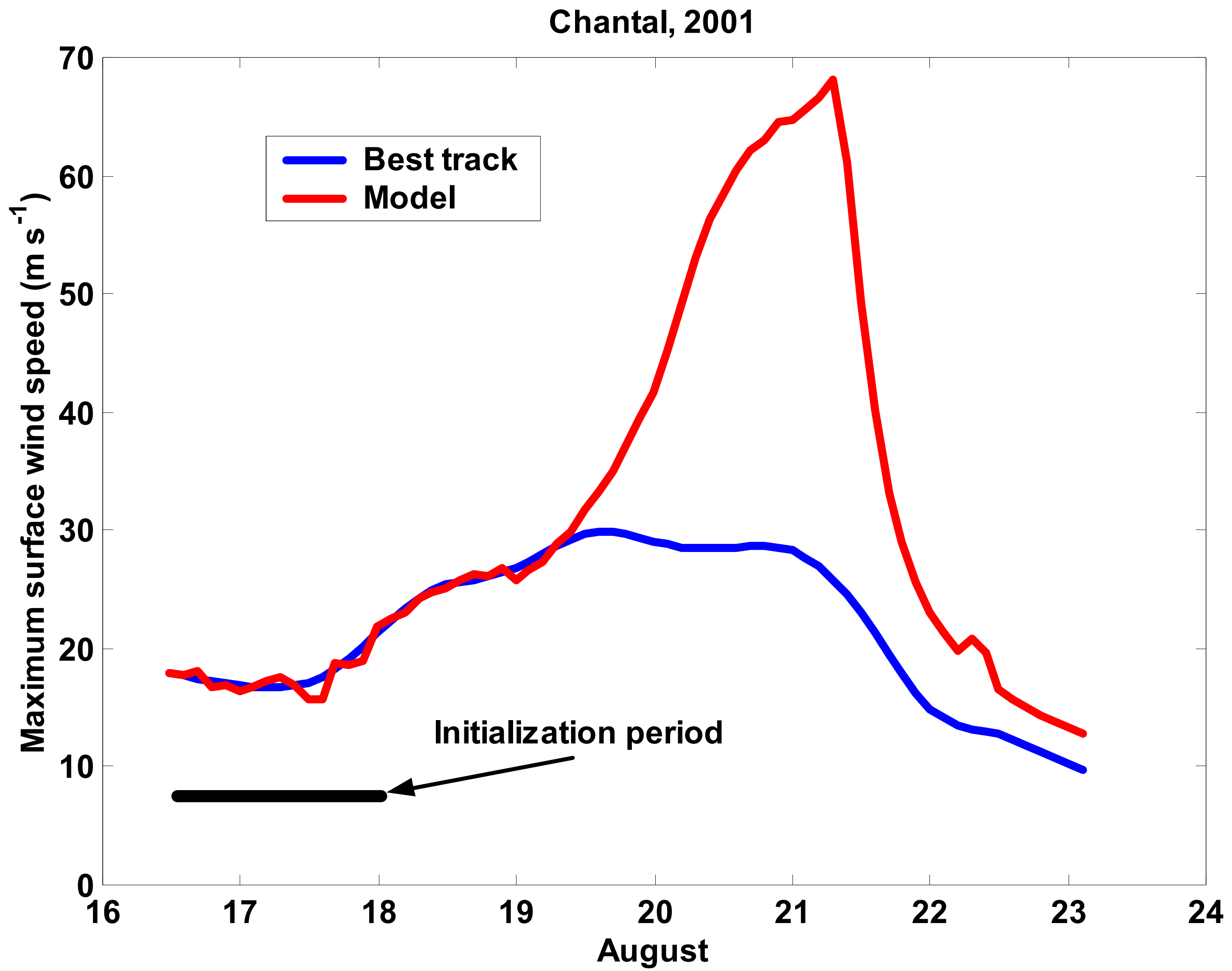

850 – 200 hPa environmental shear:

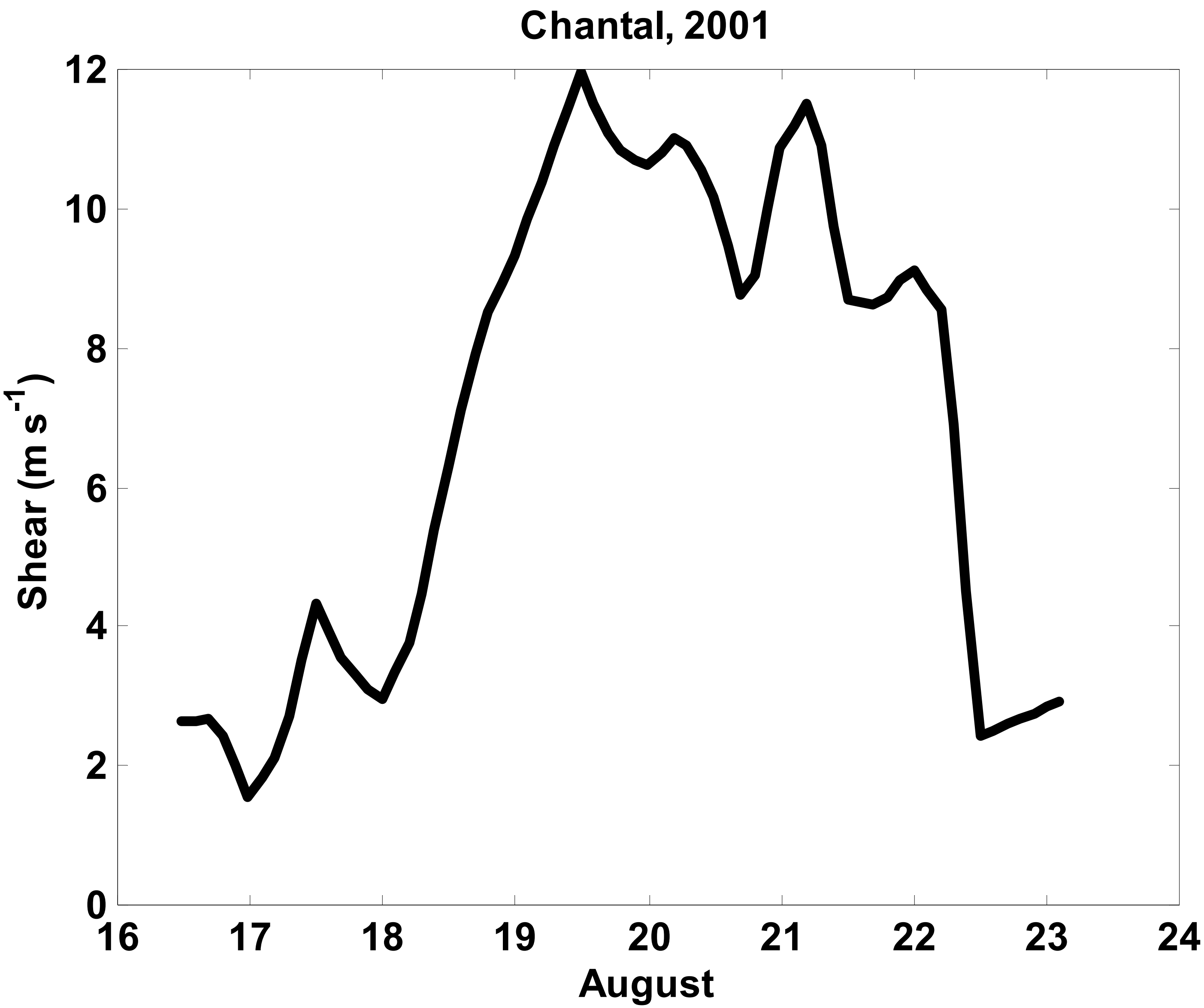

Add “ventilation” term to model equation governing middle level θ_e. Coefficient determined by matching model to long record of observations:

$$\frac{\partial \theta_e}{\partial t} = \ldots - \mathbf{V}\left(\theta_e - \theta_{e0}\right)$$

$$\mathbf{V} = V_{max}^2 V_{shear}^2$$

Result:

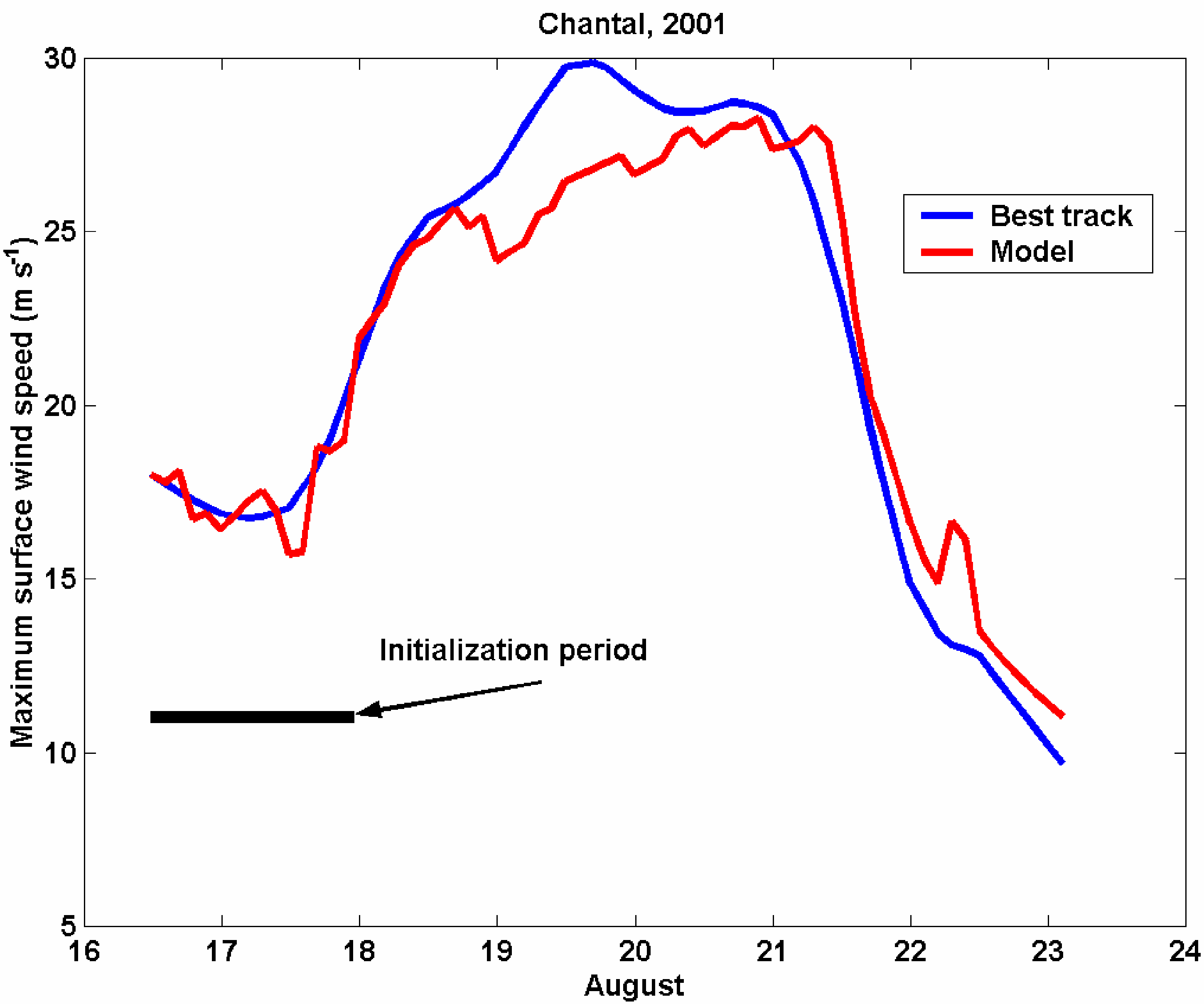

Chantal, 2001
Maximum surface wind speed (m s-1)
30
25
20
15
10
5
16
17
18
19
20
21
22
23
24
August
Best track
Model
Initialization period

But model sensitive to shear: This shows the results of varying Shear magnitude by +/- 5 kts and +/- 10 kts:

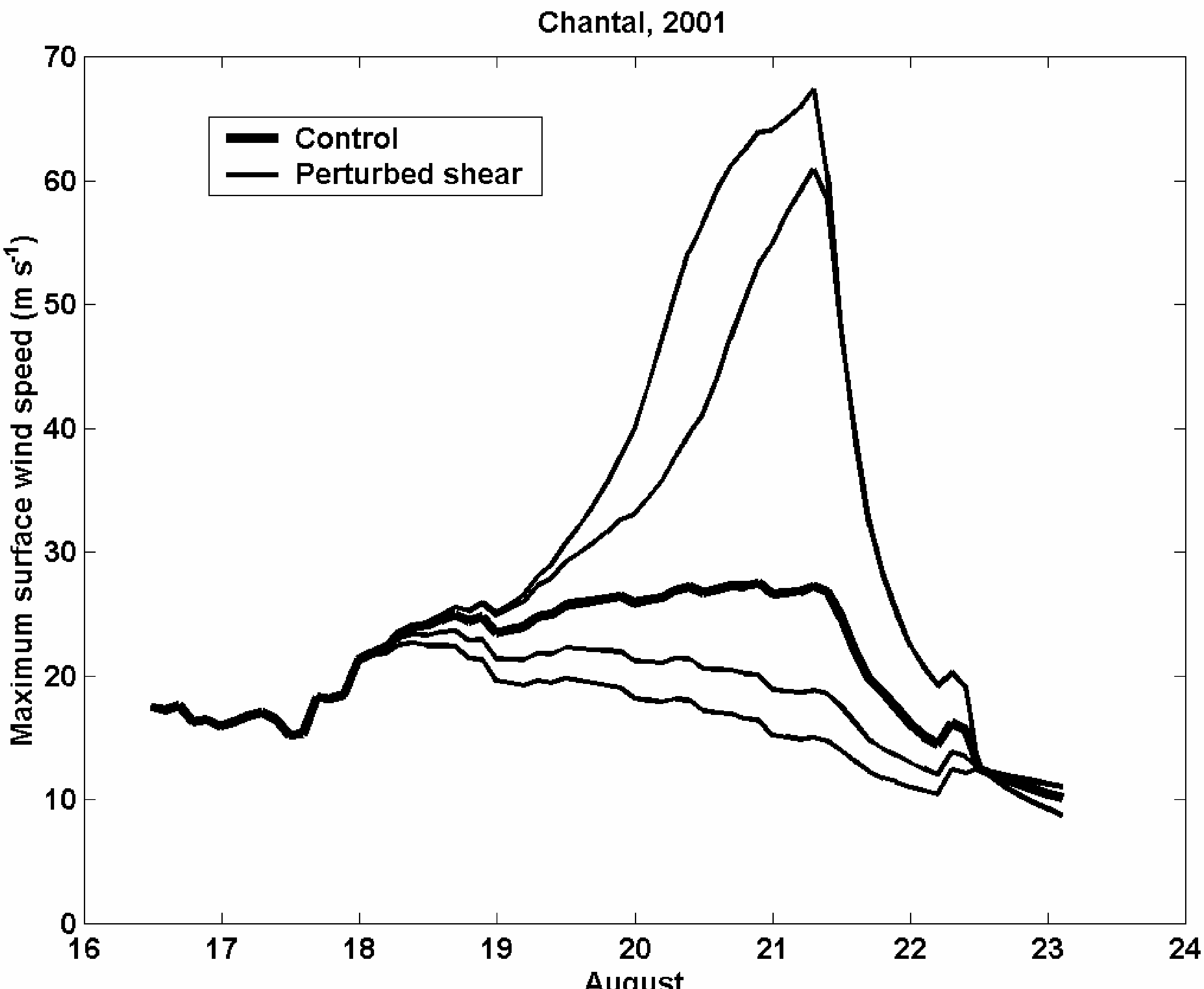

Presence of shear also makes model sensitive to initial conditions. Here the initial intensity is varied by +/- 3 m/s and +/- 6 m/s:

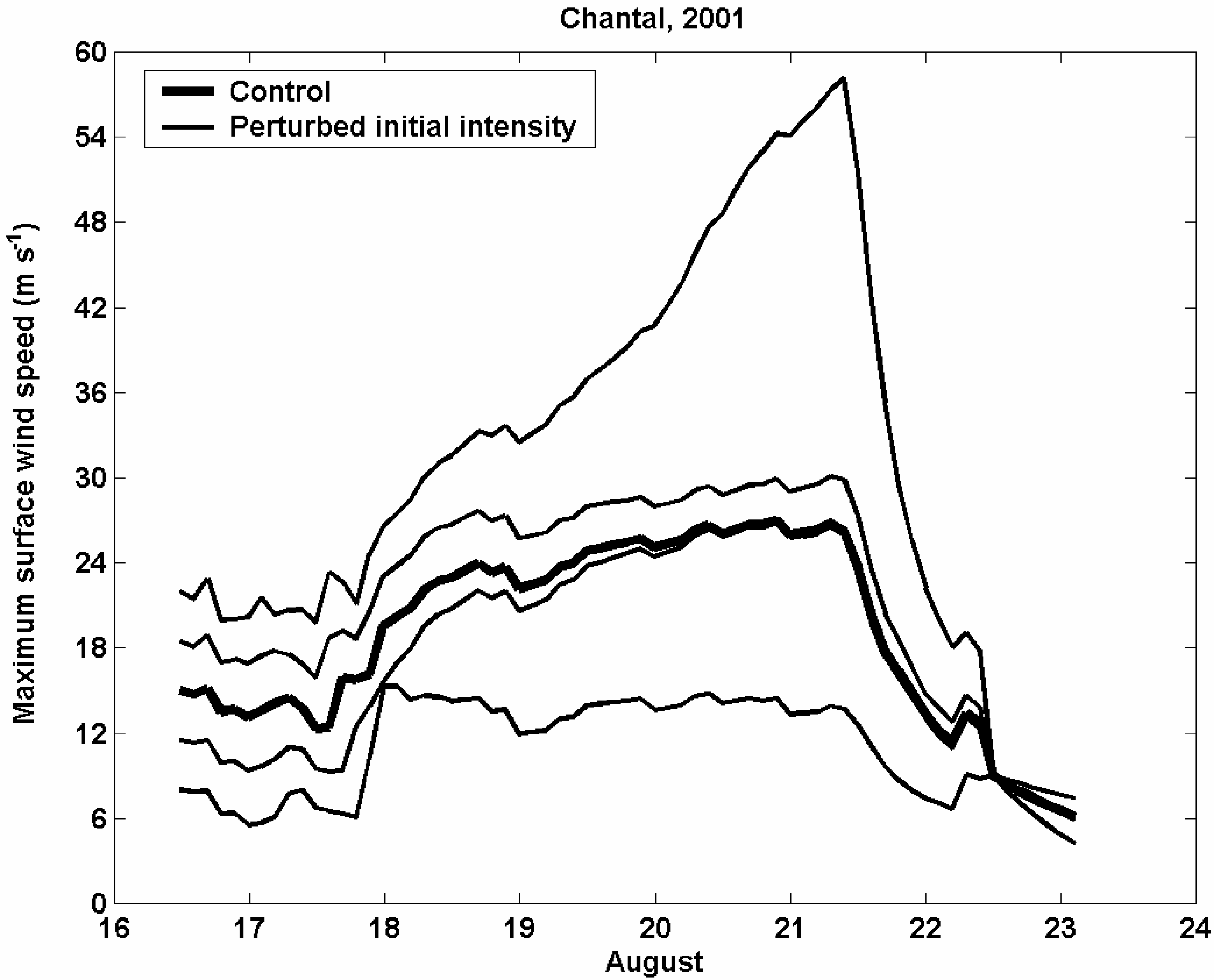

Some storms are influenced by upper ocean anomalies from monthly climatology. An example is that of Typhoon Maemi of 2003, which passed over a warm eddy in the western North Pacific:

Typhoon Maemi, 2003

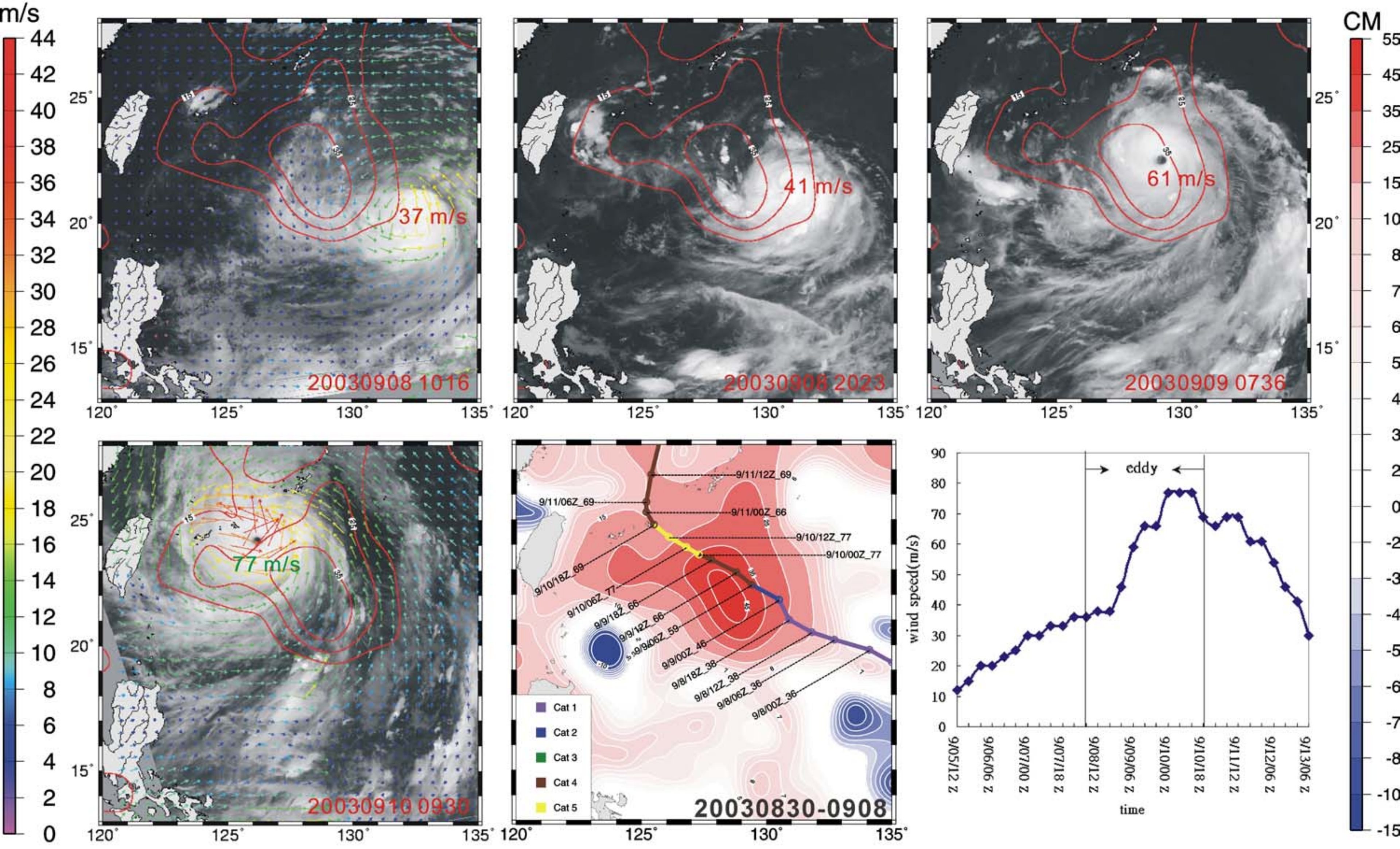

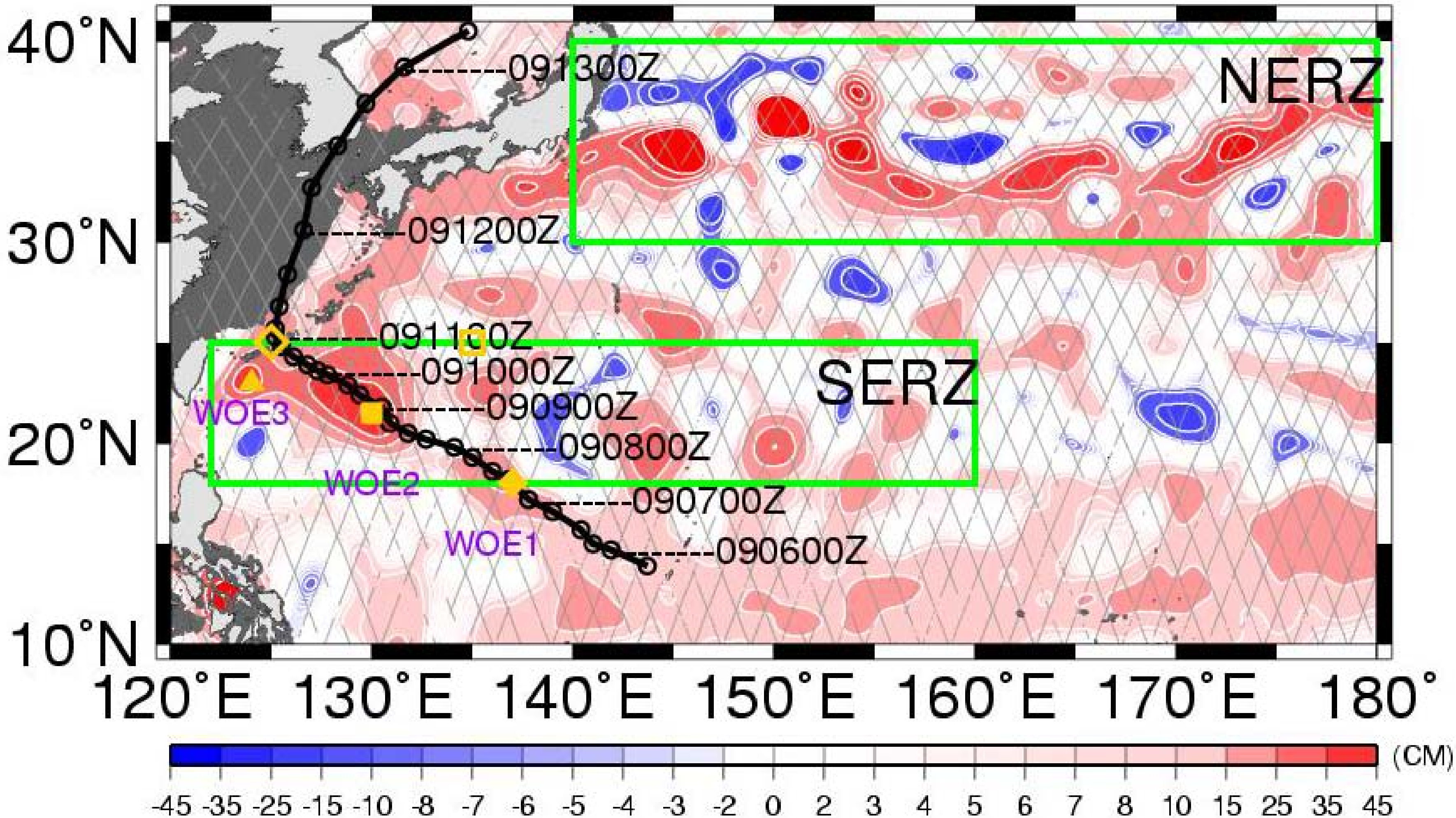

tj_20030827-0905

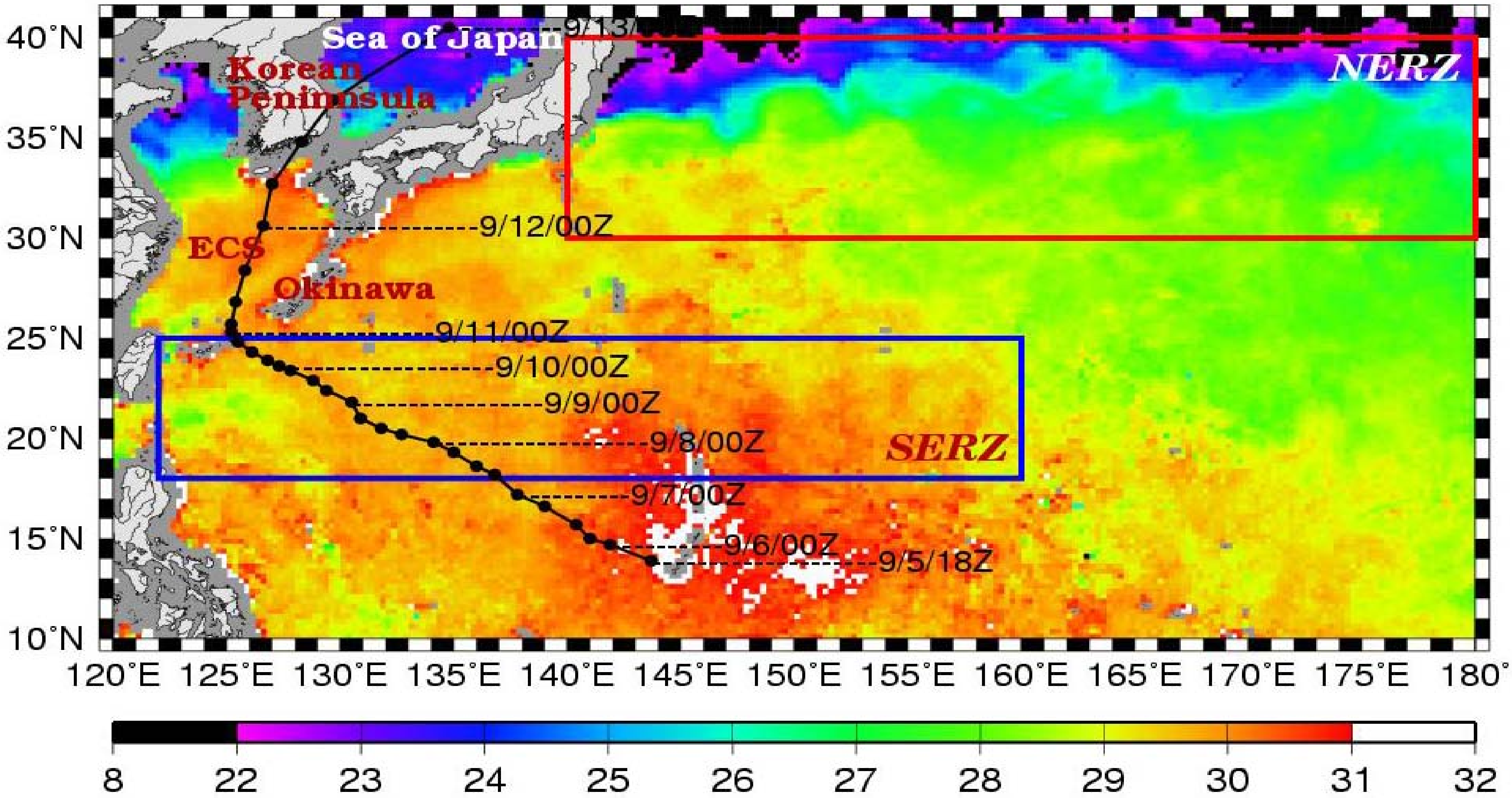

Sea of Japan
Korean Peninmsula
ECS
Okinawa
NERZ
SERZ
9/12/00Z
9/11/00Z
9/10/00Z
9/9/00Z
9/8/00Z
9/7/00Z
9/6/00Z
9/5/18Z
40°N
35°N
30°N
25°N
20°N
15°N
10°N
120°E 125°E 130°E 135°E 140°E 145°E 150°E 155°E 160°E 165°E 170°E 175°E 180°
8 22 23 24 25 26 27 28 29 30 31 32

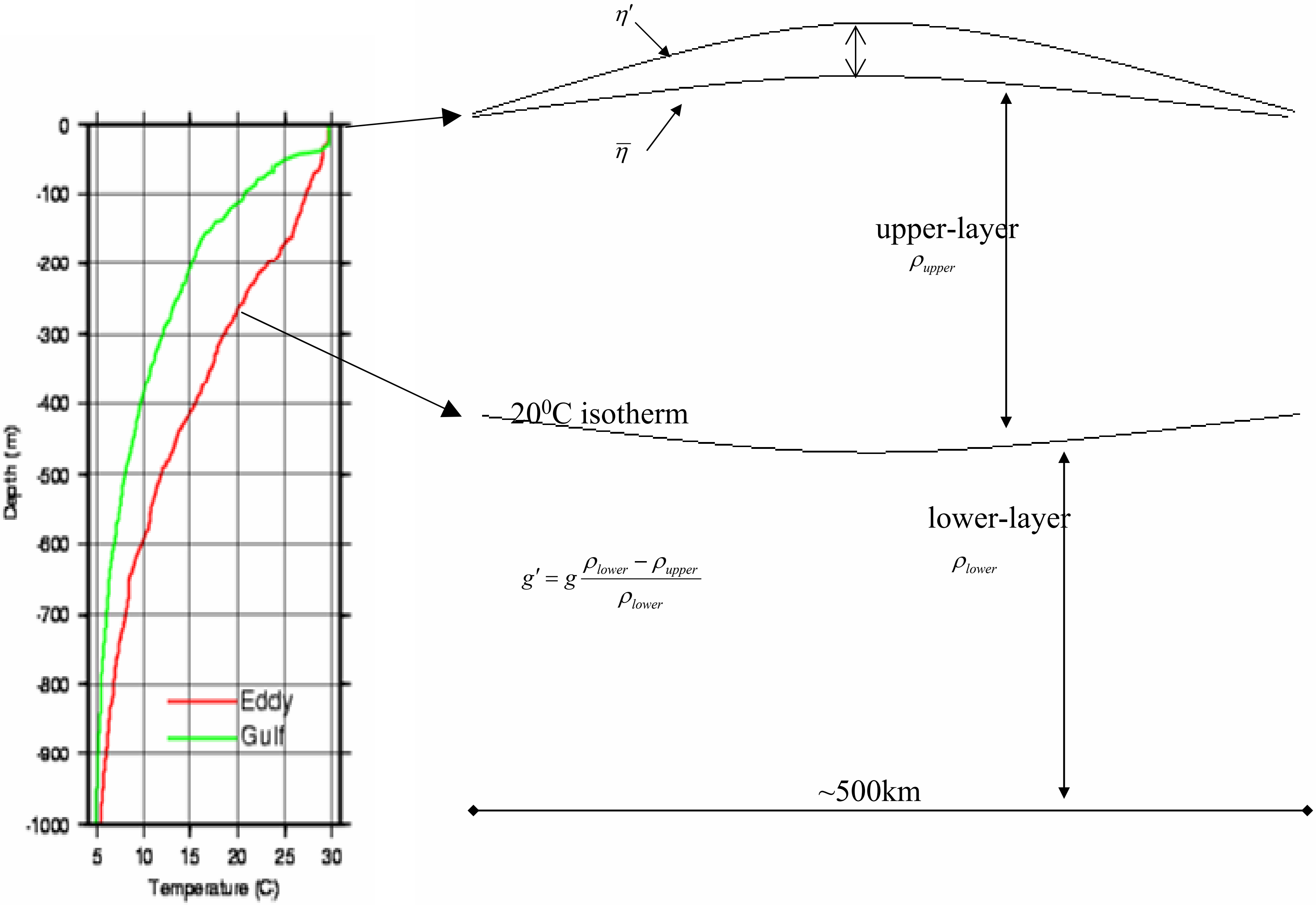

Depth (m)
0
-100
-200
-300
-400
-500
-600
-700
-800
-900
-1000
5
10
15
20
25
30
Temperature (C)
Eddy
Gulf
η'
$\overline{\eta}$
upper-layer
ρ_{upper}
20^0C isotherm
lower-layer
ρ_{lower}
$g' = g\frac{\rho_{lower} - \rho_{upper}}{\rho_{lower}}$
~500km

Standard Simulation:

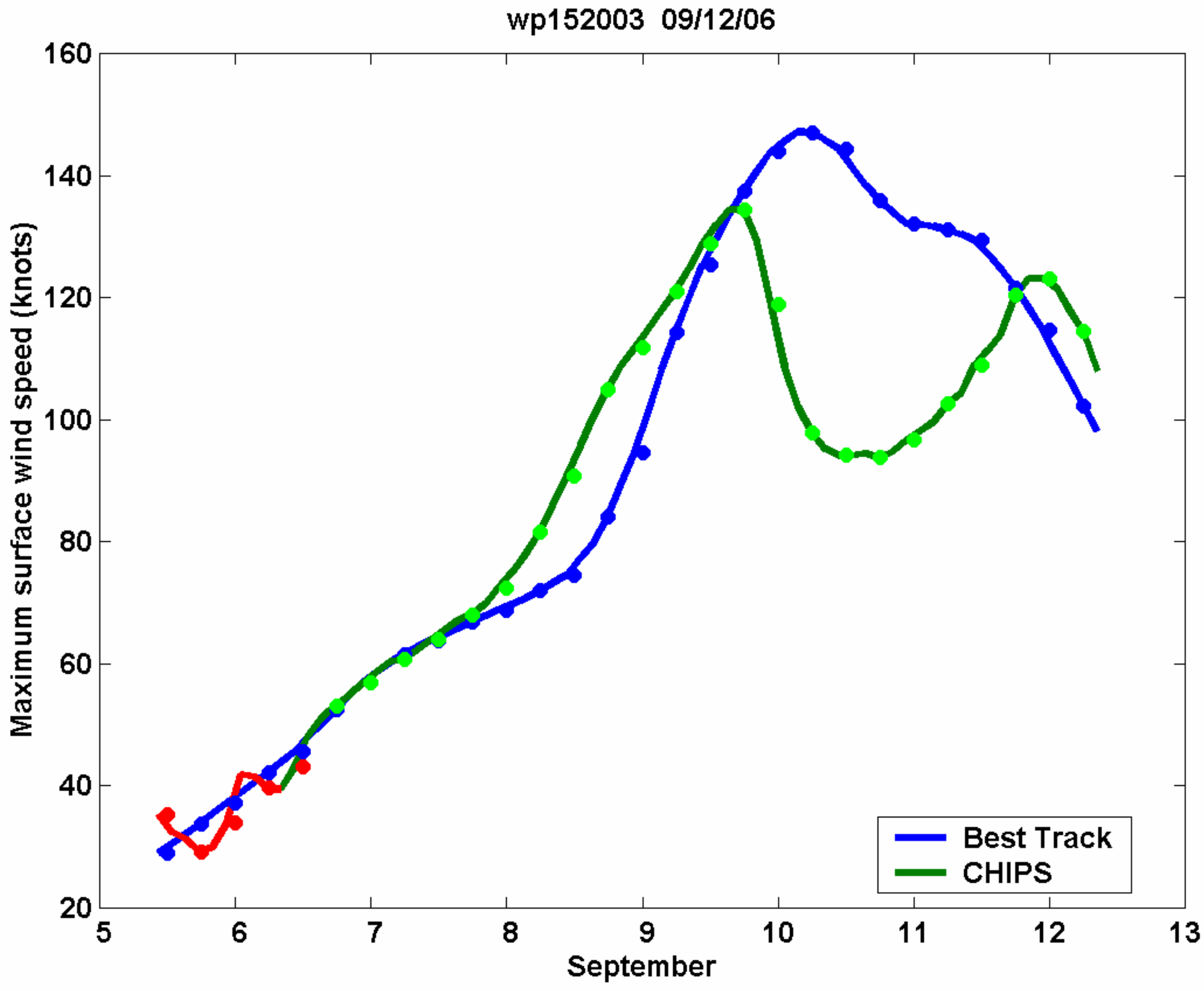

Using Sea Surface Altimetry to Estimate Upper Ocean Thermal Structure:

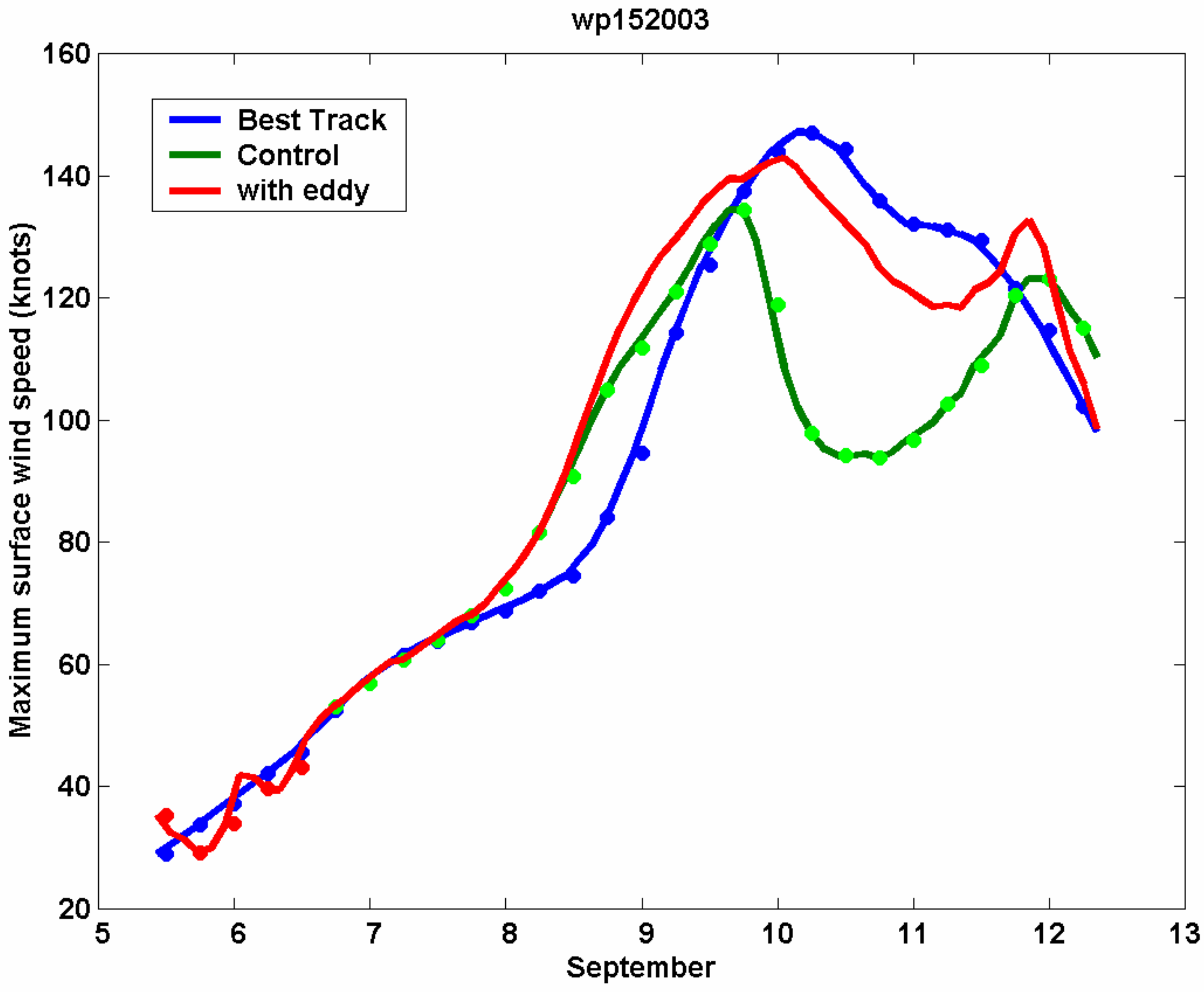

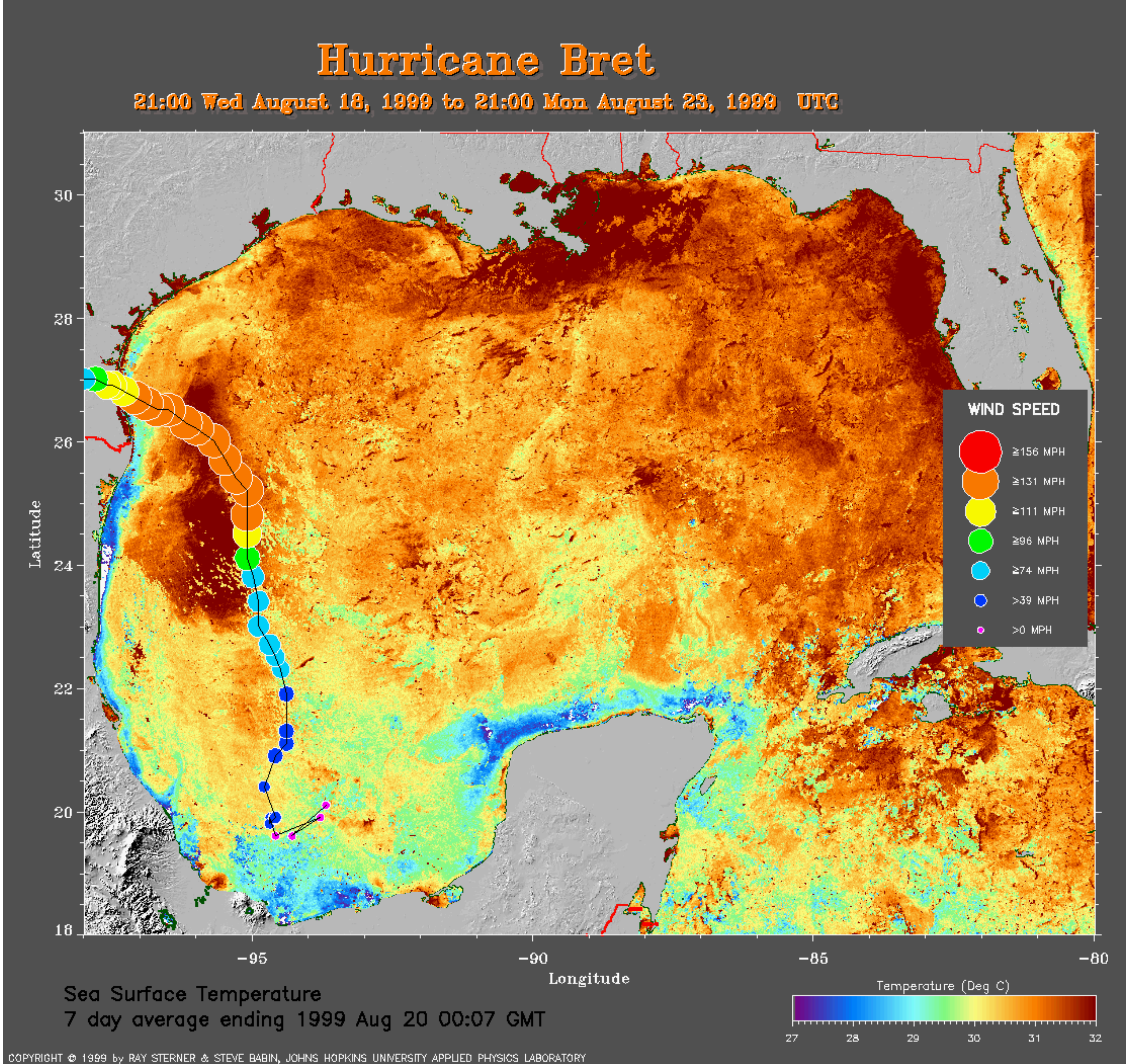
Hurricane Bret
21:00 Wed August 18, 1999 to 21:00 Mon August 23, 1999 UTC
WIND SPEED
≥156 MPH
≥131 MPH
≥111 MPH
≥96 MPH
≥74 MPH
>39 MPH
>0 MPH
30
28
26
24
22
20
18
Latitude
-95
-90
-85
-80
Longitude
Sea Surface Temperature
7 day average ending 1999 Aug 20 00:07 GMT
Temperature (Deg C)
27
28
29
30
31
32
COPYRIGHT © 1999 by RAY STERNER & STEVE BABIN, JOHNS HOPKINS UNIVERSITY APPLIED PHYSICS LABORATORY

This shows model hindcasts with and without the ocean eddy, as estimated from sea surface altimetry data:

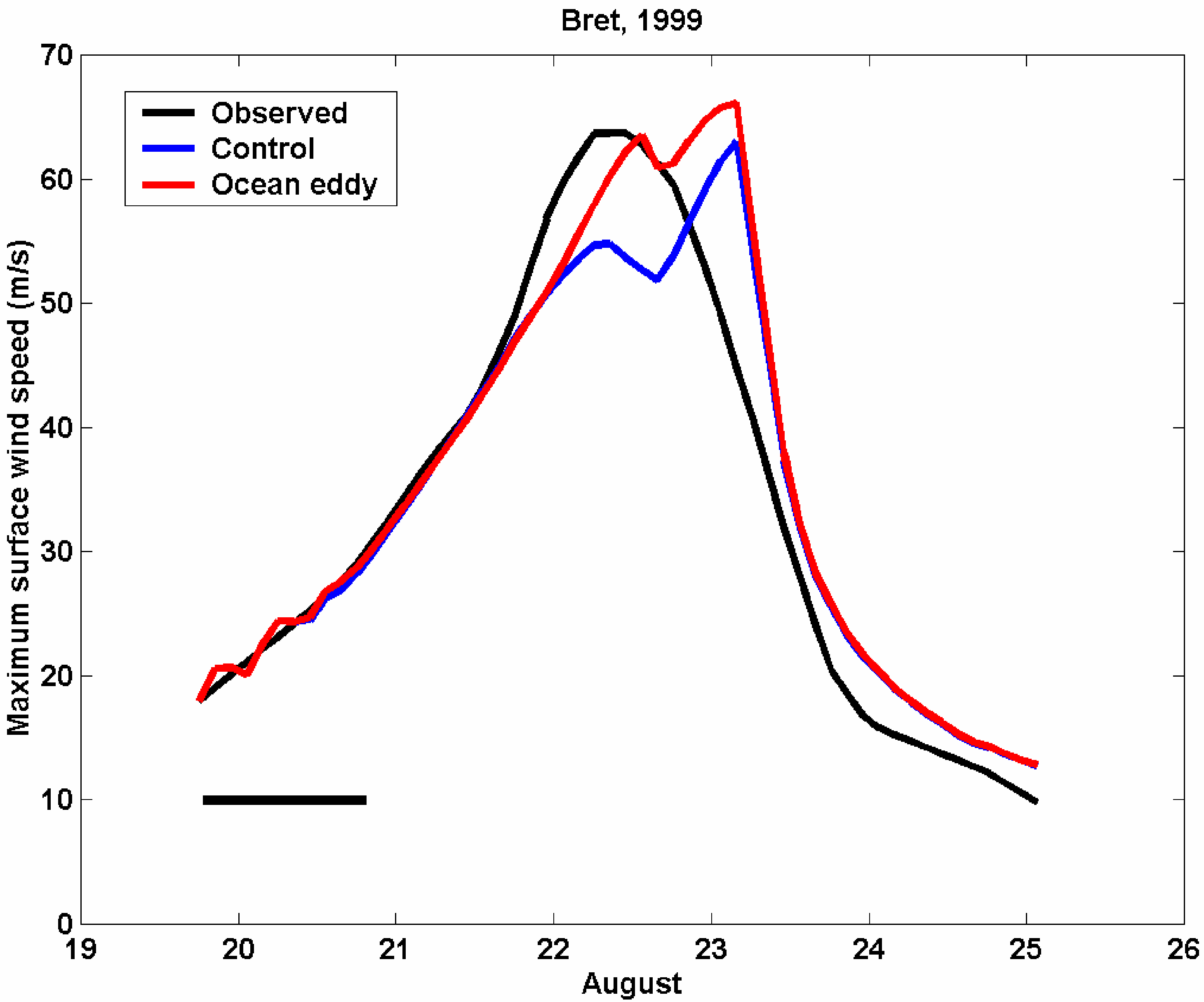

As TCs approach shore, shoaling water isolates surface mixed layer... surface cooling ceases.

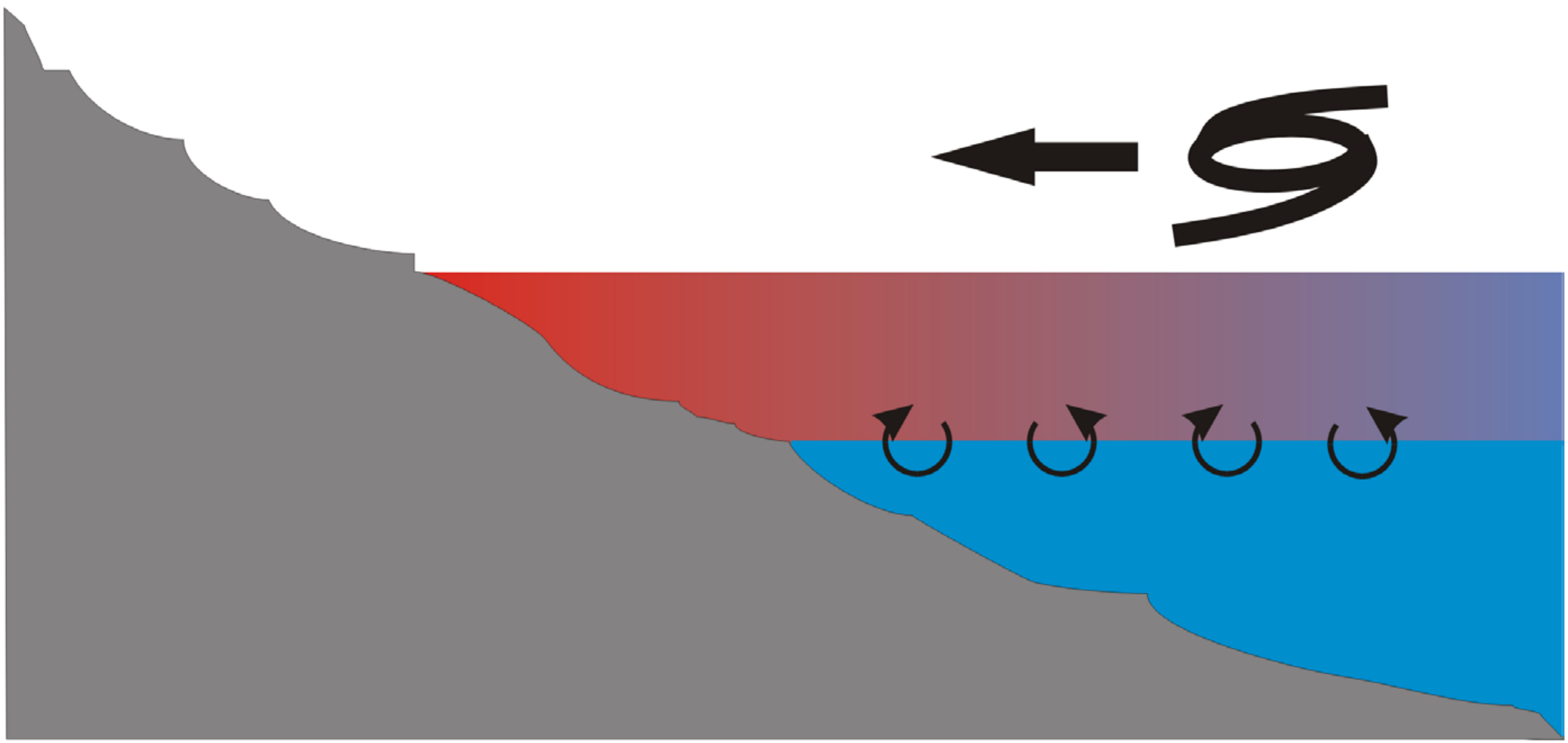

Hurricane Camille, August, 1969

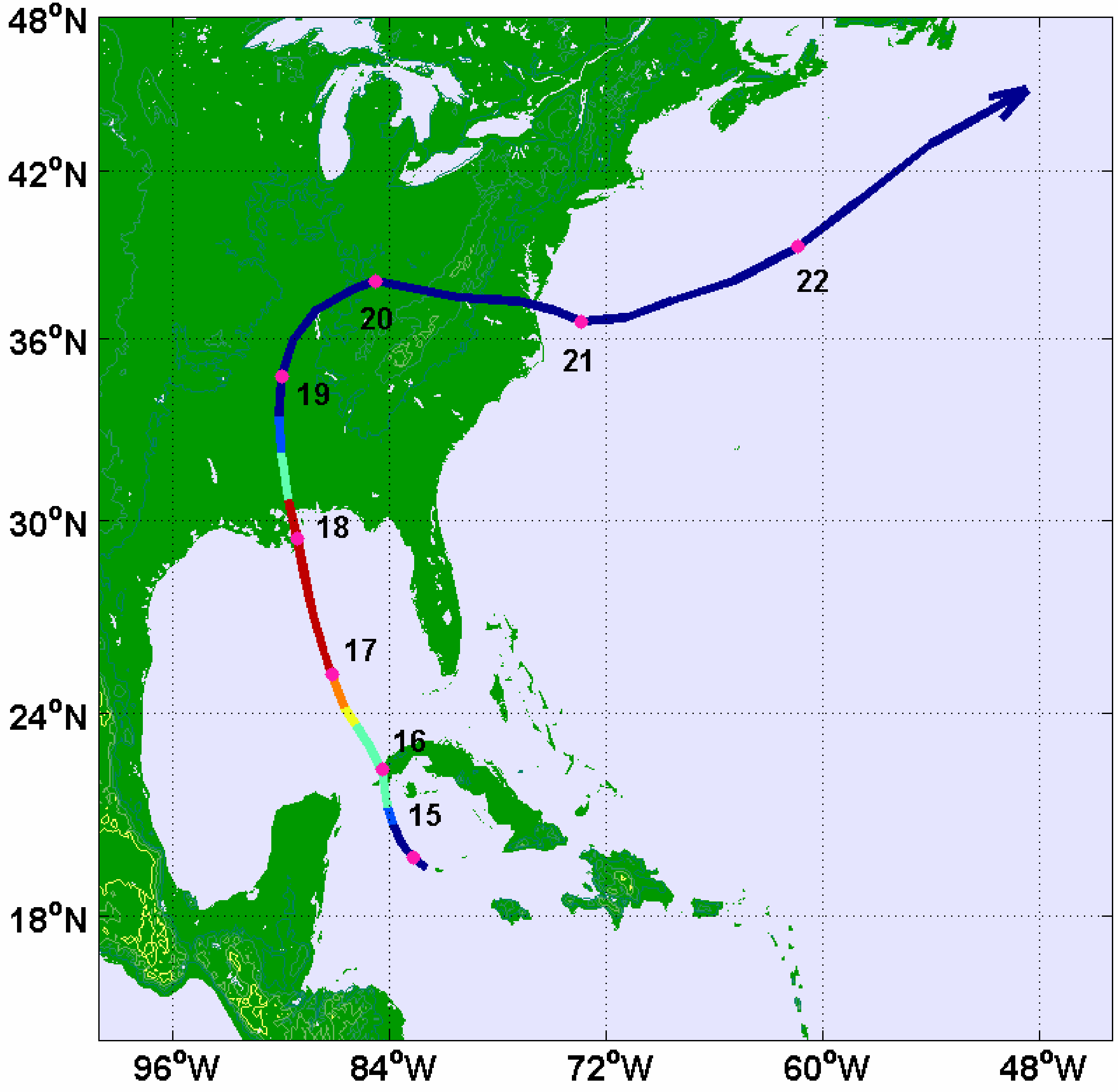

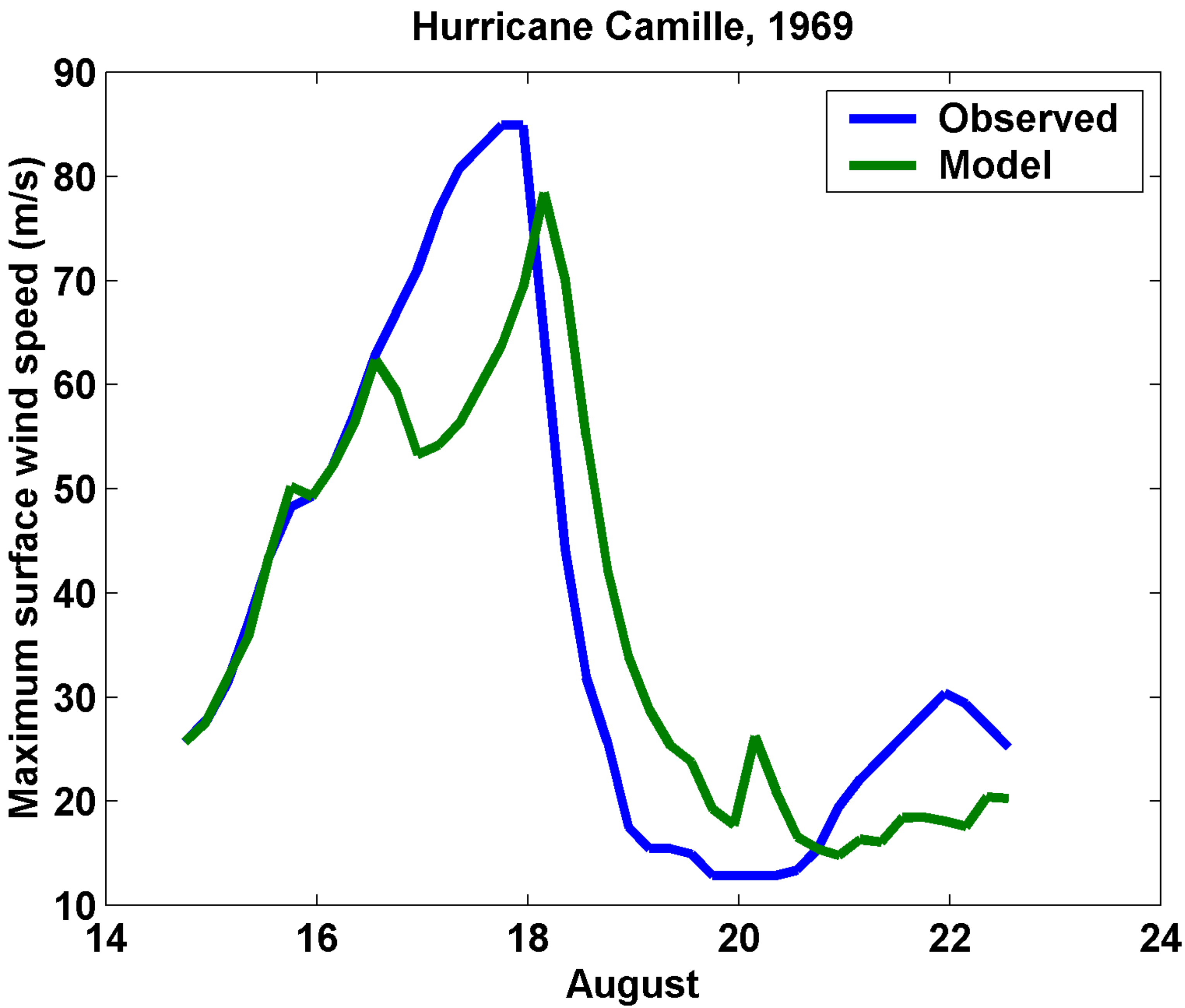
Hurricane Camille, 1969
Maximum surface wind speed (m/s)
90
80
70
60
50
40
30
20
10
14
16
18
20
22
24
August
Observed
Model

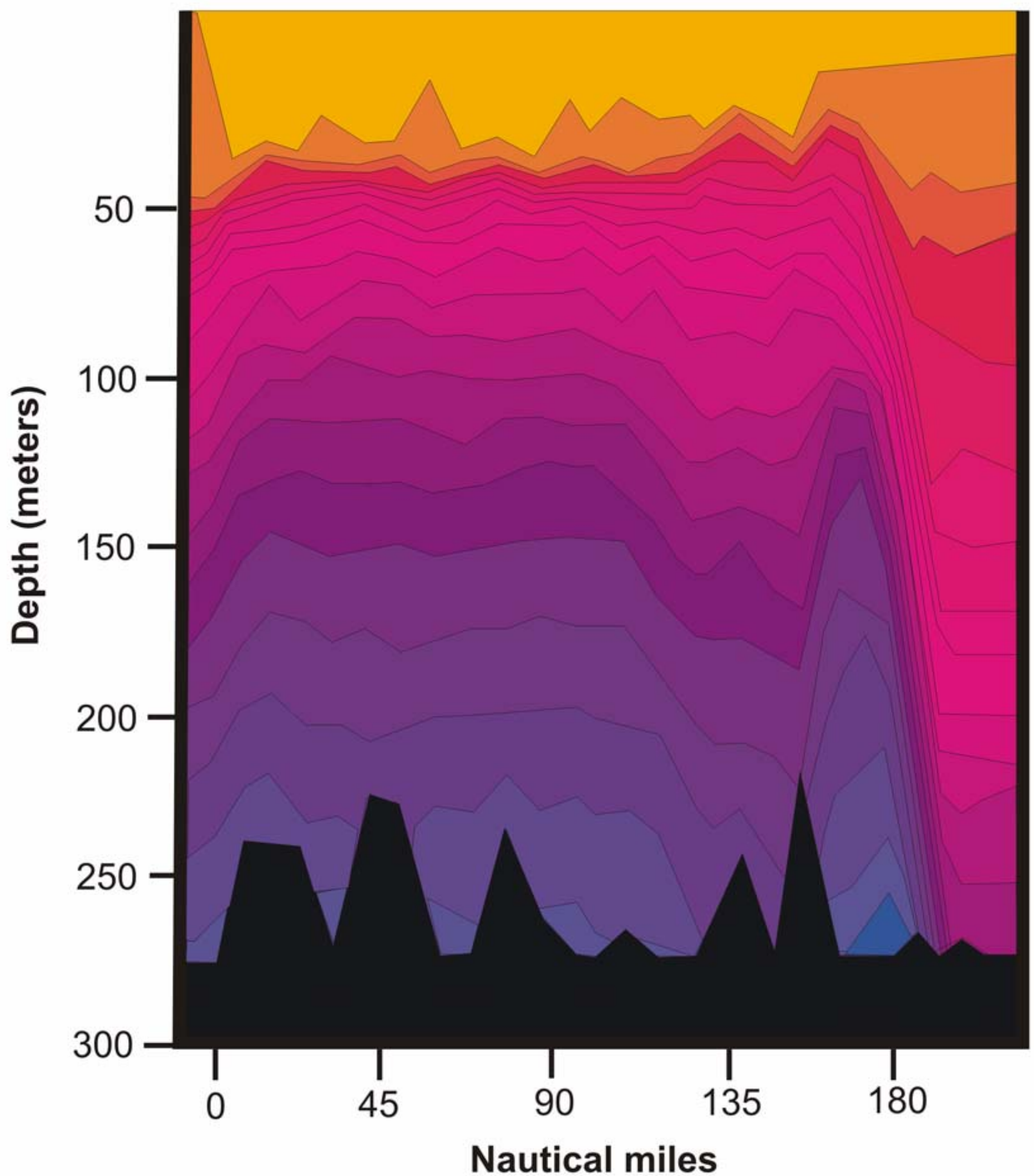
Depth (meters)
50
100
150
200
250
300
0
45
90
135
180
Nautical miles

A good simulation of Camille can only be obtained by assuming that it traveled right up the axis of the Loop Current:

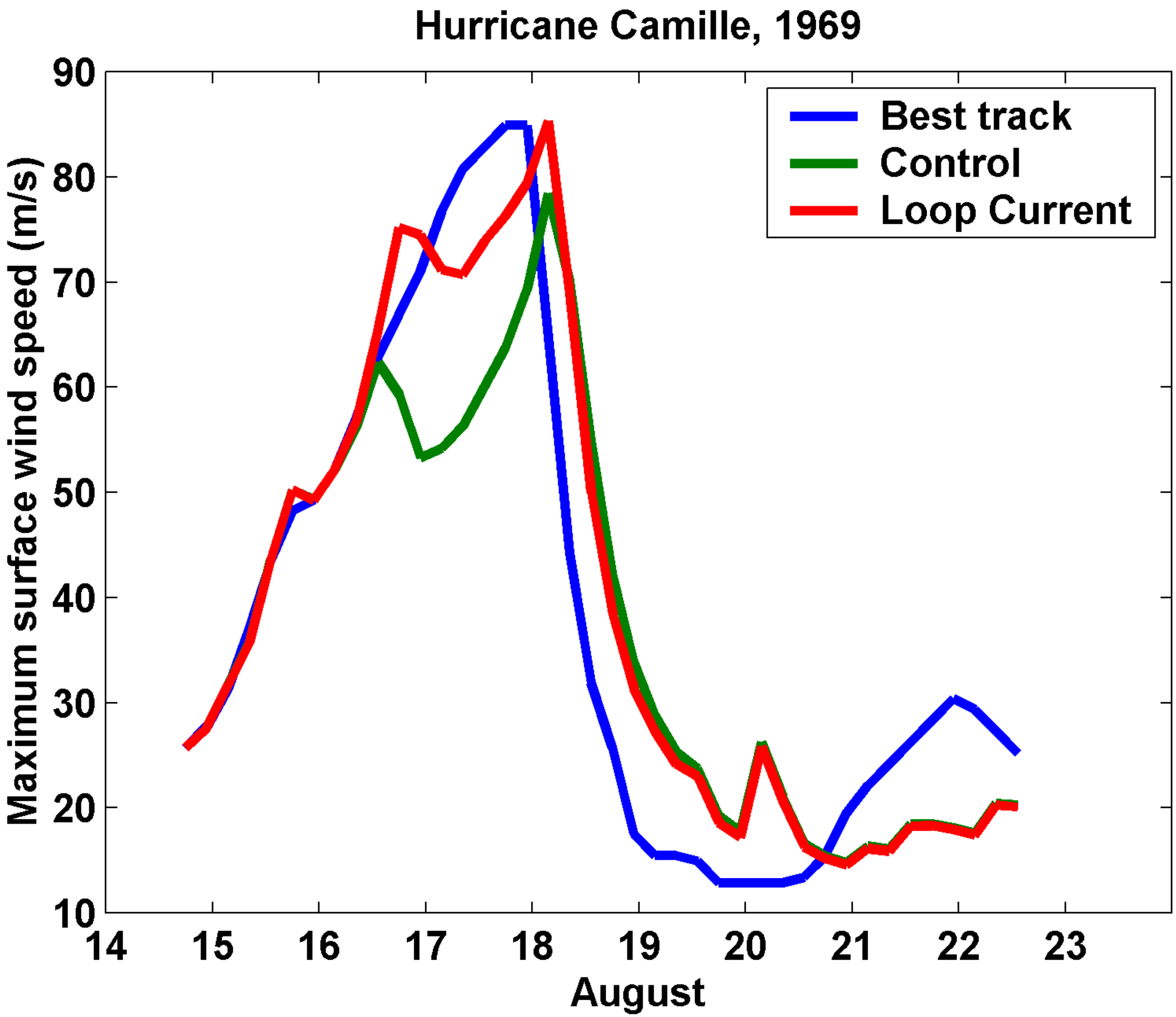

Mitch was also influenced by an ocean eddy. The red curve used TOPEX altimetry modified by de-aliasing the estimated peak amplitude:

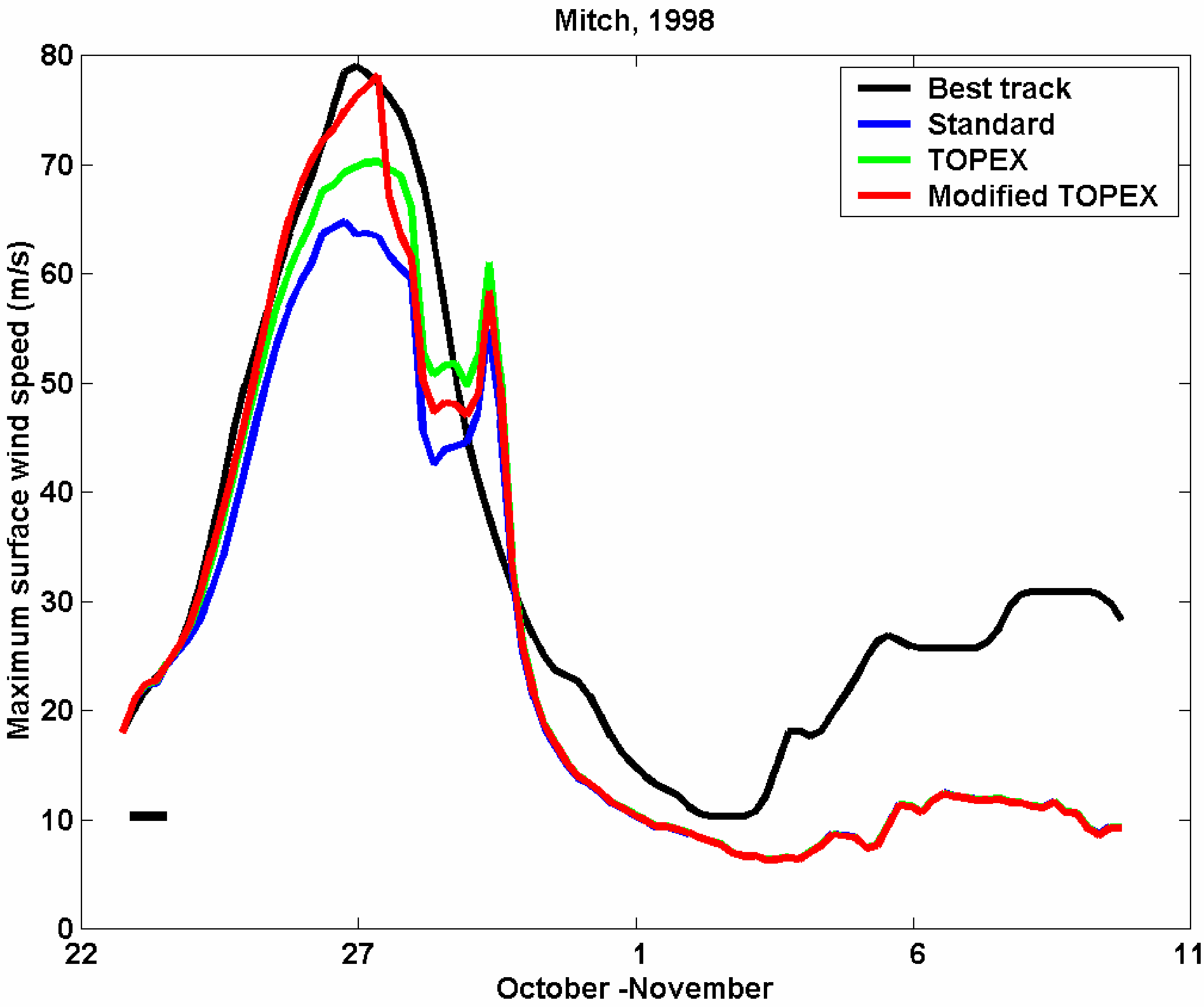

Effect of standing water can be seen in these idealized simulations of storm landfall over dry land and over swamps with indicated depths of standing water:

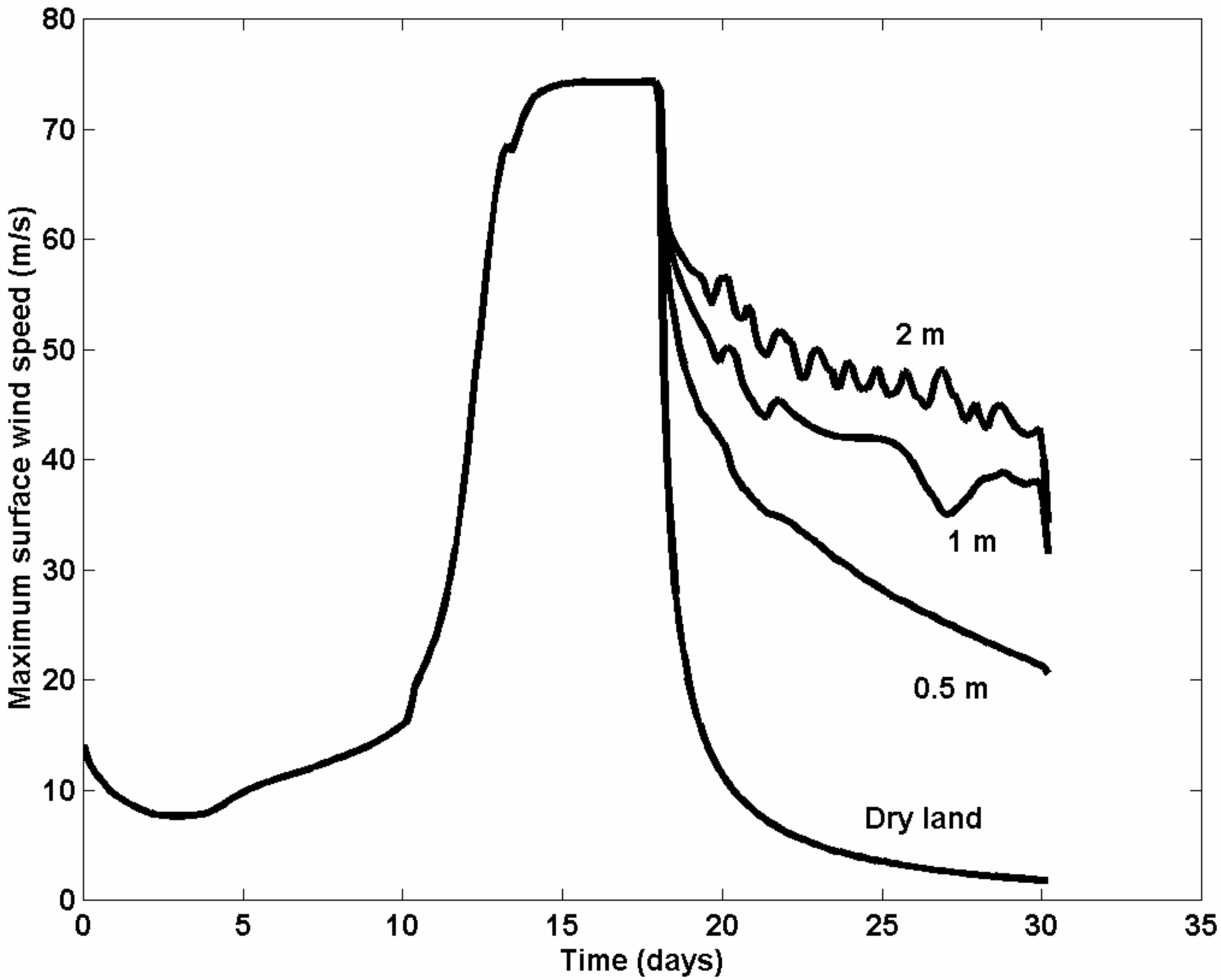

August 1992

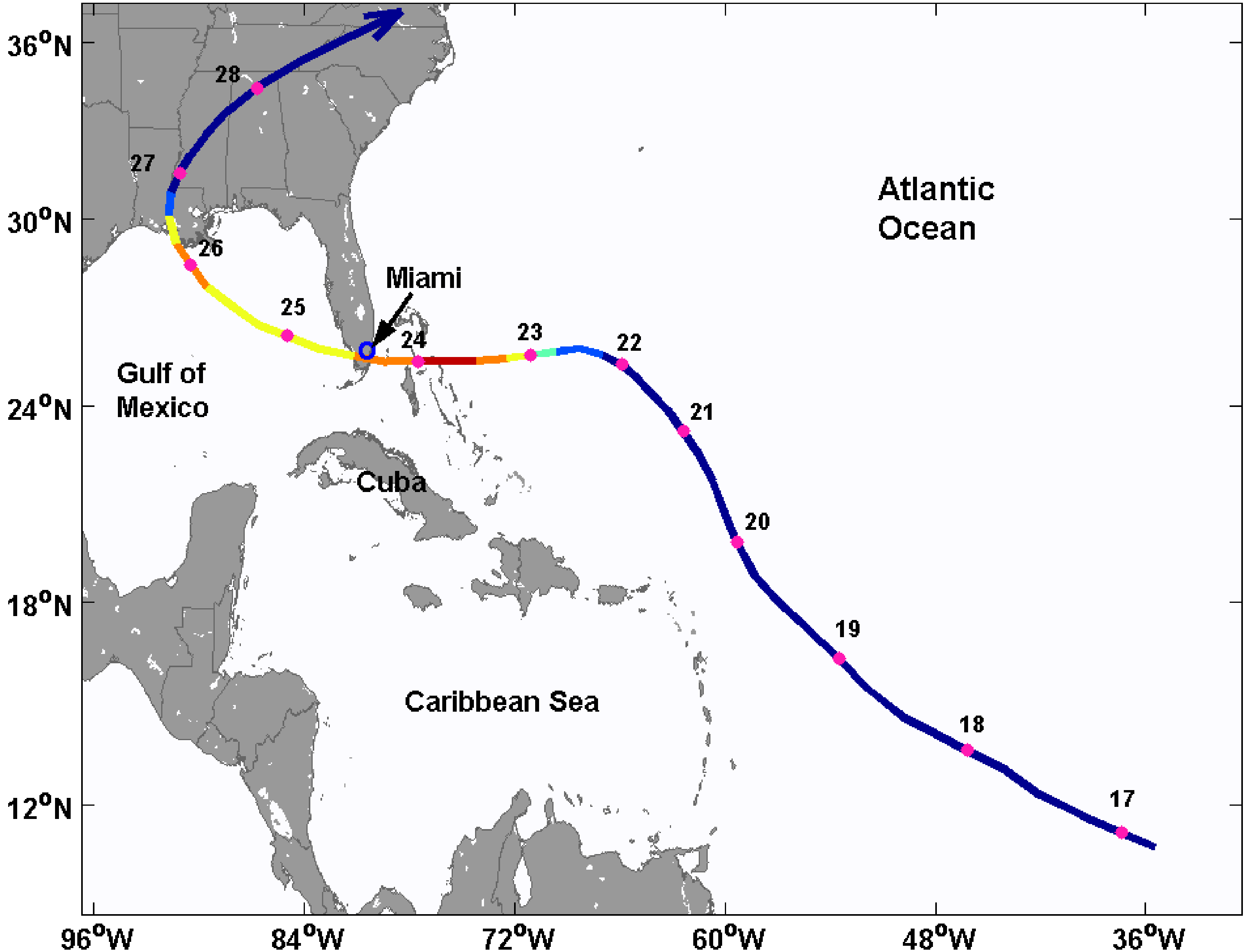
36°N
30°N
24°N
18°N
12°N
96°W
84°W
72°W
60°W
48°W
36°W
Atlantic Ocean
Gulf of Mexico
Cuba
Caribbean Sea
Miami
17
18
19
20
21
22
23
24
25
26
27
28

Hurricane Andrew, with and without the effect of the Everglades, as represented by a elevation-dependent heat exchange coefficient:

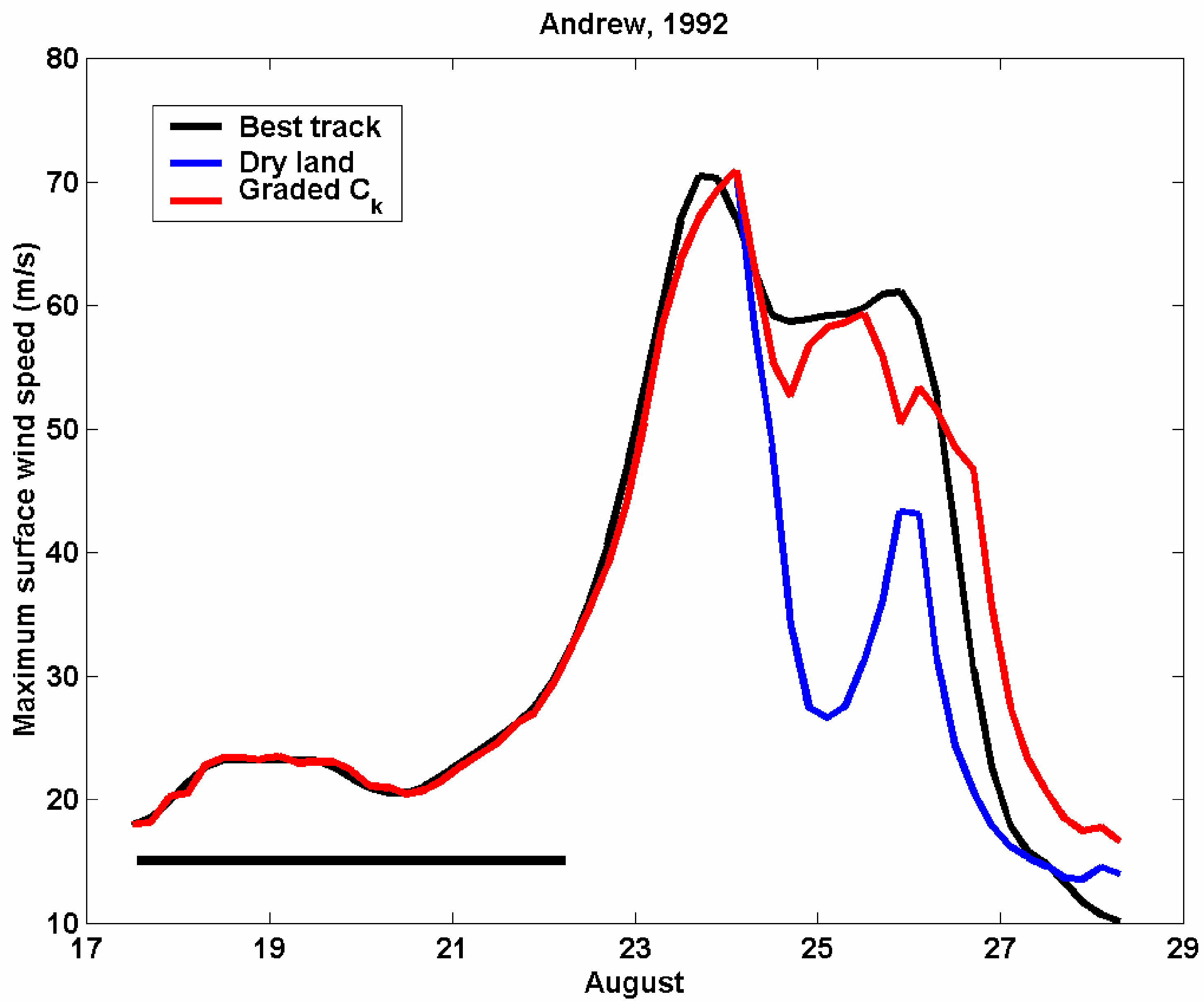

Some storms may have large internal fluctuations (e.g. Allen). CHIPS may predict the existence of these, but not their phase:

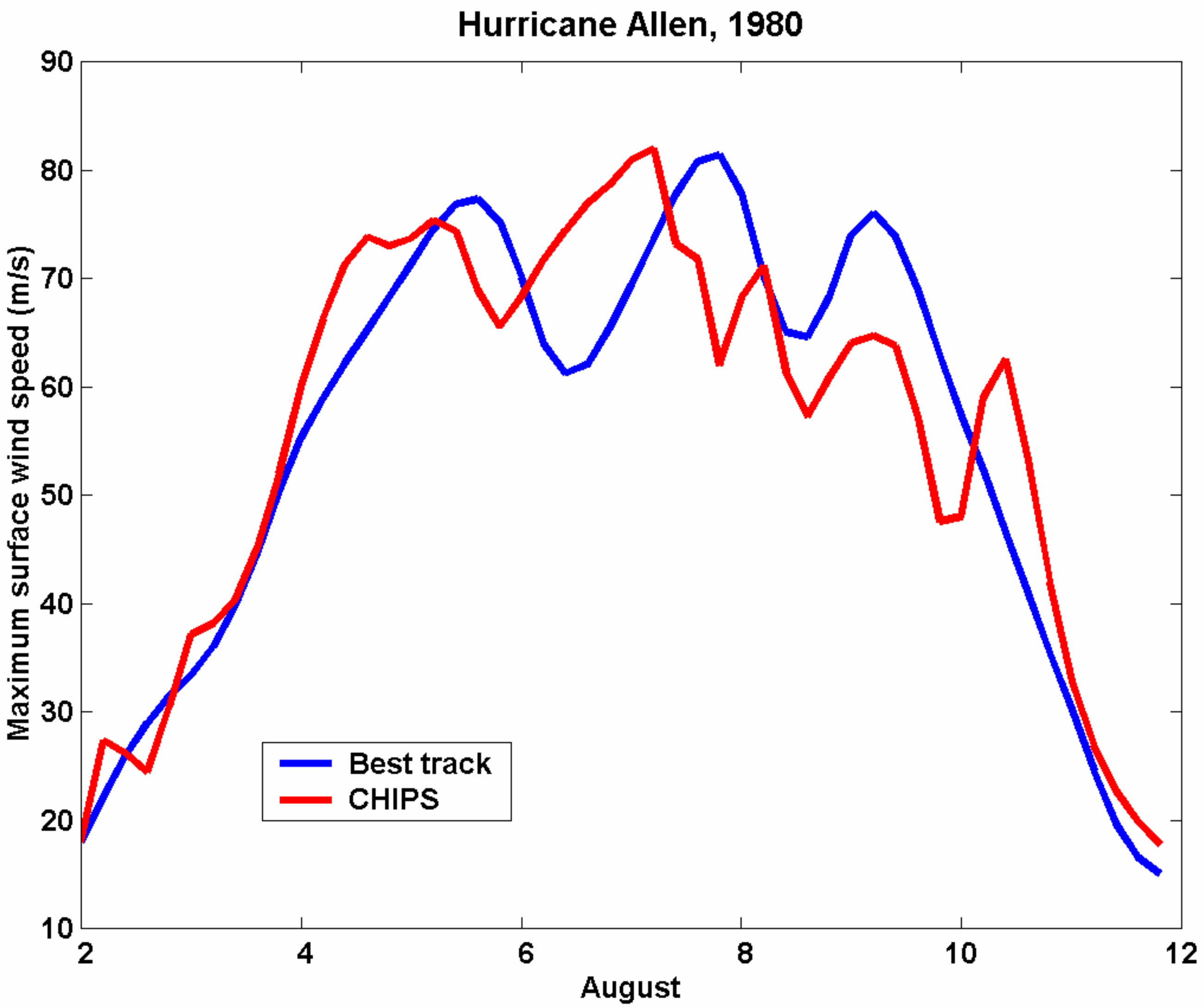

Concentric eyewalls in Hurricane Gilbert, 1988 (from Black and Willoughby, *Mon. Wea. Rev.*, 1992)

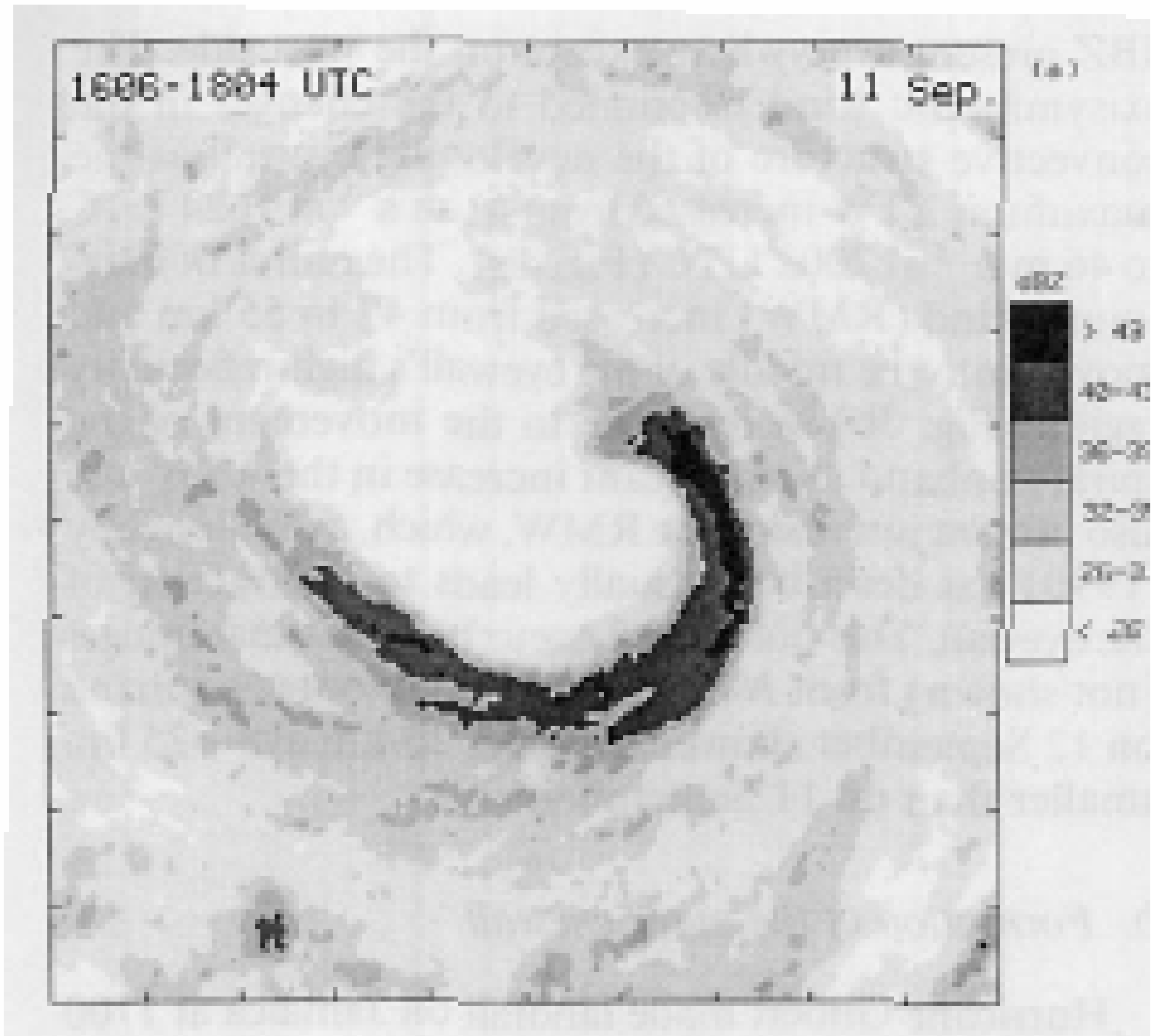

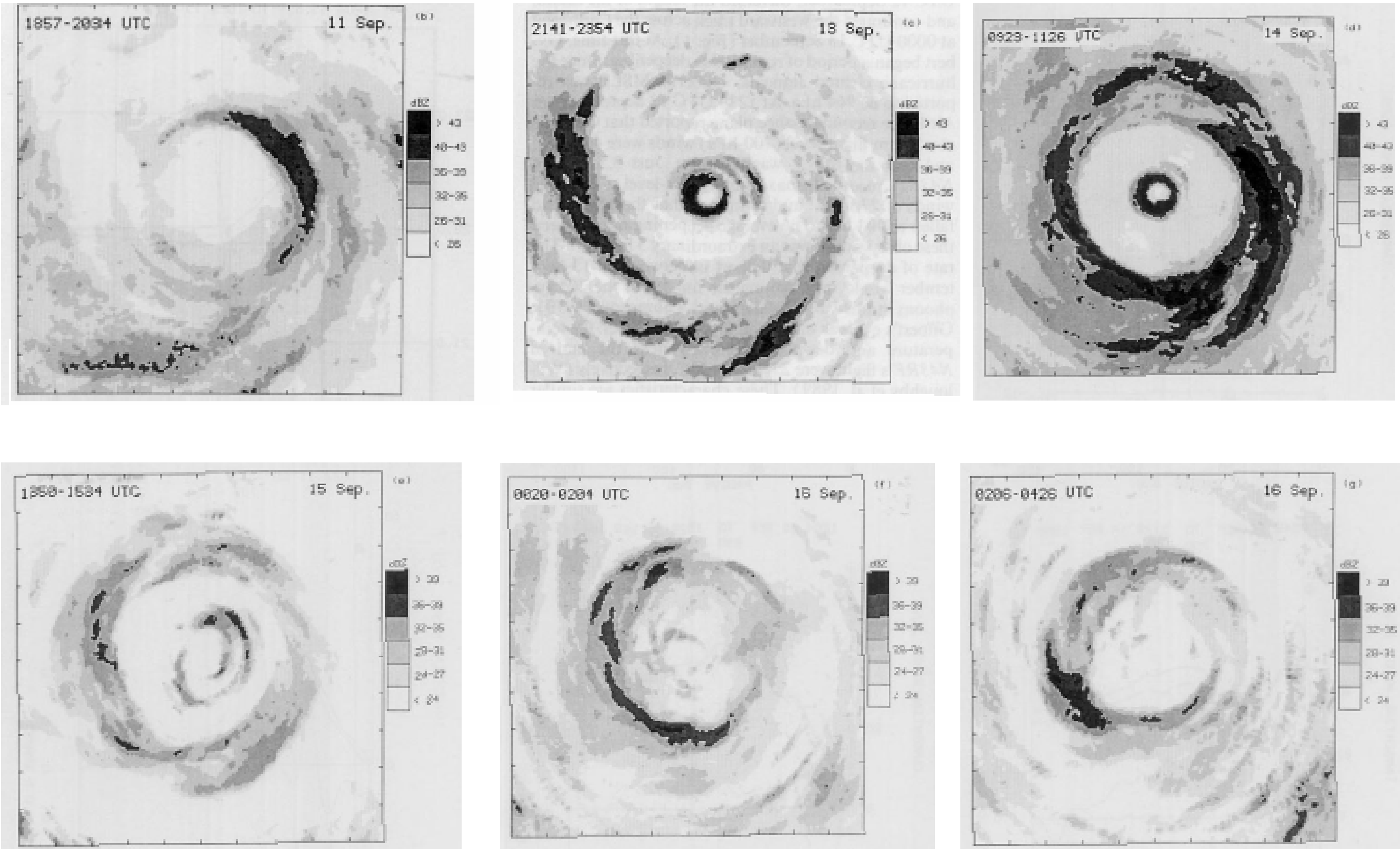
1857-2034 UTC
11 Sep.
(b)
dBZ
> 43
40-43
36-39
32-35
28-31
< 28
2141-2354 UTC
13 Sep.
(c)
0923-1126 UTC
14 Sep.
(d)
1360-1534 UTC
15 Sep.
(e)
> 39
36-39
32-35
28-31
24-27
< 24
0020-0204 UTC
16 Sep.
(f)
0206-0426 UTC
16 Sep.
(g)

Solid: Beginning of fllight; Dashed: End of flight; Dotted: Change/6hr

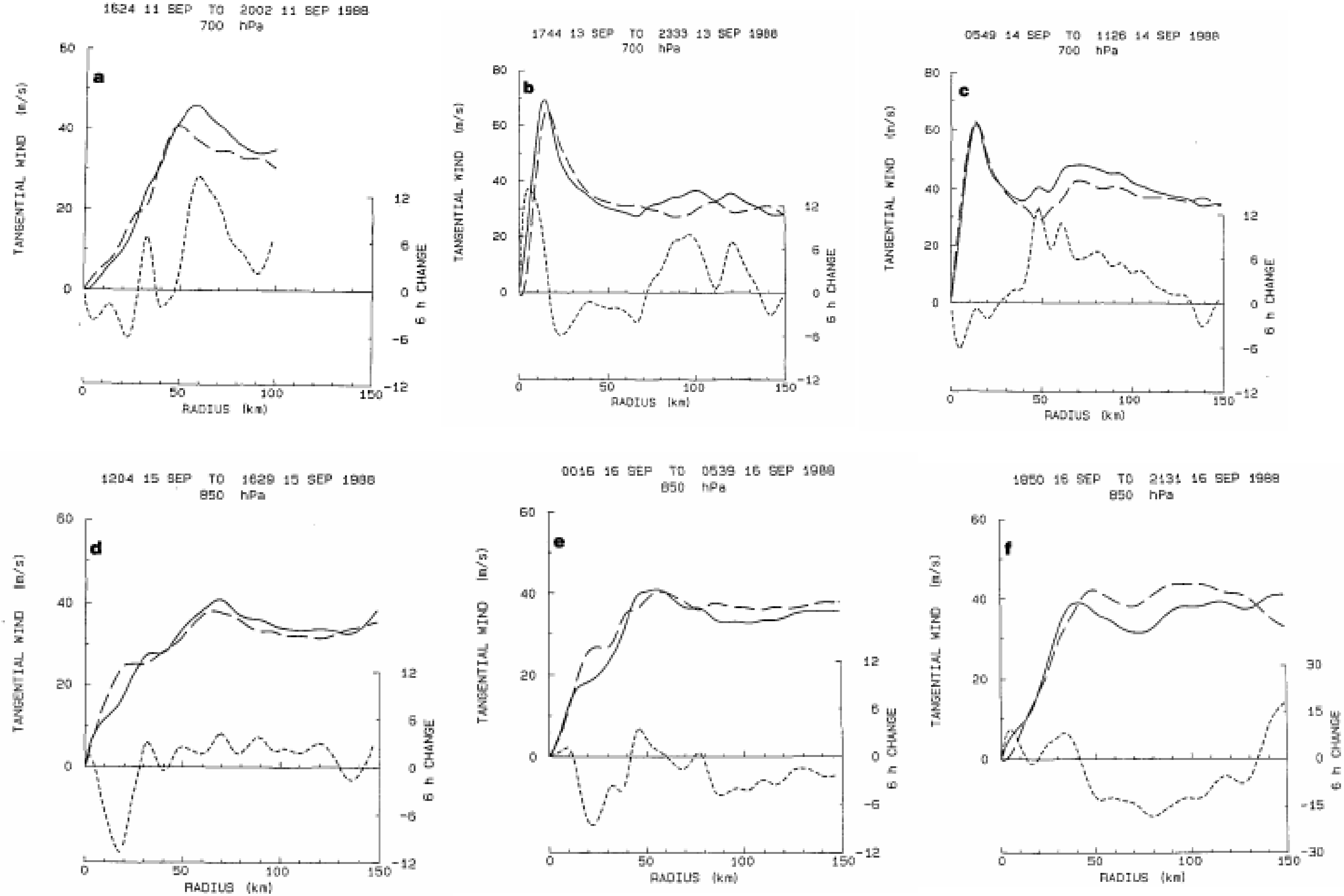

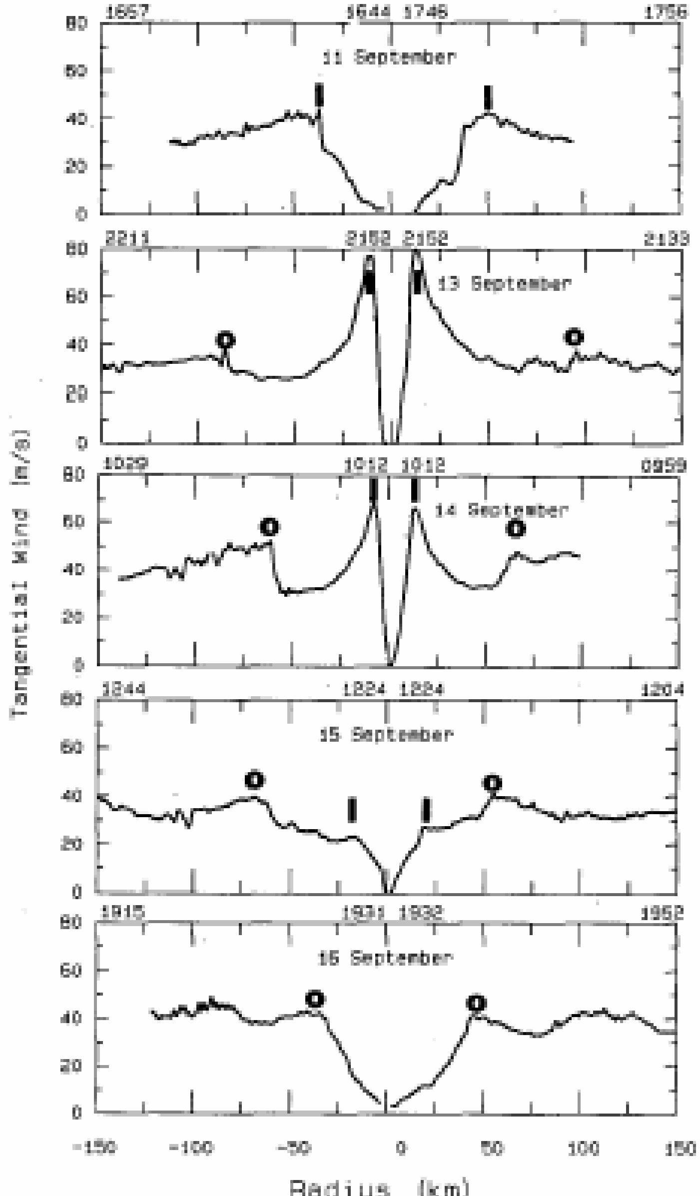

FIG. 7. Flight-level tangential wind speed from south–north traverses through the center of Hurricane Gilbert for five of the six reconnaissance flights listed in Table 1. Bold *I*'s and *O*'s denote the location of the inner- and outer-eyewall wind maxima, respectively. Times at the beginning and end of each radial pass are plotted at the top of the panels.

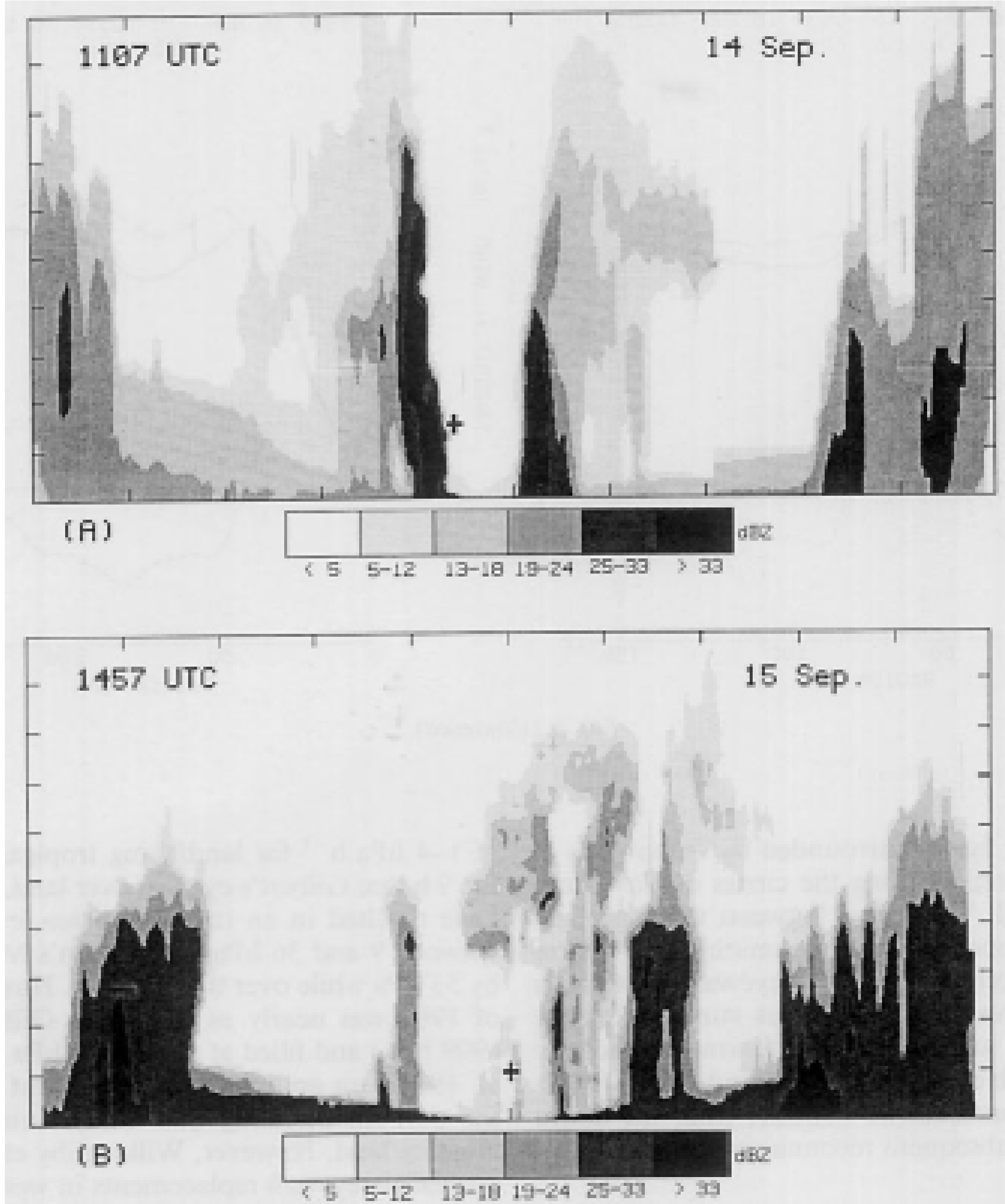

FIG. 5. Vertical cross sections of radar reflectivity from single sweeps of the tail radar while the aircraft was near the center of Hurricane Gilbert: (a) 1107 UTC 14 September and (b) 1457 UTC 15 September. West is on the left and east on the right in both (a) and (b). The domain is 160×15 km^2, with tic marks at 16 and 1.5 km in the horizontal and vertical, respectively. The plus sign in the lower center of the images indicates the aircraft's location, and the reflectivity scale is at the bottom.

Environmental factors critical to intensity prediction:

- Potential intensity along track
- Upper ocean thermal structure
- Environmental wind shear
- Bathymetry
- Land surface characteristics

Major sources of uncertainty:

- Uncertain forecasts of vertical shear
- Shear reduces predictability
- Little real-time knowledge of upper ocean thermal structure
- Low predictability of internal variability

Hurricanes and Climate

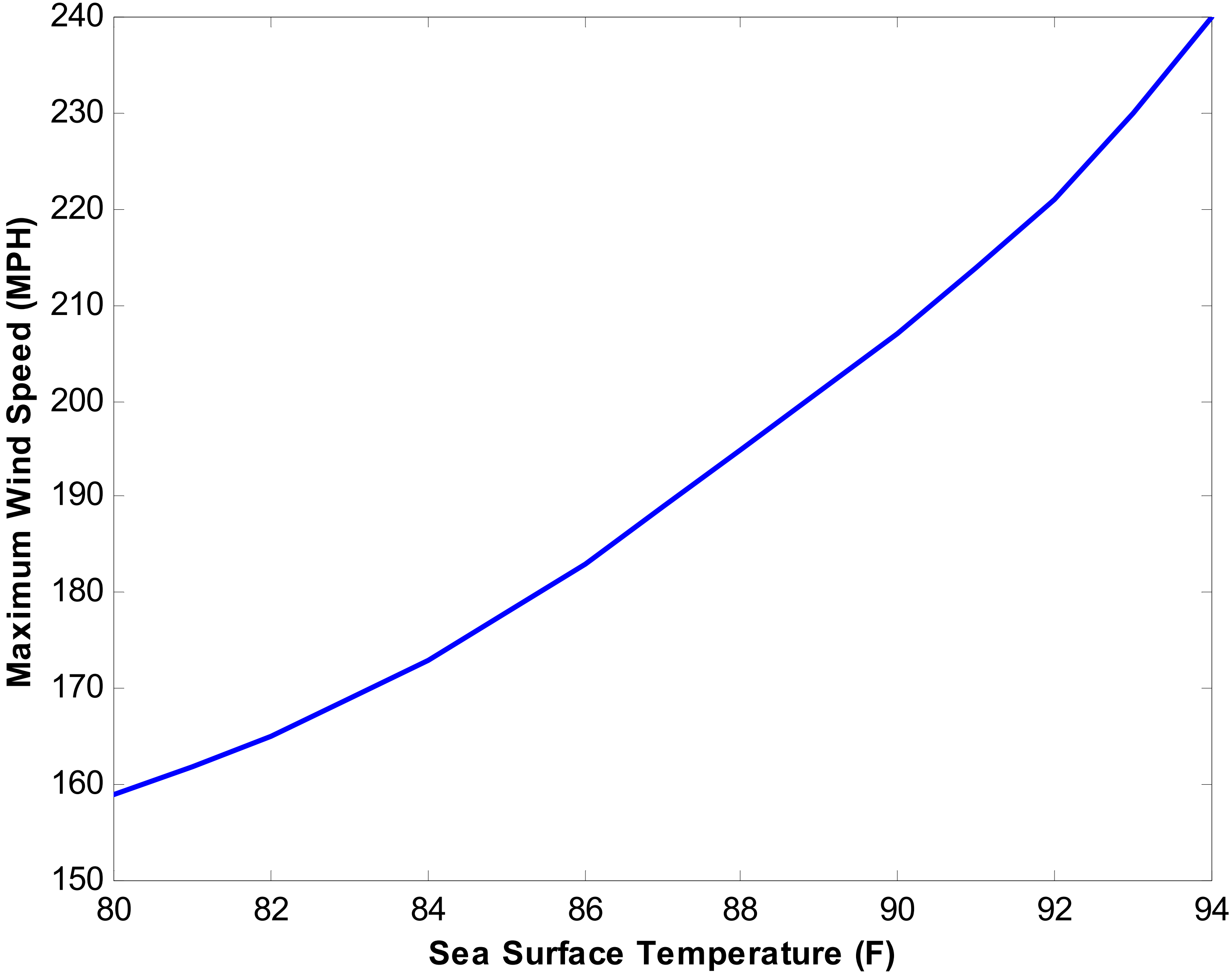
Maximum Wind Speed (MPH)
150
160
170
180
190
200
210
220
230
240
80
82
84
86
88
90
92
94
Sea Surface Temperature (F)

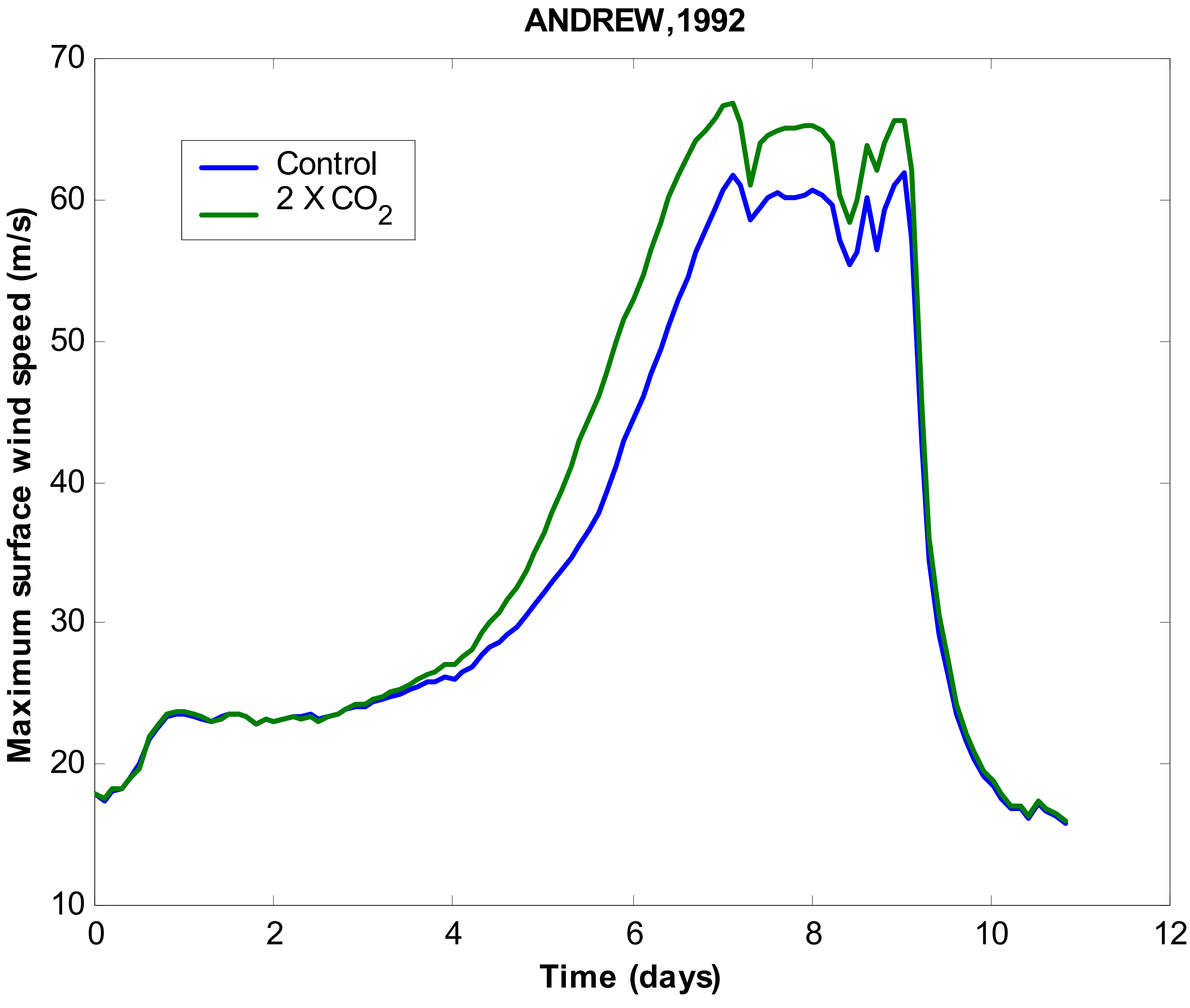
ANDREW,1992
Control
2 X CO2
Maximum surface wind speed (m/s)
Time (days)
70
60
50
40
30
20
10
0
2
4
6
8
10
12

Empirical Index:

$$I = \left|10^5 \eta\right|^{3/2} \left(\frac{\mathcal{H}}{50}\right)^3 \left(\frac{V_{pot}}{70}\right)^3 \left(1 + 0.1 V_{shear}\right)^{-2},$$

$\eta \equiv 850\, hPa\ absolute\ vorticity\ (s^{-1}),$

$V_{pot} \equiv Potential\ wind\ speed\ (ms^{-1}),$

$\mathcal{H} \equiv 600\, mb\ relative\ humidity\ (\%),$

$V_{shear} \equiv \left|\mathbf{V}_{850} - \mathbf{V}_{250}\right|\ \ (ms^{-1}).$

Atlantic

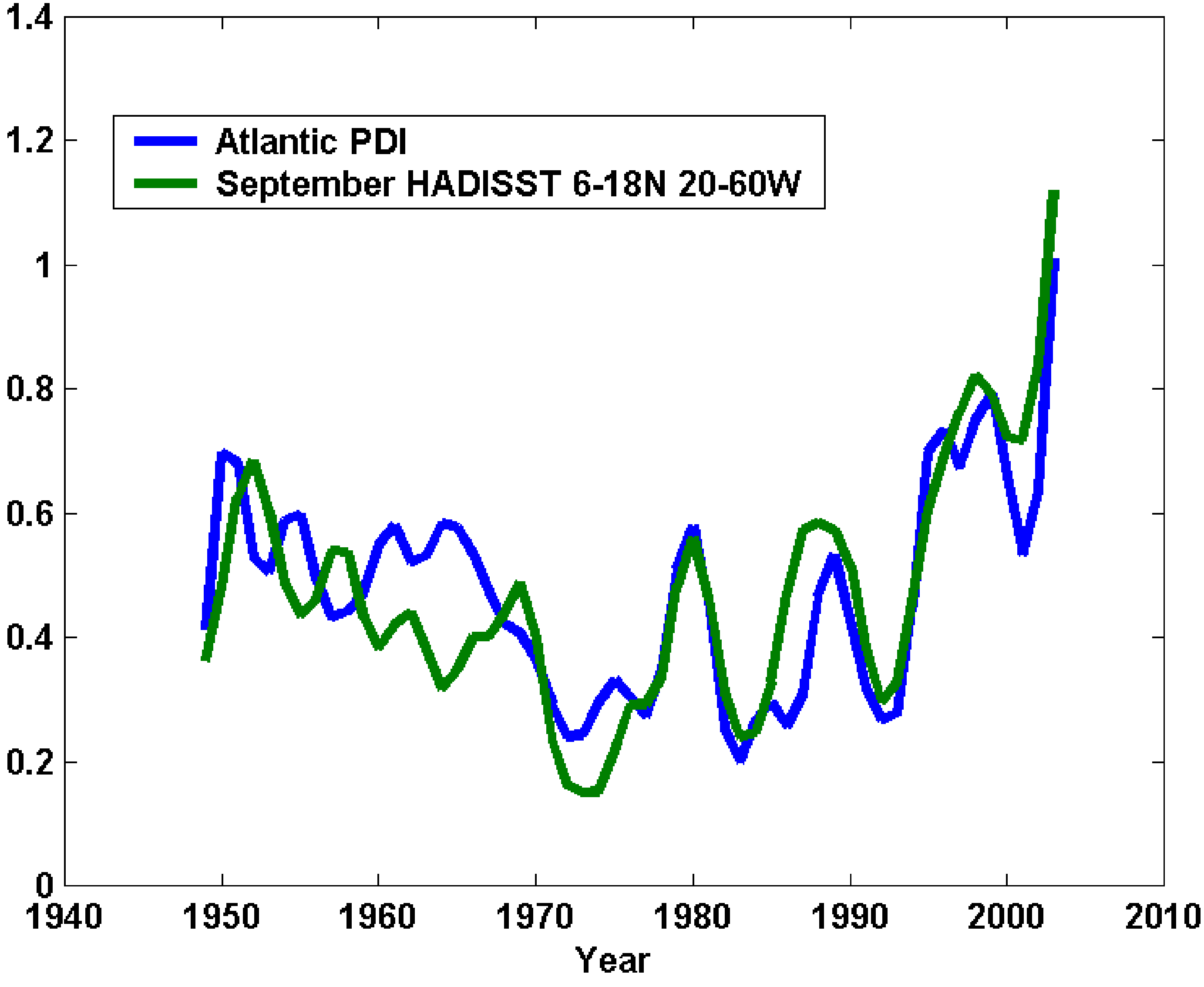

1.4
1.2
1
0.8
0.6
0.4
0.2
0
1940
1950
1960
1970
1980
1990
2000
2010
Year
Atlantic PDI
September HADISST 6-18N 20-60W

Western North Pacific

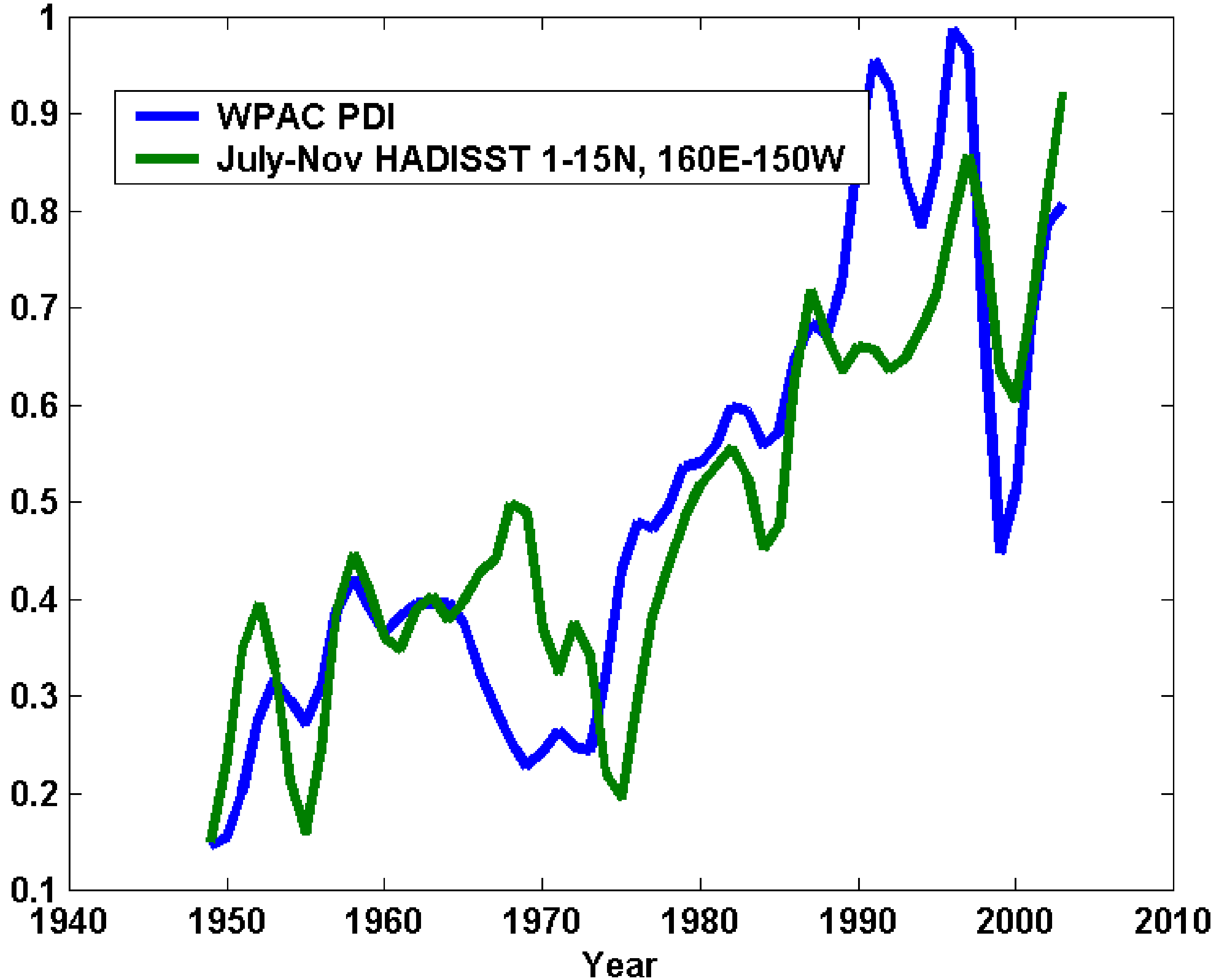

Paleotempestology

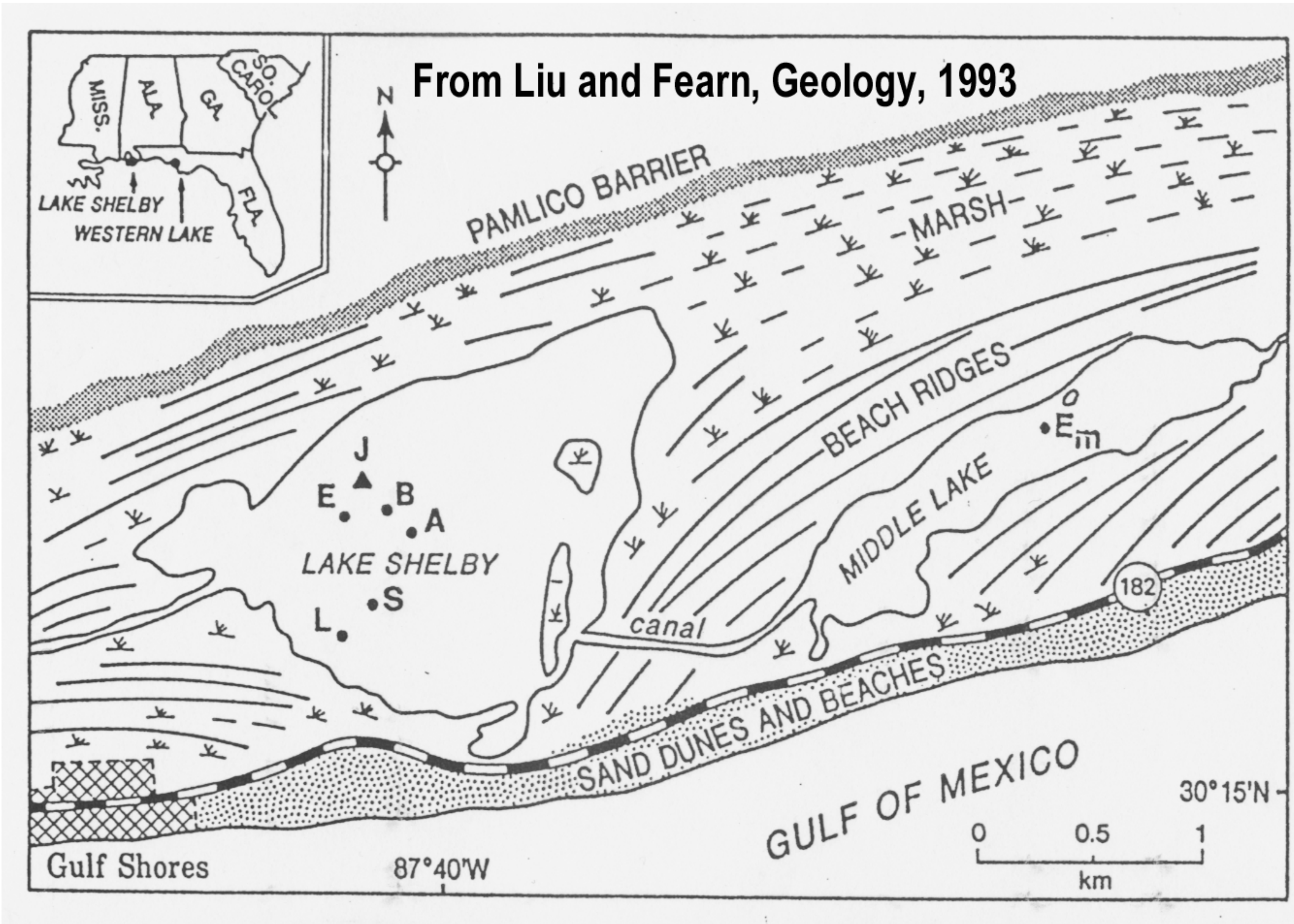

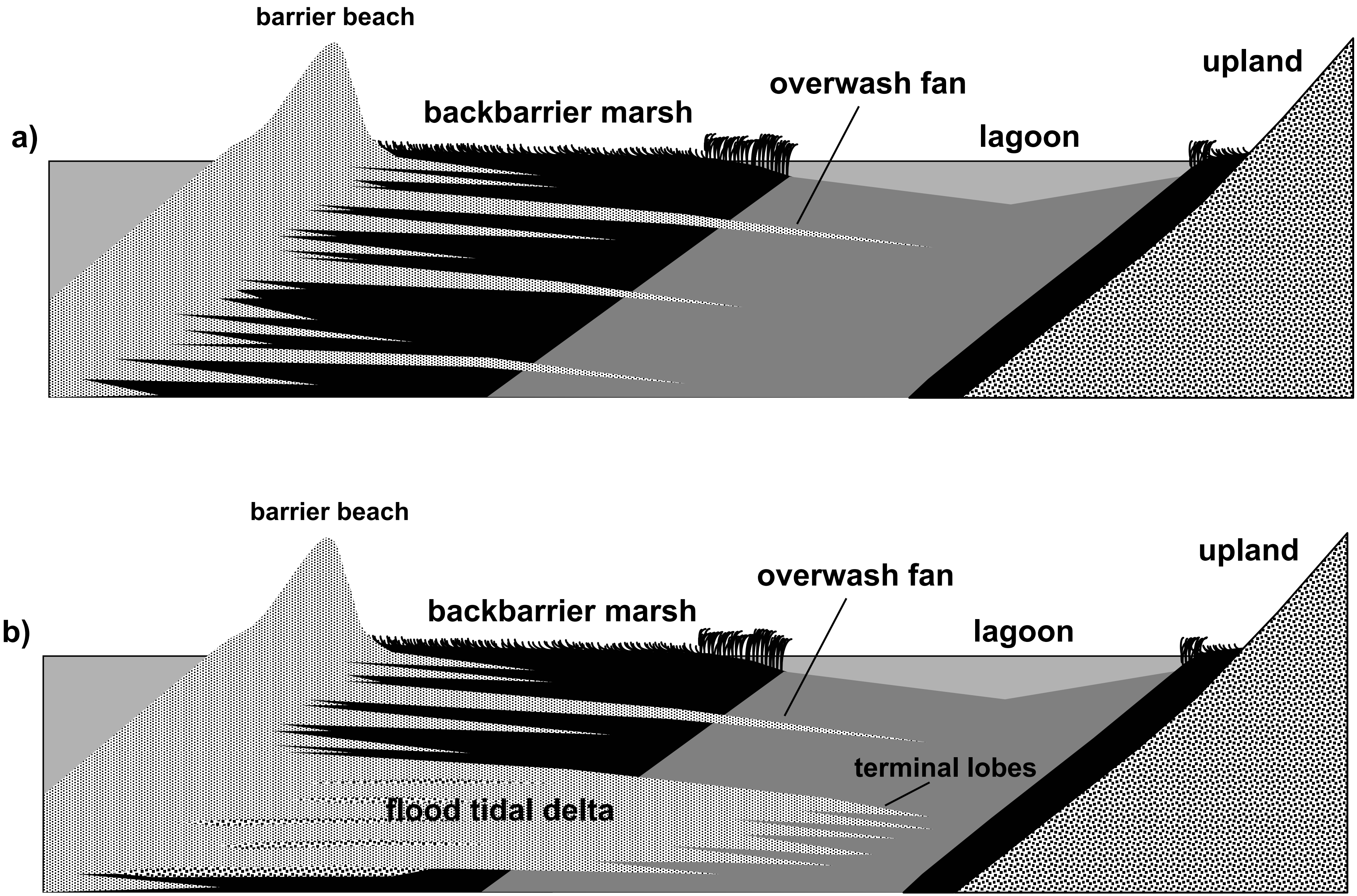

Donnelly – Figure 2

Work of Liu, 2000 (Science News)

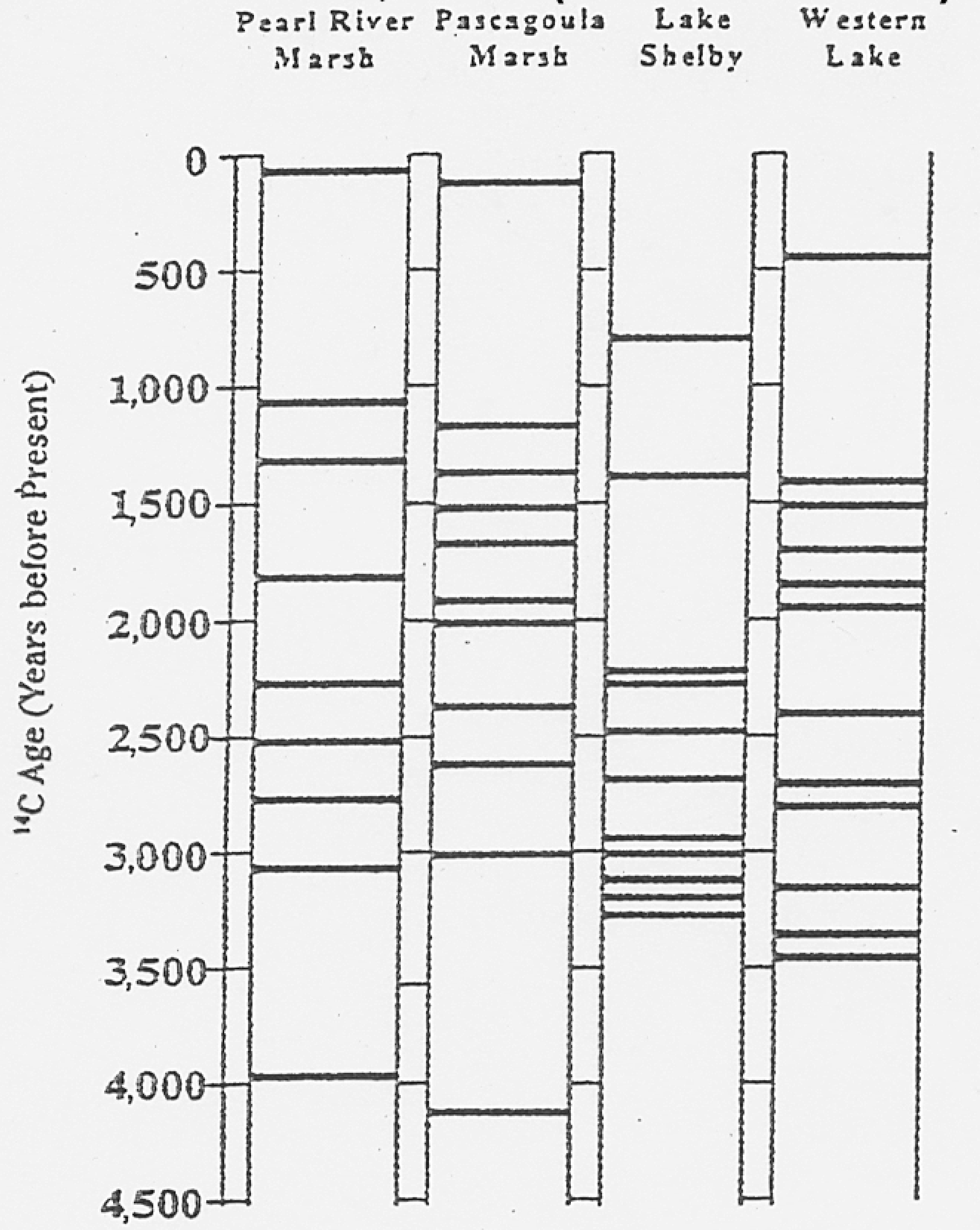

Whale Beach

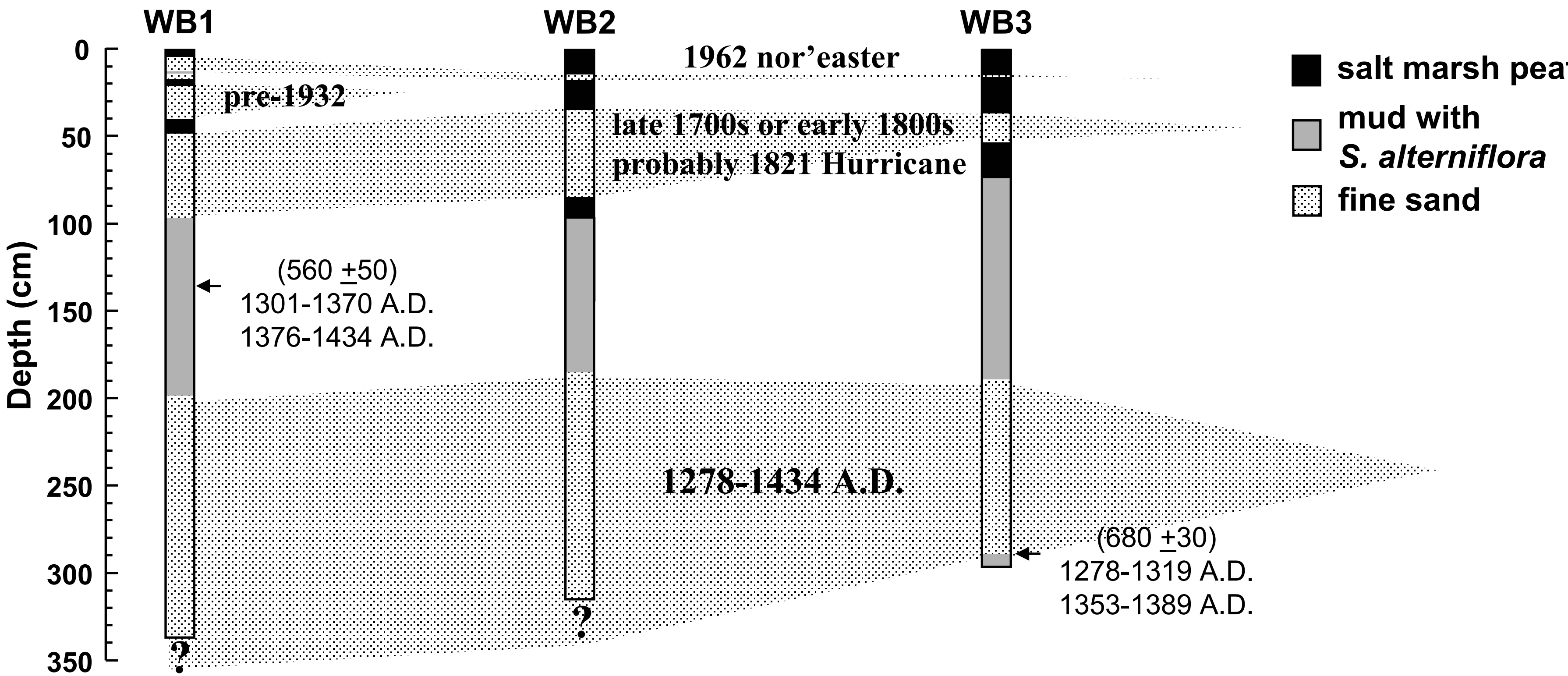

Jeffrey Donnelly, WHOI

Beach Deposits

Nott and Hayne, 2001

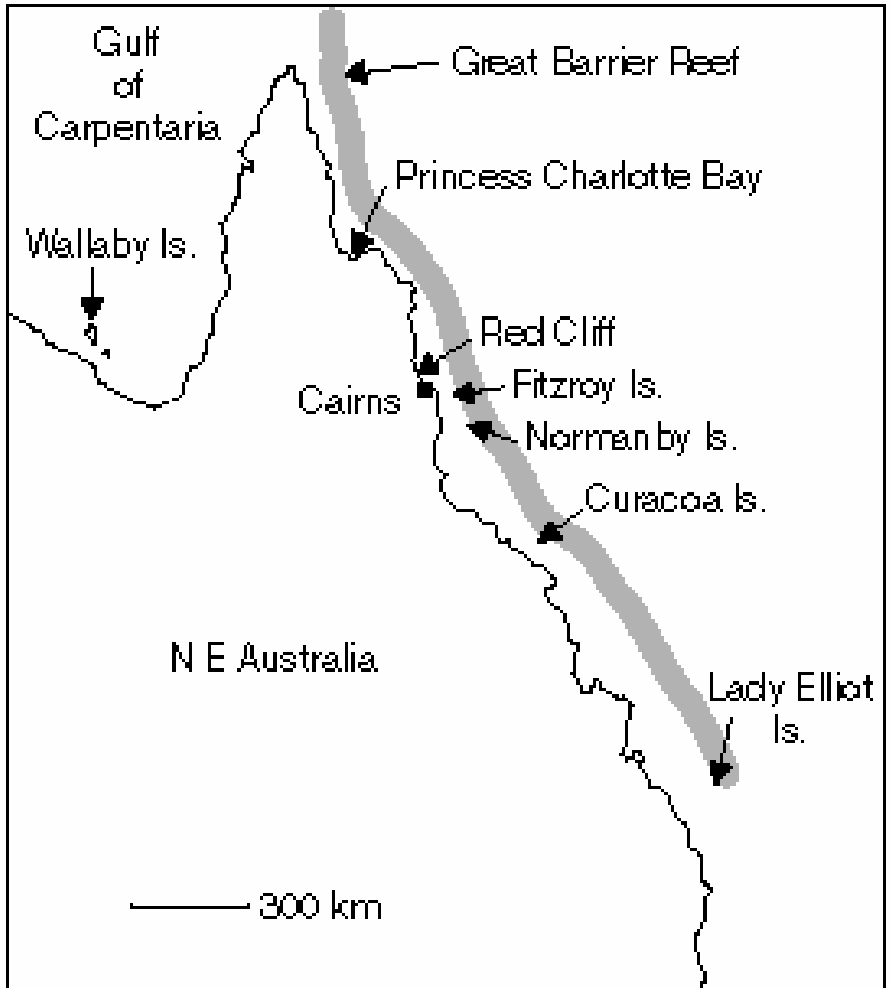

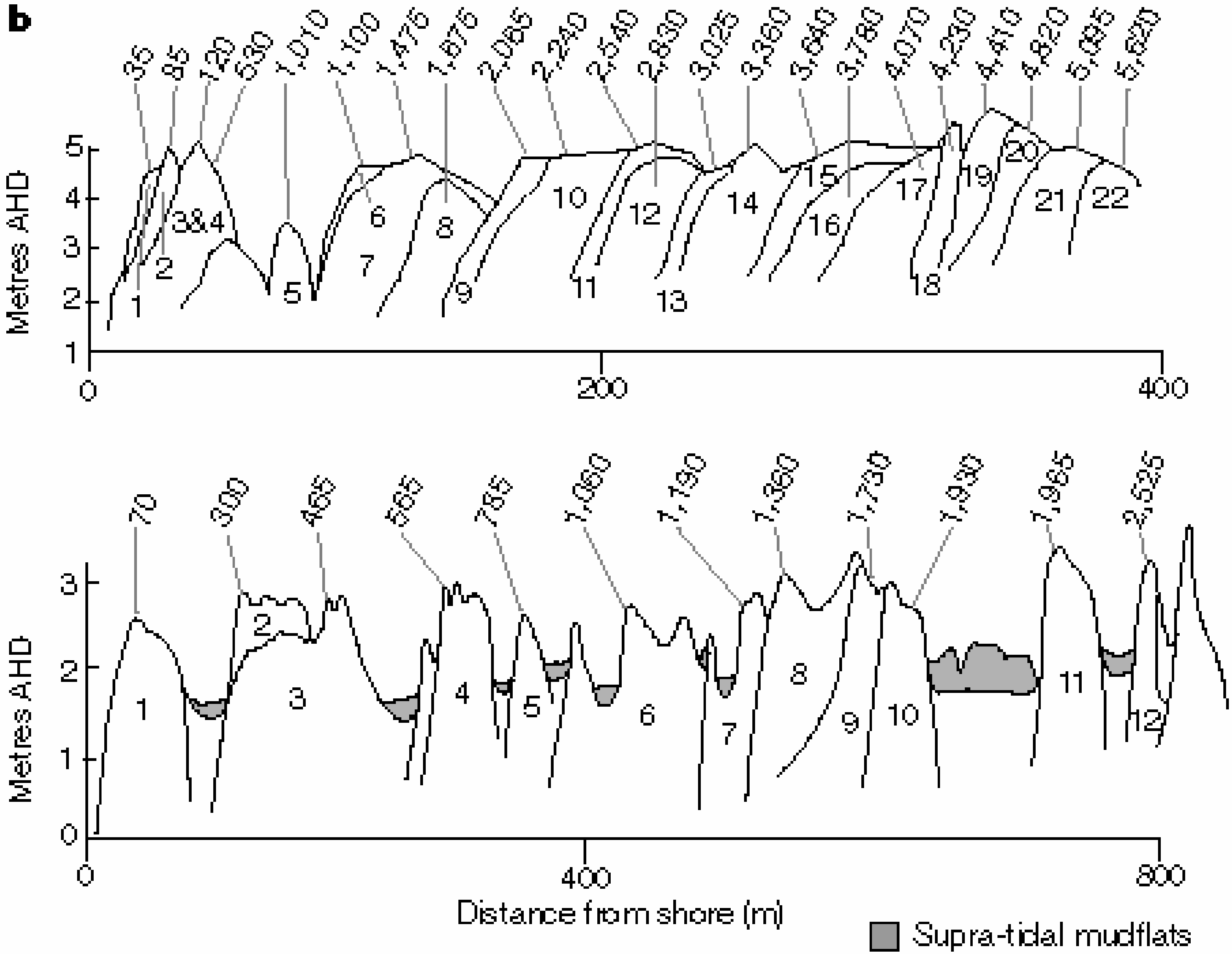
b
Metres AHD
Metres AHD
Distance from shore (m)
Supra-tidal mudflats

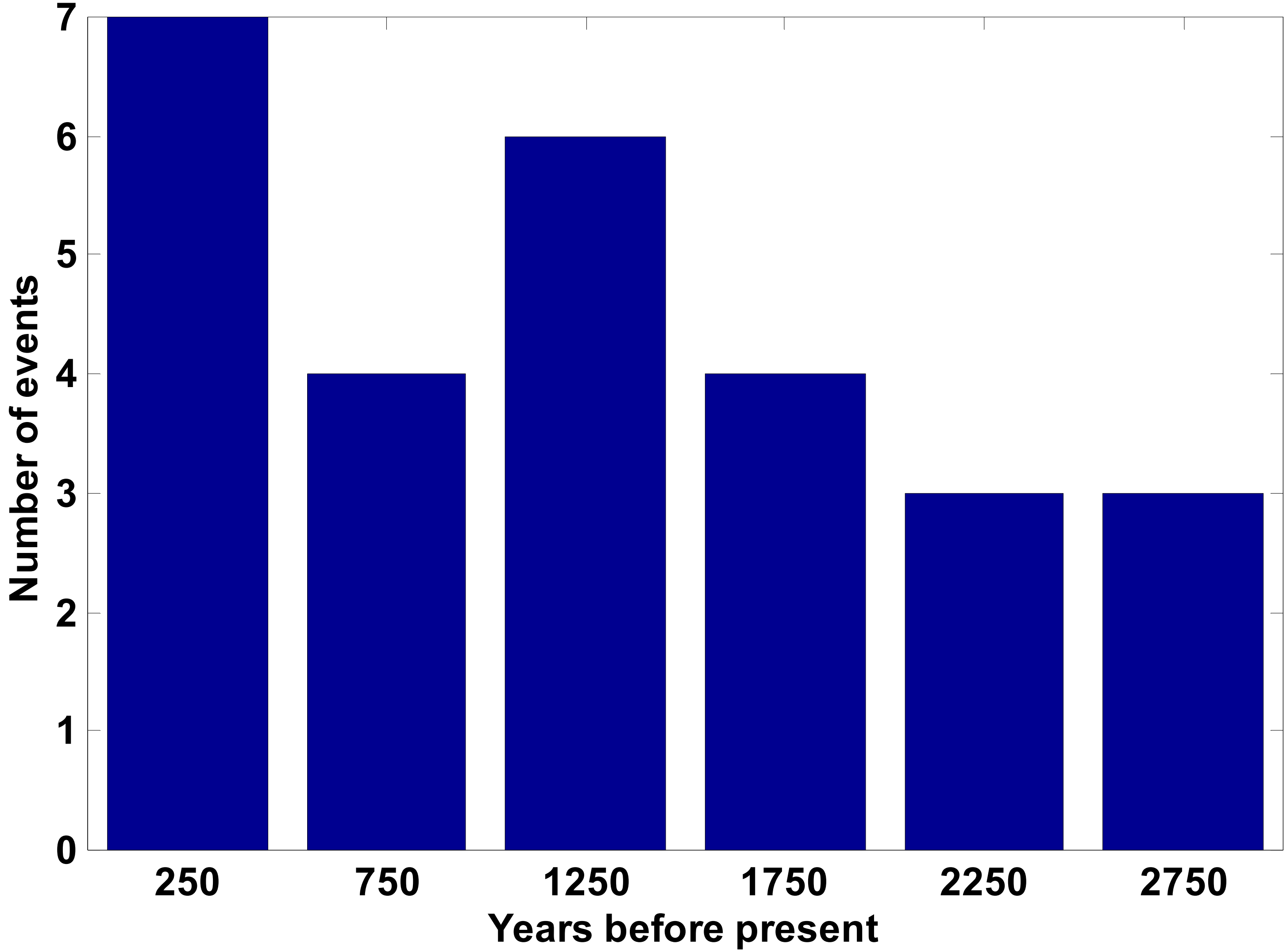

7
6
5
4
3
2
1
0
Number of events
250
750
1250
1750
2250
2750
Years before present

Lake Inwash Deposits

Noren et al., 2002

Core stratigraphies

Sedimentation event histogram

GISP2 sea salt

GISP2 non-sea salt

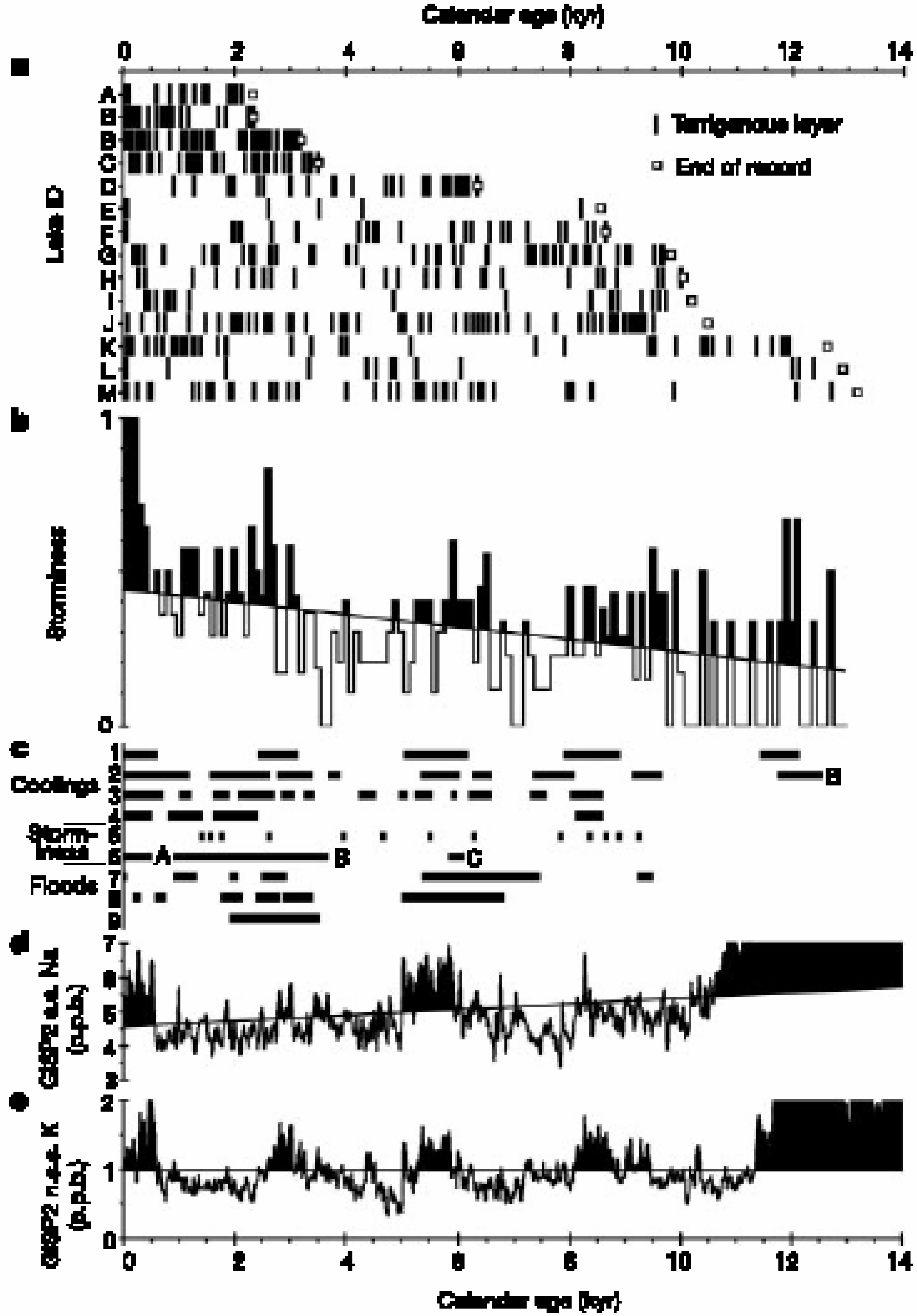

Hummocky Cross-Stratification

Duke, 1985

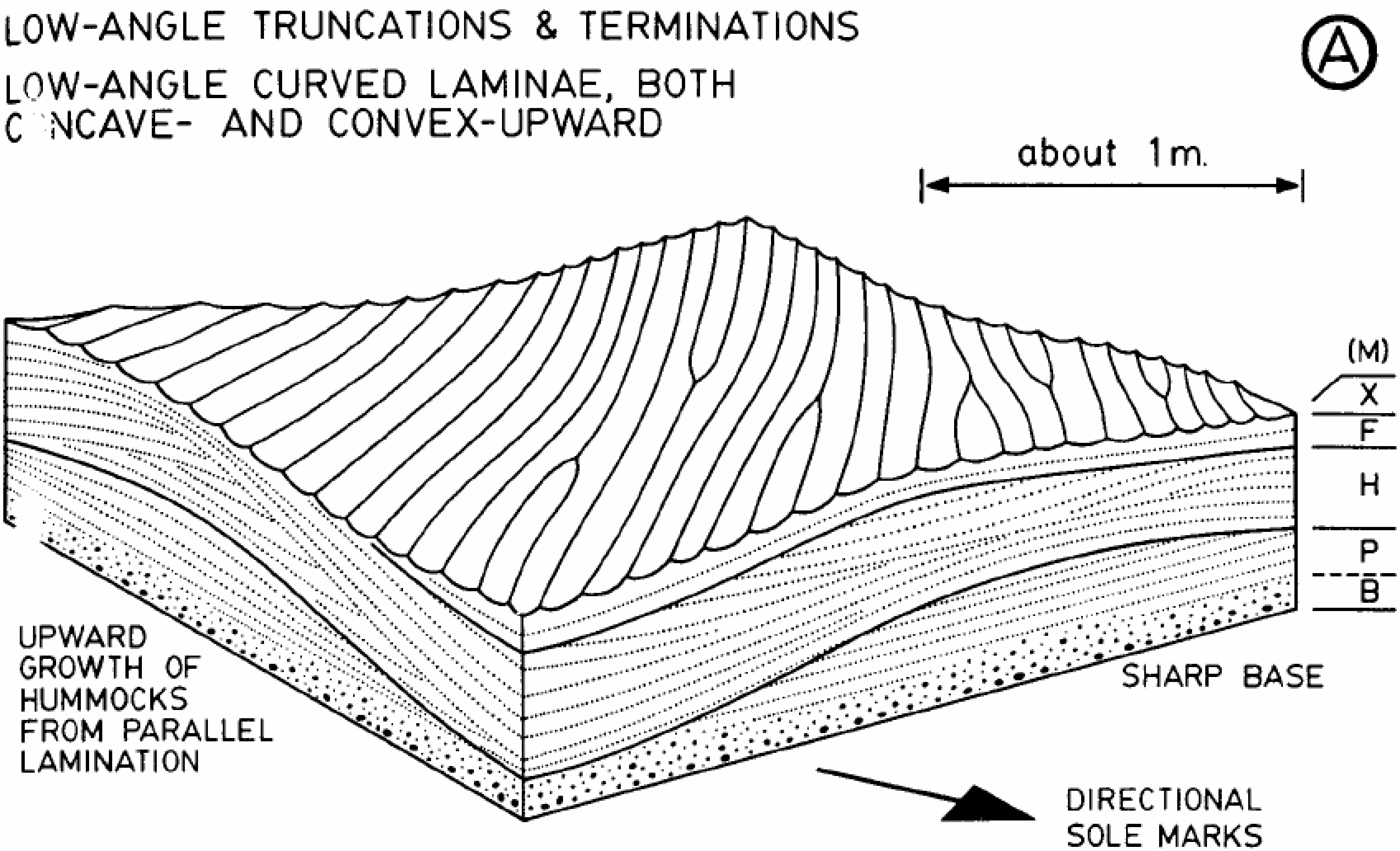

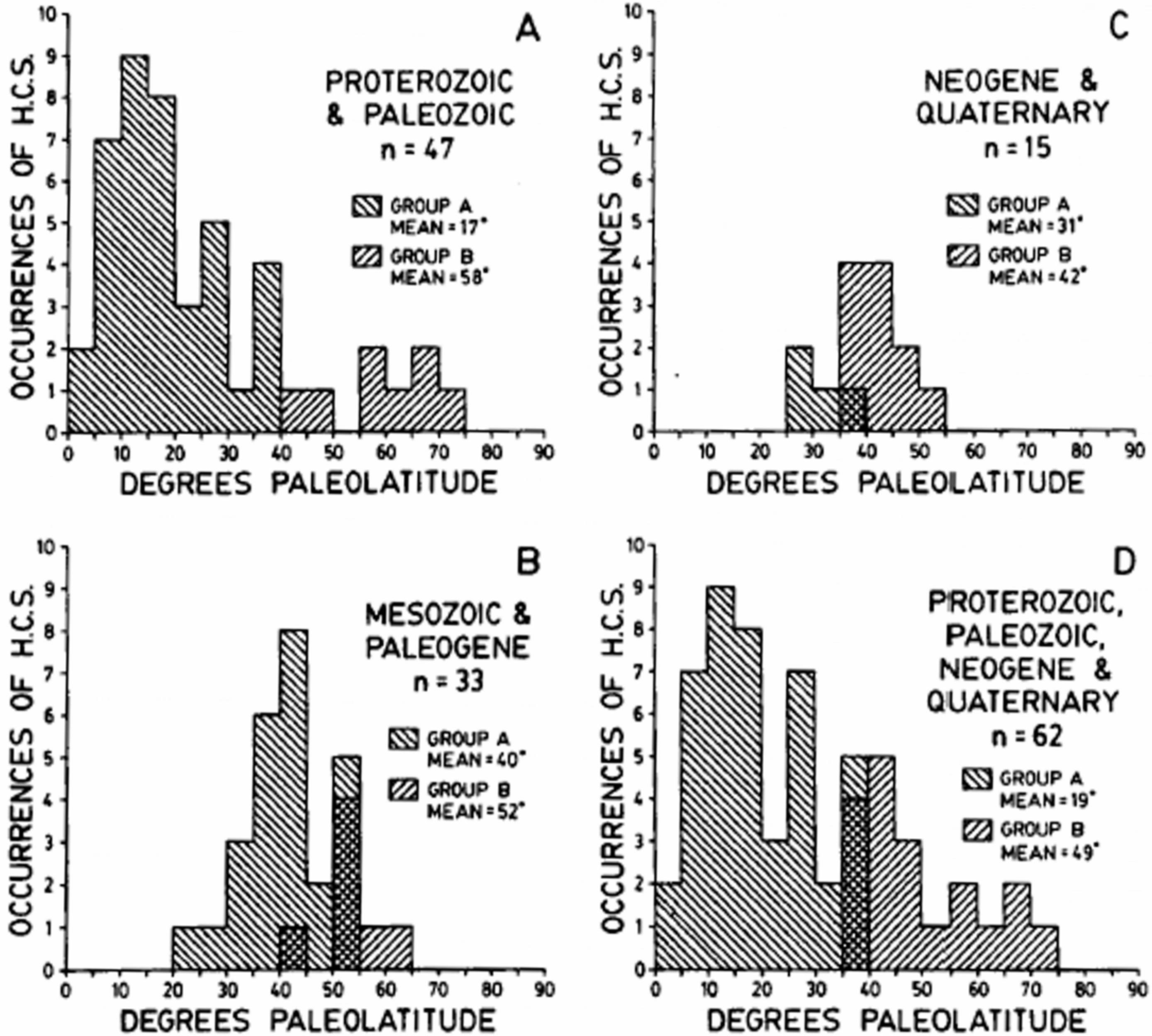
A
PROTEROZOIC & PALEOZOIC
n = 47
GROUP A MEAN = 17°
GROUP B MEAN = 58°
C
NEOGENE & QUATERNARY
n = 15
GROUP A MEAN = 31°
GROUP B MEAN = 42°
B
MESOZOIC & PALEOGENE
n = 33
GROUP A MEAN = 40°
GROUP B MEAN = 52°
D
PROTEROZOIC, PALEOZOIC, NEOGENE & QUATERNARY
n = 62
GROUP A MEAN = 19°
GROUP B MEAN = 49°
OCCURRENCES OF H.C.S.
DEGREES PALEOLATITUDE

Brandt and Elias, 1989

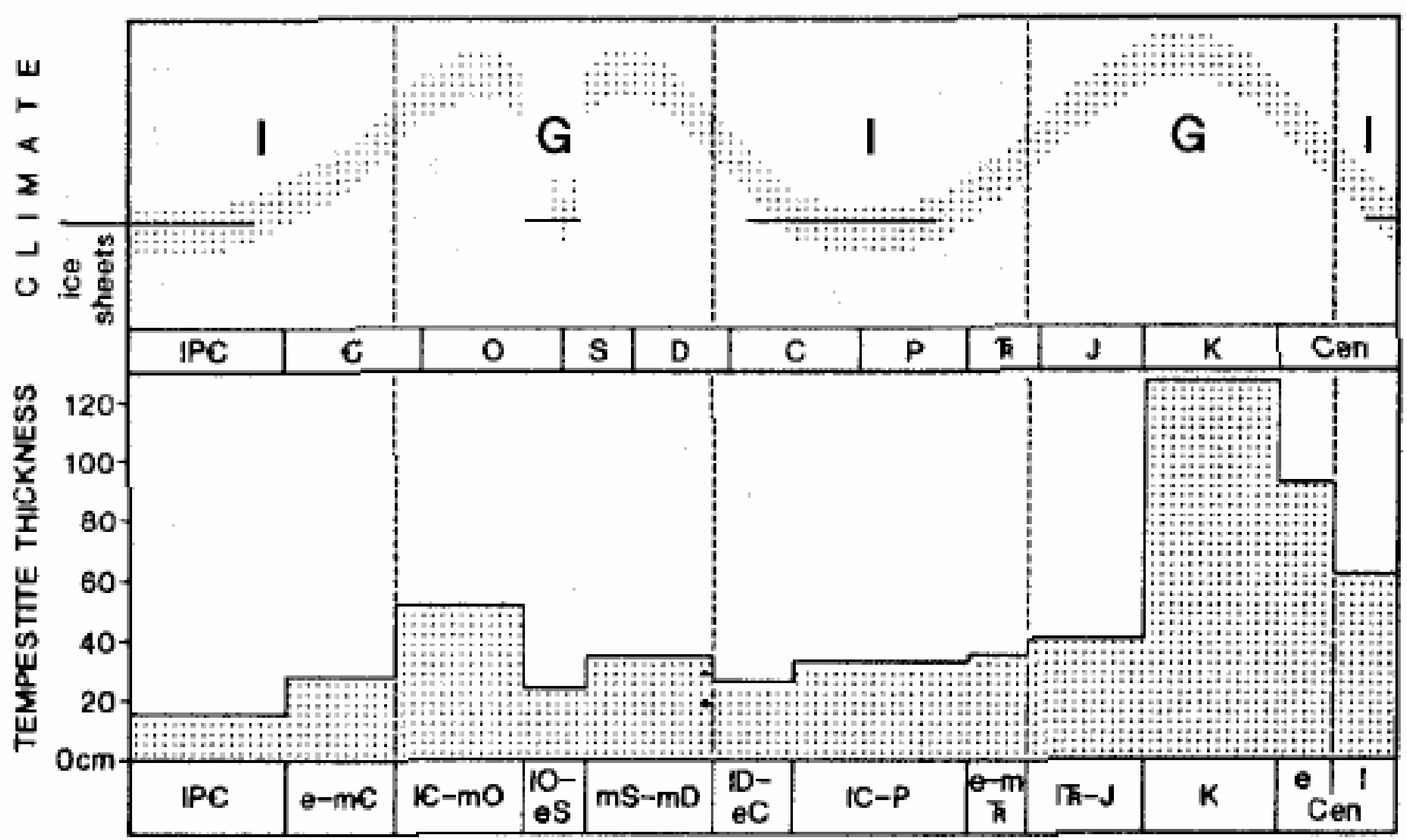

Do tropical cyclones play a role in the climate system?

- The case for tropical cyclone control of the thermohaline circulation
- Feedback of tropical cyclone activity on climate

Tropical Cyclone-Climate Feedback

- Sensitive dependence of tropical cyclone frequency and intensity on tropical SSTs

+

- Dependence of tropical SSTs on global tropical cyclone activity

= Tropical thermostat

Ocean Feedback

Ocean Thermohaline Circulation

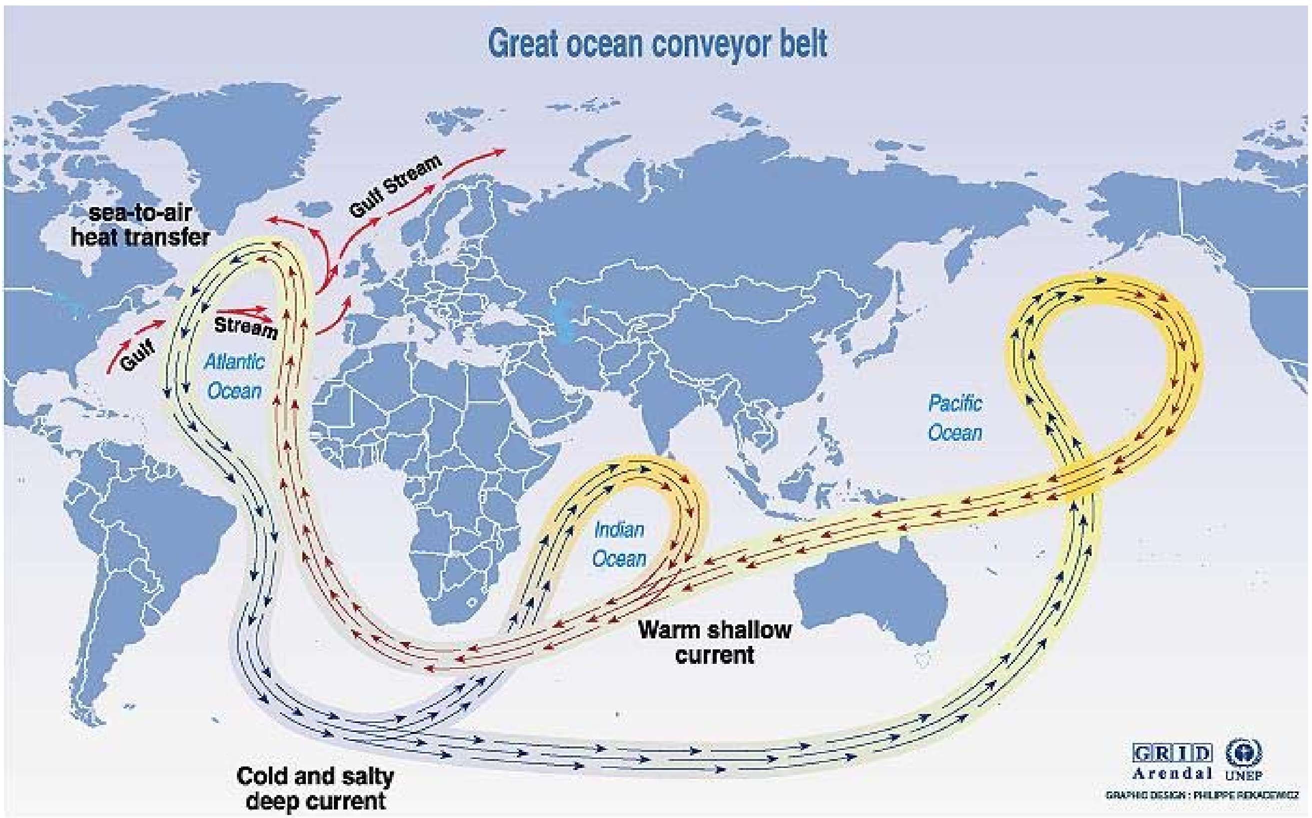

Source: Broecker, 1991, in Climate change 1995, Impacts, adaptations and mitigation of climate change: scientific-technical analyses, contribution of working group 2 to the second assessment report of the intergovernmental panel on climate change, UNEP and WMO, Cambridge press university, 1996.

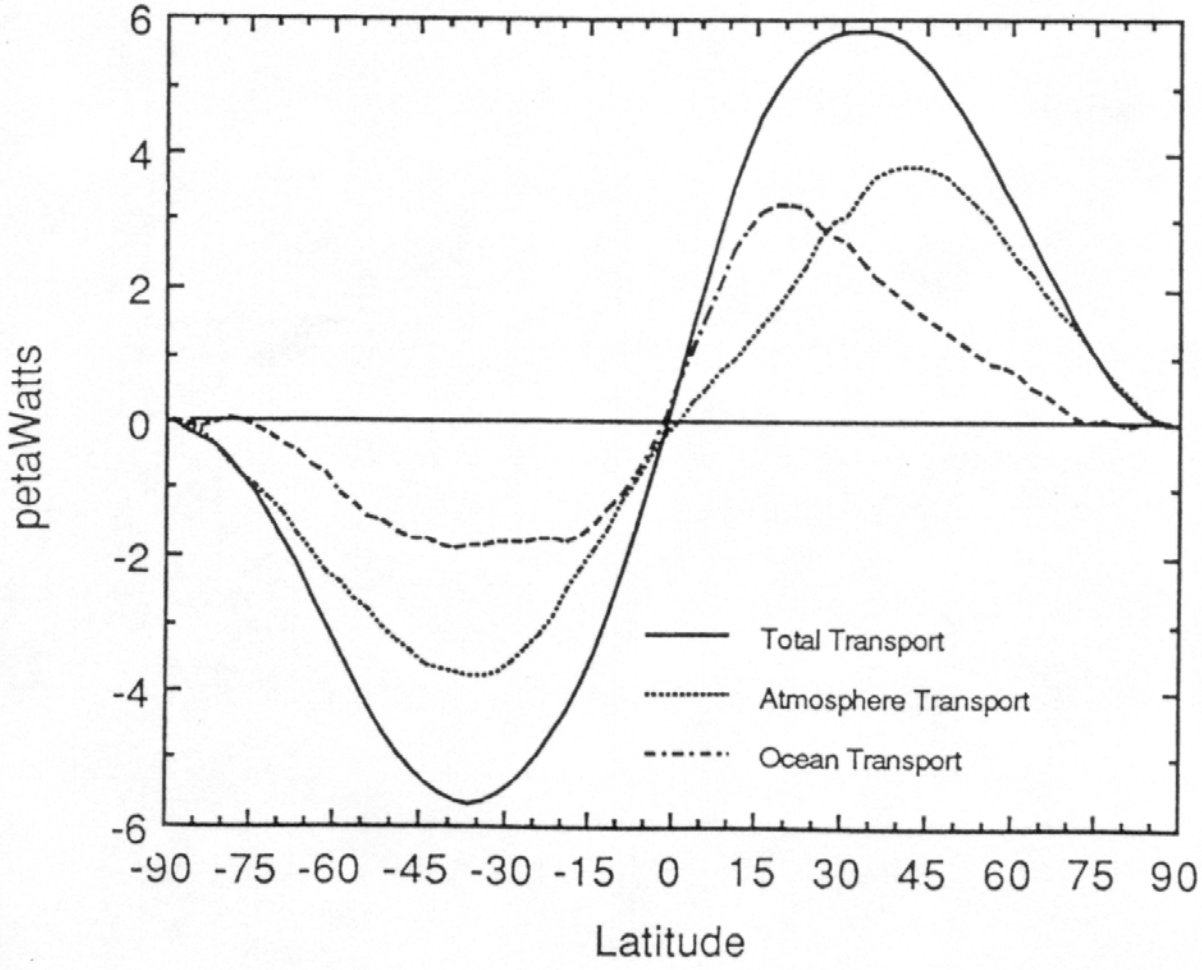

Heat Transport by Oceans and Atmosphere

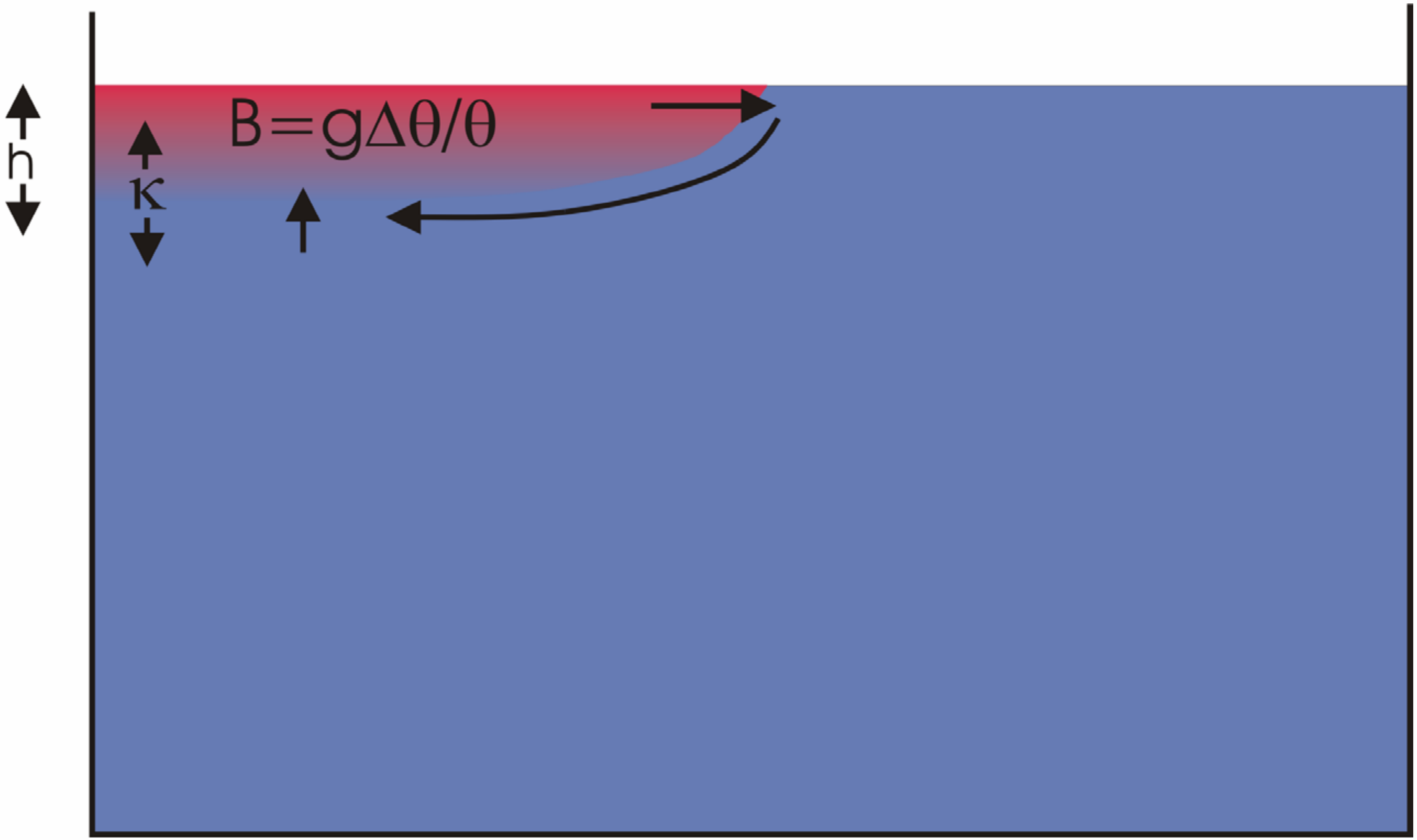

A hot plate is brought in contact with the left half of the surface of a swimming pool of cold water. Heat diffuses downward and the warm water begins to rise. The strength of the circulation is controlled in part by the rate of heat diffusion. In the real world, this rate is very, very small.

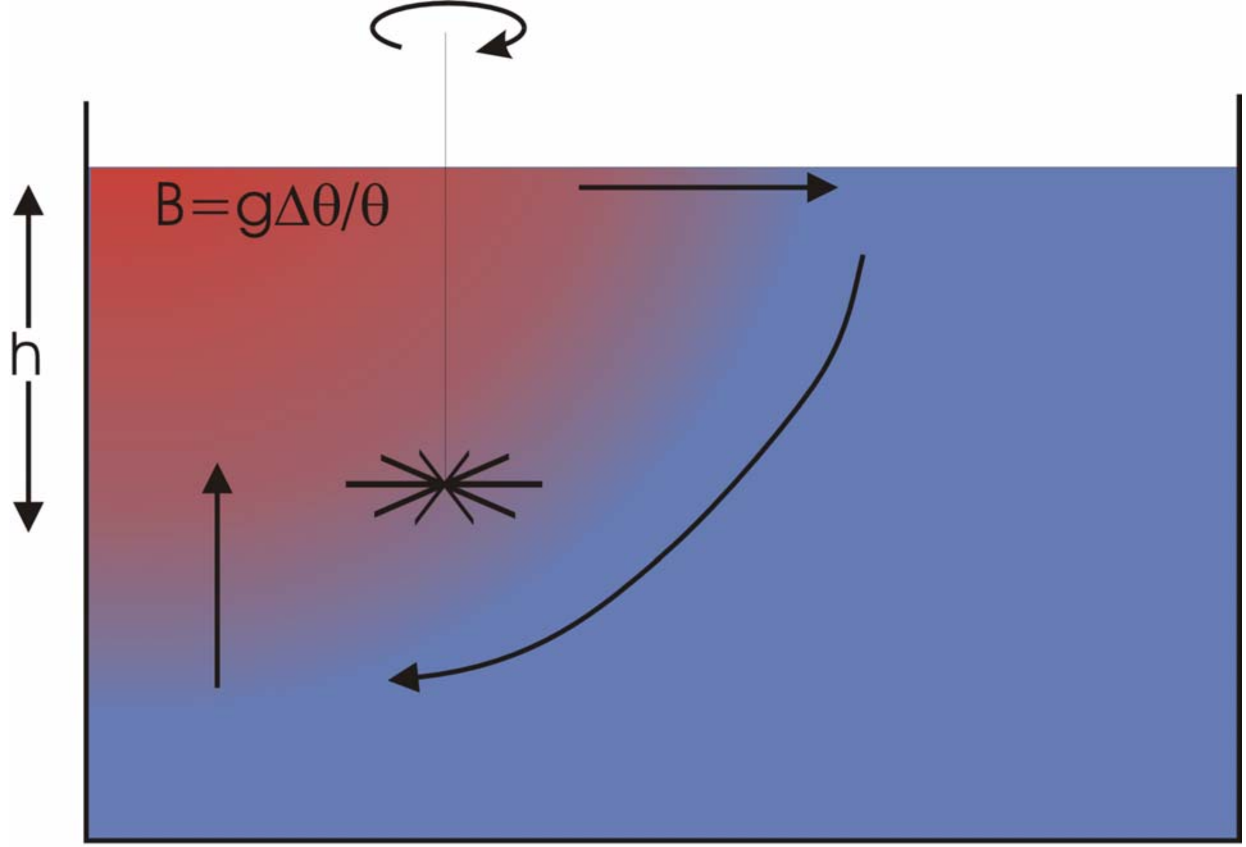

$$\text{Heat Flux} \sim P^{2/3} B^{2/3}$$

$$h \sim P^{1/3} B^{-2/3}$$

Adding a stirring rod to this picture greatly enhances the circulation by mixing the warm water to greater depth and bringing more cold water in contact with the plate. The strength of the lateral heat flux is proportional to the 2/3 power of the power put into the stirring, and the 2/3 power of the temperature of the plate.

Coupled Ocean-Atmosphere model run for 67 of the 83 tropical cyclones that occurred in calendar year 1996

Accumulated TC-induced ocean heating divided by 366 days

Result:

Net column-integrated heating of ocean induced by global tropical cyclone activity:

$$\left(1.4 \pm 0.7\right) \times 10^{15}\, W$$

Trenberth et al., 2001

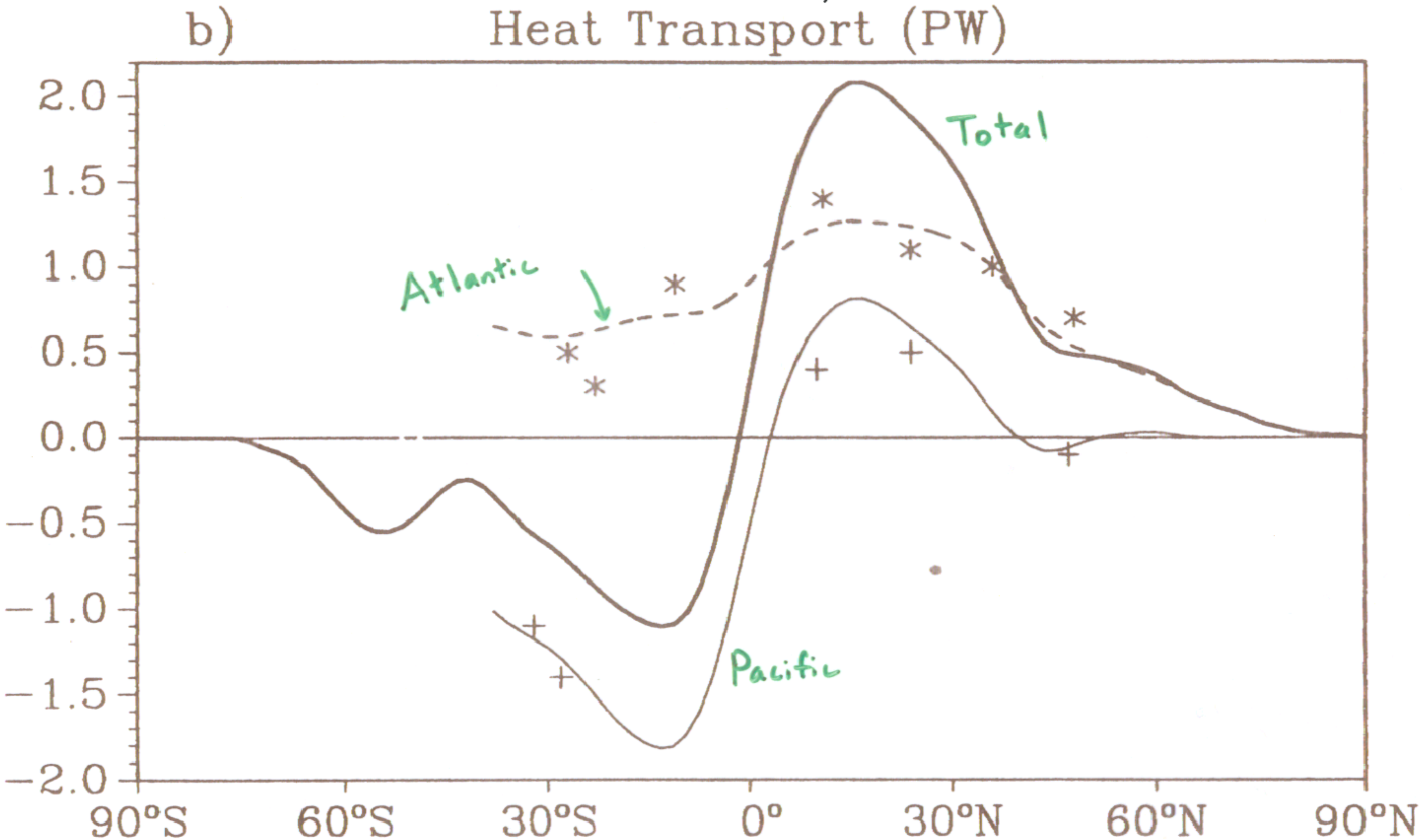

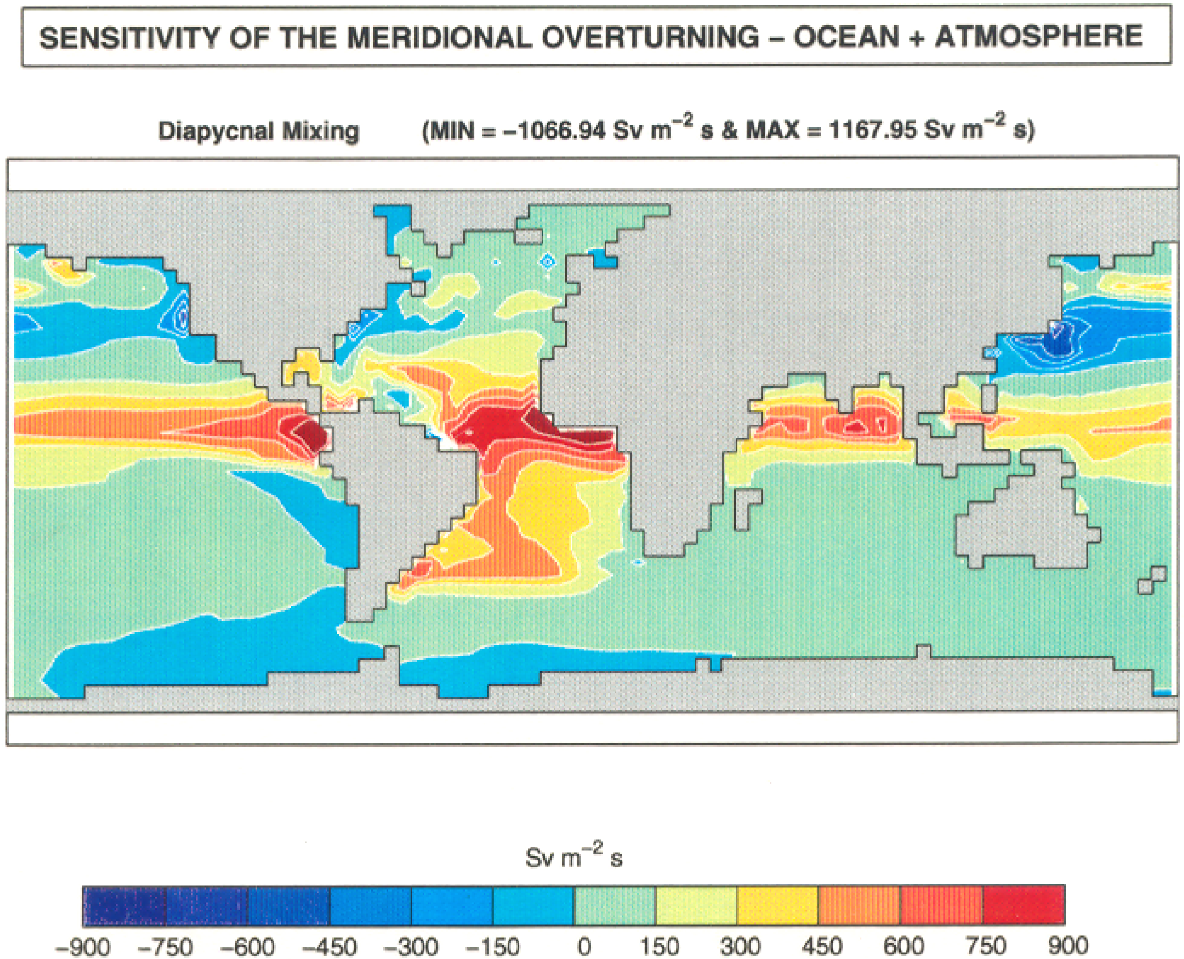

Veronique Bugnion used an ocean model to calculate the sensitivity of the total poleward heat flux by the world oceans to the strength and distribution of vertical mixing. This sensitivity, shown here, is concentrated in the Tropics, where hurricanes occur.

The Role of Wind Forcing

Vertical profiles in the tropics

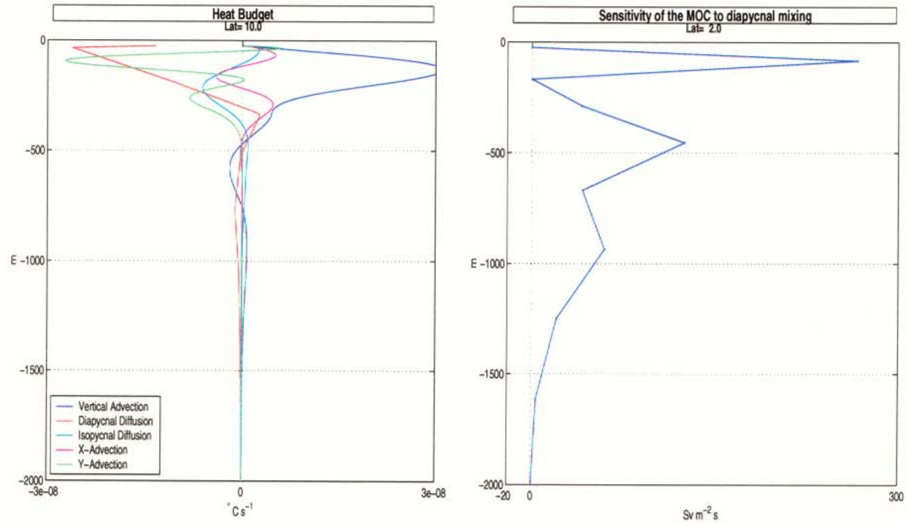

- Near surface heat fluxes are three times larger than without wind
- Near surface sensitivities dominate
- The secondary maximum occurs at the depth of transition between the wind driven and diffusive thermoclines

These diagrams show the currents generated by a very localized source of vertical mixing at 20° N and 25° E. The upper diagram shows the currents near the top of the ocean, while the bottom diagram show currents closer to the bottom. Note in particular the strong northward flow of warm water along the western boundary of the ocean, near the surface. These plots have been generated using a complex ocean model set in a simple rectangular basin.

Courtesy of Jeff Scott

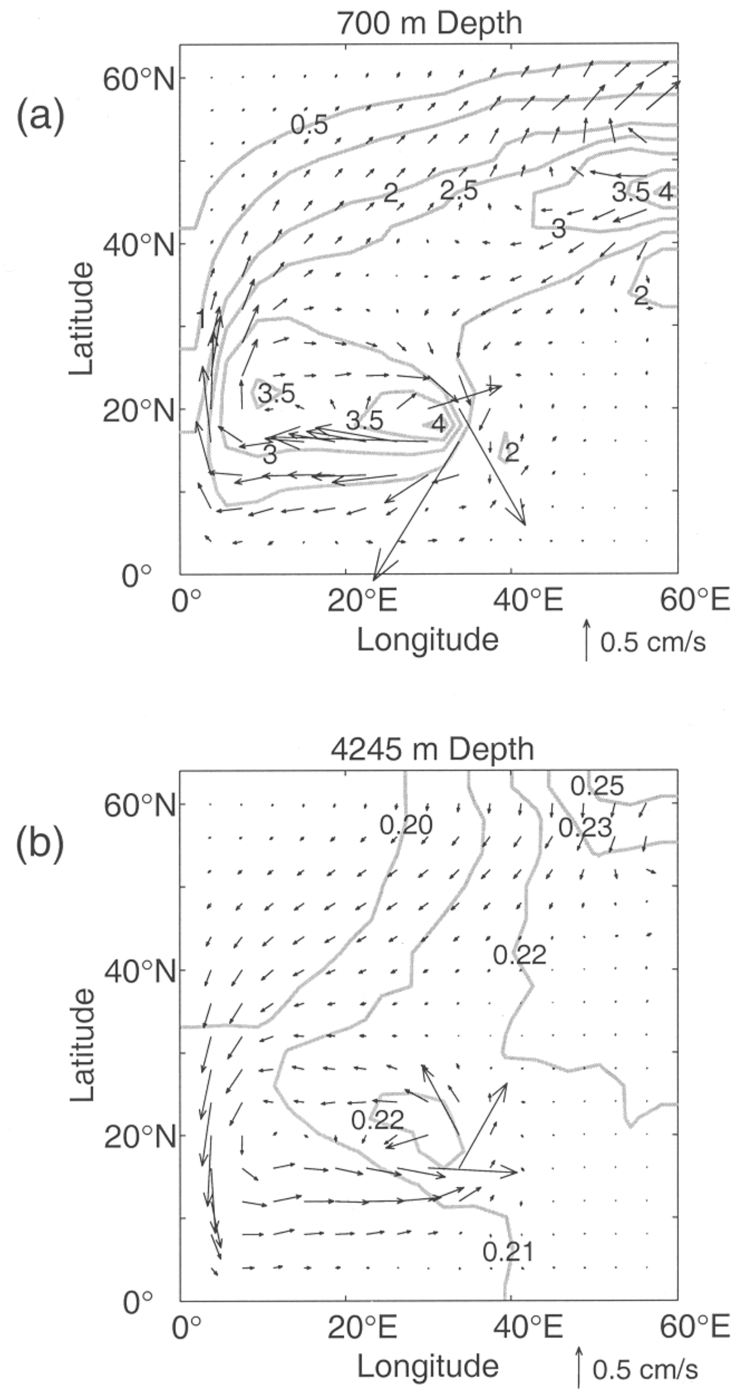

Implications for Climate:

$$Poleward\ Heat\ Flux \sim FP^{2/3}$$

$$F \sim PI^3$$

$$P \sim PI^3$$

$$\rightarrow Poleward\ Heat\ Flux \sim PI^5$$

May be conservative, in view of Nolan's results

This plot shows a measure of El Niño/La Niña (green) and a measure of the power put into the far western Pacific Ocean by tropical cyclones (blue). The blue curve has been shifted rightward by two years on this graph. There is the suggestion that powerful cyclones in the western Pacific can trigger El Niño/La Niña cycles.

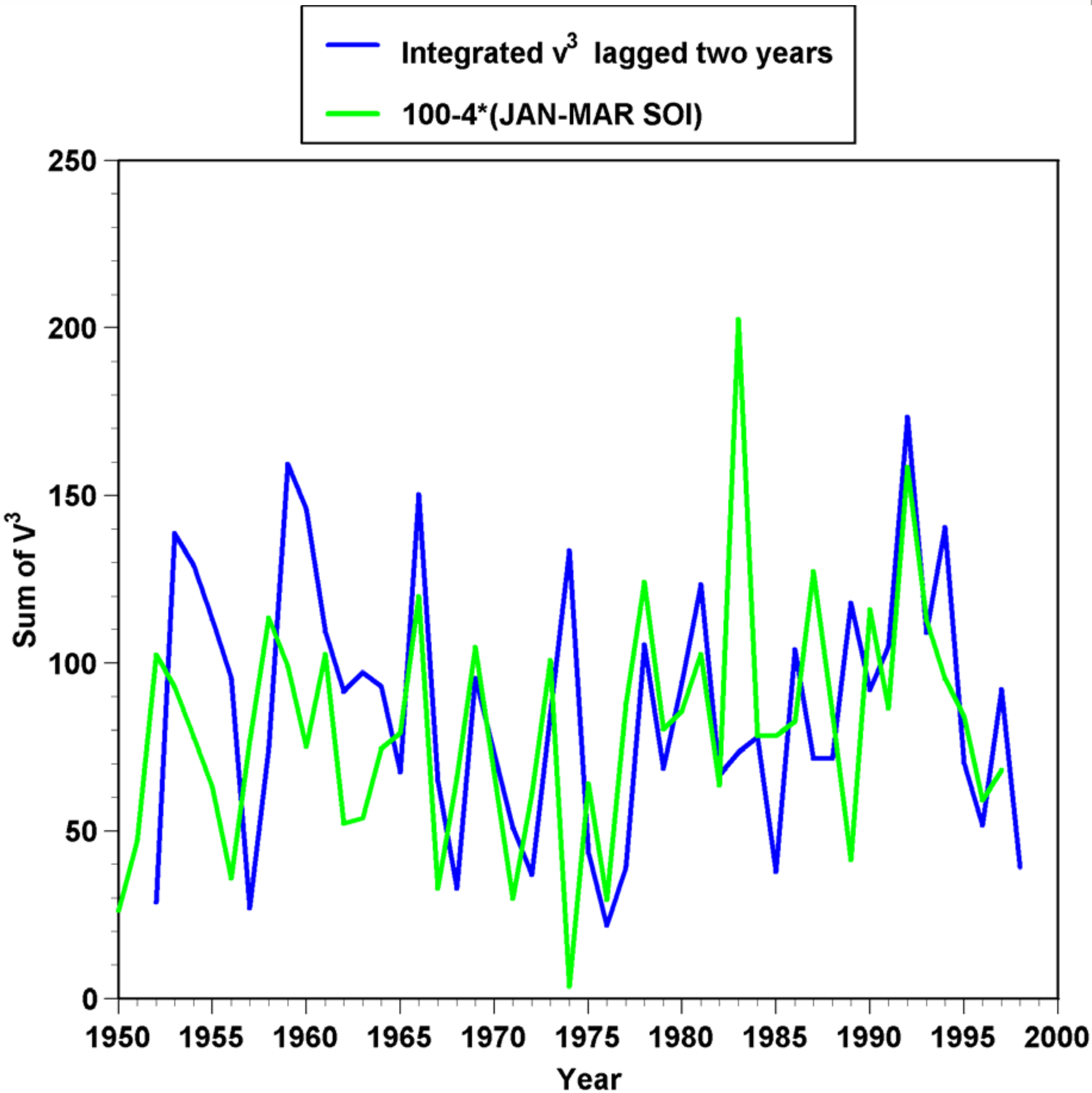

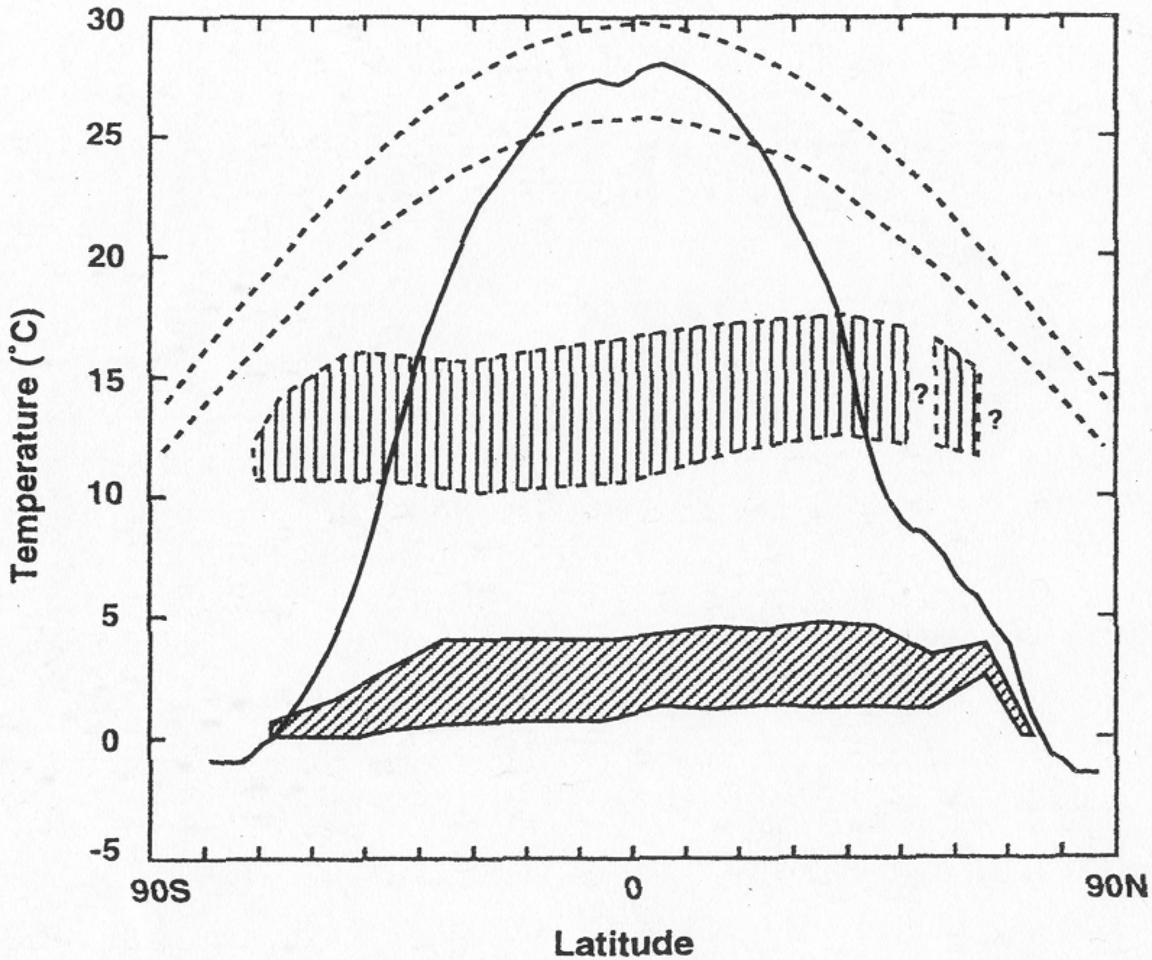

Figure 4.1. Modern (solid line) and estimated early Eocene (dashed lines) zonal sea surface temperatures. Modern (diagonal hatch) and estimated early Eocene (vertical hatch) water temperatures at bottom depths between 1000 m and 5000 m. Modern data are from the *World Ocean Atlas data set* (Levitus and Boyer, 1994). The cooler Eocene SST profile is based on Zachos *et al.* (1994); the warmer SST profile is based on Crowley and Zachos (Chapter 3, this volume).